

**Research of transcriptome response after gamma-ray irradiation
exposure in Japanese medaka (*Oryzias latipes*)**

(トランスクリプトーム解析によるメダカにおけるガンマ線被ばく
の生物影響の研究)

令和6年3月申請 博士 (生命科学)

東京大学大学院 新領域創成科学研究科

李 多琳

Index

| | |
|--|-----|
| General Introduction | 1 |
| Chapter 1. RNA-seq of medaka after low dose/dose rate irradiation | |
| Introduction | 4 |
| Materials and Methods | 6 |
| Results | 11 |
| Discussion | 20 |
| Figures and Tables | 41 |
| Chapter 2. Single Cell RNA-seq of Medaka Testis | |
| Introduction | 60 |
| Materials and Methods | 63 |
| Results | 68 |
| Discussion | 79 |
| Figures | 84 |
| General discussion | 95 |
| References | 99 |
| Acknowledgements | 118 |

General Introduction

Modern technology employs ionizing radiation (IR) for several purposes, such as medical testing, radiotherapy and nuclear power plant. Radiation can affect cell either through direct action by breaking single or double DNA strands or indirectly through the formation of reactive oxygen species (ROS) and other free radicals through the radiolysis of water in cells. Both mechanisms can cause chemical changes (e.g. oxidative changes in DNA, lipid peroxidation, protein oxidation), leading to biological damage. The biological effect of high dose / high dose rate irradiation usually leads to cell death, chromosomal aberrations, DNA damage, mutagenesis and carcinogenesis (Lowe et al., 2022). However, experiments reveal that the effects and risks to low dose / low dose rate irradiation are different from high dose / high dose rate irradiation (Ebrahimian et al., 2017; Ina & Sakai, 2005; Ishida et al., 2010; Mathias et al., 2015; H. Nakamura et al., 2005). The biological responses following low dose / low dose rate irradiation are sometimes contradictory, DNA damage might not be primary response of low dose / low dose rate irradiation. While high dose / high dose rate irradiation causing DNA damage by direct effects of irradiation, it is believed that low dose / low dose rate irradiation can damage tissues and cells by indirect effects, such as oxidative stress induced by reactive oxygen species (ROS) generated from water molecules within the cell due to irradiation (Halliwell, 1991; Halliwell & Aruoma, 1991). The irradiation-induced ROS not only can damage cell components, but also can trigger epigenetic responses, which leads to more complex and non-linear irradiative responses (Schofield & Kondratowicz, 2018). Over

the last 20 years, researchers have tried to reveal low dose / low dose rate irradiation effects, however, there still be limitations of studying low dose / low dose rate irradiation effects in addition to the complexity of low dose / low dose rate irradiation effect itself, such as accuracy of dose estimations, controlling of confounding factors or limited statistic power towards low dose / low dose rate irradiation effect.

The small freshwater fish, Japanese Medaka (*Oryzias latipes*), has long served as a model organism in radiobiology research (Kuwahara et al., 2002, 2003; Shima & Mitani, 2004; Yasuko & Nobuo, 1985). With a body length of approximately 3 cm, medaka is well-suited for laboratory-level breeding and radiobiology experiments. Its suitability is enhanced by the ease of isolating organs through dissection and the relatively straightforward extraction of RNA from the whole body. These characteristics make medaka highly conducive for comprehensive analysis of gene expression at the systemic level, contributing to a deeper understanding of the biological effects of irradiation.

The objective of this study is to evaluate the biological effects of low dose / low dose rate irradiation on medaka at the transcriptomic level. In the first part of the study, radiosensitive tissues, intestine, testis and ovary were selected, and transcriptomic profiles were obtained using next-generation sequencing (NGS) technology. By identifying and analyzing differentially expressed genes (DEGs) between low dose / low dose rate gamma-ray irradiated and control groups, I aim to infer the biological impacts of this irradiation dose on medaka. Furthermore, the small size of medaka allows for sequencing at the whole-body level, enabling the investigation of potential systemic responses to ionizing radiation.

Given that tissues are composed of various cell types with distinct functions, bulk RNA-seq, which analyzes whole tissues, lacks the resolution to differentiate between these cell populations. This limitation is particularly pertinent in the testis, where different cell types may exhibit diverse irradiation response expectations. Therefore, in the second part of this study, I focus on the medaka testis for more detailed investigation. Single-cell RNA sequencing (scRNA-seq) offers much higher resolution than bulk RNA-seq, allowing for the effective separation of germ cells from somatic cells in the testis, facilitating a more nuanced understanding of irradiation effects on male germ cells.

The previous experiments in irradiated *p53* deficient (*p53* knockout; *p53KO*) medaka testis revealed the presence of a cell type resembling an oocyte, called testis-ova. To further explore this phenomenon, this study will compare scRNA-seq data from the testis of wild-type and *p53* deficient medaka under irradiated and control conditions, aiming to elucidate the differences in response between these groups.

Chapter One

RNA-seq of medaka after low dose/dose rate irradiation

Introduction

The nuclear disasters like Chernobyl and Fukushima have intensified researches on the prolonged effects of low dose / low dose rate irradiation on living organisms. Understanding the molecular and cellular processes involved in biological responses to extended irradiation is crucial. Traditionally addressing acute exposures, guidelines from the International Commission on Radiological Protection (ICRP) are now being reevaluated in the context of chronic exposure scenarios. The ICRP considers that, in a population including both adults and children, there is a 0.5% increase in the probability of cancer death per 100 millisieverts (mSv) of radiation exposure. Therefore, it is generally believed that radiation exposure below approximately 100 mSv does not show a significant increase in the risk of cancer (incidence or death). This research informs public health policies, refines risk assessments, and shapes irradiation protection

strategies, emphasizing the need for ongoing efforts to advance our understanding of low dose / low dose rate irradiation and its impact on biological systems.

Even in low dose / low dose rate irradiation, irradiation induced ROS will cause indirect impact of oxidative stress (Azzam et al., 2012). Organisms have developed defense mechanisms against oxidative stress. Enzymes such as superoxide dismutase (SOD) and catalase work to remove reactive oxygen species (ROS) that are generated, thereby reducing the harmful effects of oxidative stress (Matés, 2000).

This study aims to elucidate more comprehensive responses induced by IR at transcriptome level in individual organisms through low dose / low dose rate irradiation using inbred adult medaka fish. For this purpose, tissues with presumed both high sensitivity to irradiation (intestine, testis and ovary) as well as the whole body will be subjected to transcriptome analysis following exposure to approximately 100 mGy of low dose / low dose rate gamma-ray irradiation. The goal is to provide insights into the systemic impacts of IR at the transcriptomic level, and to achieve a comprehensive understanding of the biological responses induced by low dose / low dose rate irradiation.

Materials and Methods

1. Fish husbandry

Inbred medaka strain Hd-rR maintained in the laboratory at the University of Tokyo Kashiwa Campus was used in this study. For daily maintain in laboratory, fish were kept in indoor environment with 26-28 °C water temperature and 14h day-10h night light cycle. Brine shrimp (*Artemia franciscana*) was fed once a day in the morning, powder food (tetra-fin, spectrum brands Japan inc., Tokyo, Japan) was fed twice a day in morning and afternoon. During irradiation experiments in Radiation Research Center at Kyoto University, fish were kept in double layered glass tanks with same temperature and light-dark cycle condition. Air pumps and ammonia filters were utilized for maintaining a suitable rear water environment. Only powder food was fed by automatic feeder.

Animal experimental procedures were conducted in accordance with the ethical guidelines and regulations of the University of Tokyo. The study was approved by the Animal Care and Use Committee of the University of Tokyo, with approval permit number C-09-01 and C-21-5.

2. Irradiation exposure

Transportation: In order to use the low dose long-term radiation exposure device owned by the Radiation Research Center at Kyoto University, both the irradiation group and the control group fish were placed in 2-liter plastic bottles (10-12 individuals per bottle) and transported by Shinkansen (bullet train).

Irradiation: The Cs-137 gamma ray irradiation device owned by the Radiation Research Center at Kyoto University was used to irradiate medaka adult fish over a period of seven days with a total dose of 100mGy (9.99 μ Gy/min, Figure. 1, 2 and 3). Irradiation was stopped once a day for feeding, water quality testing, and changing of the rearing water if needed. For the consistency, control group was placed at the room outside the irradiation room with same equipment and environment conditions.

Treatment after the irradiation: After the irradiation, all fish was brought back to Kashiwa Campus, reared in laboratory environment for 7 days since the irradiation stopped.

3. RNA extraction

Fish were euthanized 7 days after irradiation and proceed to RNA extraction.

For tissue RNA extraction, testis and intestine from male and ovary from female individuals were isolated from fish after euthanasia. Tissues isolated from adult fish were pooled into a 1.5 mL sample tube with 1 mL of Isogen. Each sample contains tissue from 6 individuals. The mixture was homogenized using a homogenizer and then placed at room temperature for 5 minutes. After 5 minutes, 0.2 mL of chloroform was added, and

the mixture was vigorously shaken for 30 seconds before being stand on ice for 5 minutes. The sample was then centrifuged at 14,000 rpm for 15 minutes at 4°C, and the aqueous phase was transferred to a new 1.5 mL tube. This step was repeated, followed by the addition of 500 µL of isopropanol to the separated aqueous phase. The mixture was inverted gently to mix, left to stand at room temperature for 30 minutes, and then centrifuged again at 14,000 rpm for 15 minutes at 4°C. The supernatant was discarded, and the pellet was air-dried at room temperature for 5 minutes before being dissolved in RNase-free water (#10977023, UltraTMDNase/RNase-Free Distilled Water, Invitrogen, USA) to obtain the total RNA solution.

For whole-body RNA extraction, fish was placed on a dry ice block immediately after euthanasia, and instantaneously frozen by another dry ice block on top. A 50 mL centrifuge tube was prepared with 15 mL of Isogen (#311-02501, NIPPON GENE Co., Tokyo, Japan) 3 individual fish of each gender were mixed into one sample, minced with scissors, and shaken by hand for a short time, followed by a 5-minute incubation at room temperature. Next, the mixture was centrifuged using a large centrifuge (#S101637, Himac CR-21G, Koki Holdings Co., Ltd., Tokyo, Japan) at 5000 rpm for 10 minutes at 4°C to remove the insoluble fraction. The supernatant was transferred to a new tube, and 2 mL of chloroform (#035-02616, FUJIFILM Wako Pure Chemical Corporation, Osaka, Japan) was added, followed by vigorous mixing for 30 seconds and a 5-minute incubation on ice. The sample was then centrifuged at 12000 rpm for 15 minutes at 4°C, and the aqueous phase was transferred to a new tube. Subsequently, 5 mL of isopropanol (#166-04836, FUJIFILM Wako Pure Chemical Corporation, Osaka, Japan) was added, mixed by inversion, and centrifuged at 12000 rpm for 10 minutes at 4°C. The supernatant was

discarded, 1 mL of 70% ethanol was added, and the mixture was transferred to a 1.5 mL tube and mixed using a vortex mixer. The sample was then centrifuged at 7500 rpm for 5 minutes at 4°C, the supernatant was discarded, and the pellet was air-dried. Finally, the pellet was dissolved in RNase-free water (#10977023, Ultra™ DNase/RNase-Free Distilled Water, Invitrogen, USA) to obtain a total RNA solution.

4. RNA sequence

Total RNA was subjected to ethanol precipitation (100 µL total RNA solution, 10 µL 3M sodium acetate (#316-90081, NIPPON GENE Co., Tokyo, Japan), 250 µL 100% ethanol) and sent to MacroGen Japan Co., Ltd. for RNA-seq analysis. For library preparation, the TruSeq Stranded mRNA LT Sample Prep Kit (#RS-122-2101, Illumina, Inc., USA) was used, and the library protocol followed was the TruSeq Stranded mRNA Sample Preparation Guide, Part #15031047 Rev. E (Illumina, Inc., California, USA). For sequencing, NovaSeq 6000 (Illumina, Inc., USA) was used, with the Reagent Kit being the NovaSeq 6000 S4 Reagent Kit (#20012866, Illumina, Inc., USA), and the sequencing protocol followed was the NovaSeq 6000 System User Guide Document #1000000019358 v02.

5. Data processing

RNA sequence data were first checked for quality using fastQC (<http://www.bioinformatics.babraham.ac.uk/projects/fastqc/source>), then trimmed by Trimmomatic (Bolger et al., 2014).

Raw reads after trimming were mapped to medaka reference transcriptome (Ensemble 94; ASM223467v1) using STAR (Dobin et al., 2013) with default parameters. Mapped reads were calculated by RSEM (Li & Dewey, 2011) and the gene expression were outputted in both raw count form and normalized form of TPM (Transcripts per kilobase million).

R package edgeR (Y. Chen et al., 2024) was used to find DEGs between conditions. Raw count format of expression matrixes was utilized and to remove batch effect in DEG analysis, batch info was treated as a covariate and the experiment was designed as design = ~batch+ condition. Gene Ontology (GO) (Ashburner et al., 2000) terms were enriched from DEG lists using webpage-tool g:profiler (Kolberg et al., 2023) (<https://biit.cs.ut.ee/gprofiler/gost>). KEGG pathway (Kanehisa & Goto, 2000) analysis was performed using webpage-tool DAVID (Huang et al., 2009a, 2009b), and pathways with p value less than 0.1 were kept and further investigated with webpage-tool Kegg Mapper (Kanehisa et al., 2022; Kanehisa & Goto, 2000) (<https://www.genome.jp/kegg/mapper/>).

Results

To elucidate the physiological alterations, at the transcriptional level of medaka exposed to low doses/ low dose rates of gamma-ray irradiation, particularly during subsequent recovery phase, we performed RNA-seq analysis on adult medaka 7 days after the irradiation (Table. 1). Organ responses to radiation vary due to differences in their tolerance levels, largely depending on their rates of cellular division. Consequently, we selected intestine and testis, which are known to be more radiation-sensitive, and conducted RNA-seq analyses. In addition, to comprehensively grasp the systemic impacts of irradiation exposure, we conducted RNA-seq analyses at a whole-body level.

Transcriptome Analysis of Medaka Intestine After 1 Week of Low Dose Irradiation

Total RNA was extracted and analyzed in both intestines of the 100 mGy gamma-ray irradiated adult medaka and the non-irradiated adult medaka. Comparing gene expression between them, there were 1,045 genes differently expressed at one week after the end of the irradiation ($\log_2FC > 1$; $p_{adj} < 0.05$). In these differential expressed genes (DEGs), I found 533 up-regulated genes and 512 down-regulated genes. Furthermore, 14 and 9 GO terms were enriched in the up-regulated genes and the down-regulated genes, respectively.

“DNA binding (MF)”, “nuclear protein-containing complex (CC)”, “DNA replication (BP)”, “protein-DNA complex organization (BP)”, “mitotic cell cycle (BP)”, “catalytic activity, acting on DNA (MF)”, “nuclear chromosome (CC)”, “chromatin binding (MF)”, “methyltransferase activity (MF)”, “circadian rhythm (BP)”, “photoperiodism (BP)”, “histone methyltransferase activity (MF)”, “MCM complex (CC)” and “DNA-directed DNA polymerase activity (MF)” were enriched in the up-regulated DEGs after the irradiation, on the other hand, “extracellular region (CC)”, “serine-type endopeptidase activity (MF)”, “response to abiotic stimulus (BP)”, “circadian regulation of gene expression (BP)”, “regulation of body fluid levels (BP)”, “pancreatic juice secretion (BP)”, “transcription corepressor binding (MF)”, “sterol esterase activity (MF)” and “retinyl-palmitate esterase activity (MF)” were enriched in the down-regulated DEGs after the irradiation (Figure 4). Additionally, 15 up-regulated KEGG pathways and 10 down-regulated KEGG pathways were enriched from DEGs with p value less than 0.1. “ola03030:DNA replication”, “ola03440:Homologous recombination”, “ola03430:Mismatch repair”, “ola03420:Nucleotide excision repair”, “ola03460:Fanconi anemia pathway”, “ola04110:Cell cycle”, “ola03410:Base excision repair”, “ola00630:Glyoxylate and dicarboxylate metabolism”, “ola00240:Pyrimidine metabolism”, “ola00061:Fatty acid biosynthesis”, “ola04146:Peroxisome”, “ola00230:Purine metabolism”, “ola01232:Nucleotide metabolism”, “ola00250:Alanine, aspartate and glutamate metabolism” and “ola00310:Lysine degradation” were enriched in the up-regulated DEGs after the irradiation (Table 2). “ola00330:Arginine and proline metabolism”, “ola04068:FoxO signaling pathway”, “ola00270:Cysteine and methionine metabolism”, “ola00260:Glycine, serine and threonine metabolism”,

“ola04115:p53 signaling pathway”, “ola04110:Cell cycle”, “ola01100:Metabolic pathways”, “ola00100:Steroid biosynthesis” and “ola04080:Neuroactive ligand-receptor interaction”, “ola00561:Glycerolipid metabolism” were enriched from the down-regulated DEGs after the irradiation (Table 3, 4).

Transcriptome Analysis of Medaka Testis After 1 Week of Low Dose Irradiation

By RNA-seq analysis, expression profiles were identified and compared between irradiated and non-irradiated medaka testis. 4,096 genes were identified significantly changed at transcription level, with 2,710 genes up-regulated and 1,386 genes down-regulated one week after the low dose / low dose rate irradiation of gamma-ray.

The DEGs were divided into DEGs of up-regulated and down-regulated after the irradiation and downstream analyses were performed on these DEGs. Through GO enrichment analysis of these significantly up-regulated or down regulated genes, 34 GO terms for up-regulated genes and 31 GO terms for down regulated genes were enriched. “protein binding (MF)”, “cell communication (BP)”, “cell periphery (CC)”, “ATP binding (MF)”, “zinc ion binding (MF)”, “calcium ion binding (MF)”, “protein kinase activity (MF)”, “GTPase regulator activity (MF)”, “DNA integration (BP)”, “supramolecular fiber organization (BP)”, “defense response (BP)”, “cytoskeletal motor activity (MF)”, “calcium ion transport (BP)”, “defense response to symbiont (BP)”, “calcium ion transmembrane transporter activity (MF)”, “myosin complex (CC)”, “aspartic-type endopeptidase activity (MF)”, “synapse organization (BP)”, “cellular response to lipid (BP)”, “nuclear receptor activity (MF)”, “actin-based cell projection (CC)”, “focal

adhesion (CC)", "dynein complex (CC)", "actin filament-based movement (BP)", "positive regulation of leukocyte cell-cell adhesion (BP)", "RNA-directed DNA polymerase activity (MF)", "structural constituent of muscle (MF)", "M band (CC)", "RSC-type complex (CC)", "peptide antigen assembly with MHC class II protein complex (BP)", "peptide antigen binding (MF)", "MHC class II protein complex binding (MF)", "positive regulation of potassium ion import across plasma membrane (BP)" and "potassium channel inhibitor activity (MF)", and were enriched from the up-regulated DEGs after the irradiation. On the other hand, "mitochondrion (CC)", "small molecule metabolic process (BP)", "translation (BP)", "RNA binding (MF)", "ribosome (CC)", "oxidoreductase activity (MF)", "structural constituent of ribosome (MF)", "nuclear protein-containing complex (CC)", "ribosome biogenesis (BP)", "catalytic activity, acting on RNA (MF)", "aerobic respiration (BP)", "serine-type endopeptidase activity (MF)", "S-adenosylmethionine-dependent methyltransferase activity (MF)", "isomerase activity (MF)", "DNA replication (BP)", "tRNA processing (BP)", "translation factor activity, RNA binding (MF)", "nucleobase-containing compound kinase activity (MF)", "iron-sulfur cluster binding (MF)", "mitochondrial respiratory chain complex assembly (BP)", "RNA endonuclease activity (MF)", "oogenesis (BP)", "phosphotransferase activity, phosphate group as acceptor (MF)", "cellular modified amino acid biosynthetic process (BP)", "binding of sperm to zona pellucida (BP)", "acrosin binding (MF)", "ncRNA catabolic process (BP)", "RNA surveillance (BP)", "U4 snRNA 3'-end processing (BP)", "S-methyltransferase activity (MF)" and "deoxynucleoside kinase activity (MF)" were enriched from the down-regulated DEGs after the irradiation (Figure 5). In KEGG pathway analysis, 25 pathways from the up-regulated DEGs and 26 pathways from the

down-regulated after the irradiation were enriched. “ola04514:Cell adhesion molecules”, “ola04020:Calcium signaling pathway”, “ola04672:Intestinal immune network for IgA production”, “ola04810:Regulation of actin cytoskeleton”, “ola04510:Focal adhesion”, “ola04145:Phagosome”, “ola04512:ECM-receptor interaction”, “ola04371:Apelin signaling pathway”, “ola04060:Cytokine-cytokine receptor interaction”, “ola04270:Vascular smooth muscle contraction”, “ola04912:GnRH signaling pathway”, “ola04070:Phosphatidylinositol signaling system”, “ola04540:gap junction”, “ola04520:Adherens junction”, “ola04148: Efferocytosis”, “ola03250: Viral life cycle - HIV-1”, “ola04012:ErbB signaling pathway”, “ola04261:Adrenergic signaling in cardiomyocytes”, “ola04010:MAPK signaling pathway”, “ola00562:Inositol phosphate metabolism”, “ola03266:Virion – Herpesvirus”, “ola04144:Endocytosis”, “ola04814:Motor proteins”, “ola02010:ABC transporters” and “ola04620:Toll-like receptor signaling pathway” were enriched from up-regulated DEGs after the irradiation (Table. 5). On the other hand, “ola03010:ribosome”, “ola00190:Oxidative phosphorylation”, “ola01100:Metabolic pathways”, “ola01232:Nucleotide metabolism”, “ola01240:Biosynthesis of cofactors”, “ola03018:RNA degradation”, “ola03030:DNA replication”, “ola03020:RNA polymerase”, “ola03040:Spliceosome”, “ola00240:Pyrimidine metabolism”, “ola03410:Base excision repair”, “ola00983:Drug metabolism - other enzymes”, “ola00030:Pentose phosphate pathway”, “ola01200:Carbon metabolism”, “ola00630:Glyoxylate and dicarboxylate metabolism”, “ola00620:Pyruvate metabolism”, “ola00350:Tyrosine metabolism”, “ola00760:Nicotinate and nicotinamide metabolism”, “ola03008:Ribosome biogenesis in eukaryotes”, “ola03420:Nucleotide excision repair”, “ola00230:Purine metabolism”,

“ola00330:Arginine and proline metabolism”, “ola00010:Glycolysis / Gluconeogenesis”, “ola00040:Pentose and glucuronate interconversions”, “ola00260:Glycine, serine and threonine metabolism” and “ola00980:Metabolism of xenobiotics by cytochrome P450” were enriched from the down-regulated DEGs after the irradiation (Table. 6).

Transcriptome Analysis of Medaka Ovary After 1 Week of Low Dose Irradiation

Total RNA extracted from low dose / low dose rate gamma-ray irradiated as well as non-irradiated adult medaka ovary was sequenced. By RNA-seq analysis, DEGs were extracted between irradiated and non-irradiated groups. Comparing irradiated group to non-irradiated ovaries, 69 up-regulated genes and 428 down-regulated genes, in total 497 differentially expressed genes were collected after 1 week of low dose irradiation. “glycosaminoglycan binding (MF)”, “perineuronal net (CC)” and “positive regulation of neuroblast proliferation (BP)” were enriched from the up-regulated DEGs after the irradiation, while “membrane (CC)”, “transport (BP)”, “extracellular region (CC)”, “small molecule metabolic process (BP)”, “transition metal ion binding (MF)”, “proteolysis (BP)”, “peptidase activity (MF)”, “active transmembrane transporter activity (MF)”, “organic anion transport (BP)”, “lipid transport (BP)”, “tetrapyrrole binding (MF)”, “sodium ion transport (BP)”, “lipid catabolic process (BP)”, “monooxygenase activity (MF)”, “response to xenobiotic stimulus (BP)”, “pancreatic juice secretion (BP)”, “chylomicron(CC)” “sterol esterase activity (MF)”, “retinyl-palmitate esterase activity (MF)” and “bile acid binding (MF)” were enriched from the down-regulated DEGs after the irradiation (Figure 6). 3 KEGG pathways, “ola00532:Glycosaminoglycan

biosynthesis - chondroitin sulfate / dermatan sulfate”, “ola00860:Porphyrin metabolism” and “ola04148:Efferocytosis” were enriched from the up-regulated DEGs after the irradiation (Table 7), whereas “ola01100:Metabolic pathways”, “ola00140:Steroid hormone biosynthesis”, “ola00591:Linoleic acid metabolism”, “ola00500:Starch and sucrose metabolism”, “ola00830:Retinol metabolism”, “ola00983:Drug metabolism - other enzymes”, “ola00590:Arachidonic acid metabolism”, “ola00380:Tryptophan metabolism”, “ola00260:Glycine, serine and threonine metabolism”, “ola00053:Ascorbate and aldarate metabolism”, “ola00040:Pentose and glucuronate interconversions”, “ola00410:beta-Alanine metabolism”, “ola00860:Porphyrin metabolism”, “ola00270:Cysteine and methionine metabolism”, “ola00982:Drug metabolism - cytochrome P450”, “ola00980:Metabolism of xenobiotics by cytochrome P450”, “ola00480:Glutathione metabolism”, “ola00770:Pantothenate and CoA biosynthesis”, “ola00430:Taurine and hypotaurine metabolism”, “ola01240:Biosynthesis of cofactors”, “ola00100:Steroid biosynthesis”, “ola00520:Amino sugar and nucleotide sugar metabolism”, “ola00592:alpha-Linolenic acid metabolism” and “ola04146:Peroxisome”, “ola01200:Carbon metabolism” were enriched from the down-regulated DEGs after the irradiation (Table. 8)

Transcriptome Analysis of Medaka Whole-body After 1 Week of Low Dose Irradiation

As the final part of chapter one, transcriptome responses after the irradiation were

investigated at whole-body level. Total RNA was extracted from 3 male and 3 female medaka fish, respectively, at a whole fish scale and sequenced to find different expression genes between irradiated and non-irradiated group. As a result of DEG analysis, 1,747 DEGs were found in the male group, with 847 genes up-regulated and 900 gene down-regulated after the irradiation, and 836 up-regulated genes and 815 down-regulated genes, in total of 1,651 DEGs found in the female group after the irradiation. To focus on the common responses to low dose / low dose rate irradiation in medaka, up- or down-regulated DEGs shared in male and female group were extracted for further analysis. Among those DEGs, 430 up-regulated DEGs and 442 down-regulated DEGs after the irradiation are shared in both genders (Figure 7). Those shared genes were expected to present the common response to low dose / low dose rate irradiation in medaka. Gene Ontology (GO) enrichment analysis and KEGG pathway analysis were performed on the up-regulated or down-regulated DEGs separately.

26 GO terms were enriched from up-regulated DEGs, and 3 GO terms were enriched from down-regulated DEGs (Figure 8). This result is consistent with GO enrichment results from male and female, more pathways and biological processes are activated than repressed, which indicates that 100mGy gamma-ray may has an activating influence on medaka. “extracellular region (CC)”, “lipid metabolic process (BP)”, “oxidoreductase activity (MF)”, “defense response (BP)”, “endoplasmic reticulum (CC)”, “positive regulation of immune system process (BP)”, “lipid transport (BP)”, “carbohydrate binding (MF)”, “humoral immune response (BP)”, “serine-type endopeptidase activity (MF)”, “tetrapyrrole binding (MF)”, “iron ion binding (MF)”, “isomerase activity (MF)”, “endopeptidase inhibitor activity (MF)”, “blood coagulation (BP)”, “acyl-CoA metabolic

process (BP)", "triglyceride metabolic process (BP)", "regulation of plasma lipoprotein particle levels (BP)", "cytoskeletal rearrangement involved in phagocytosis, engulfment (BP)", "complement receptor mediated signaling pathway (BP)", "aromatic amino acid family catabolic process (BP)", "sialic acid binding (MF)", "complement receptor activity (MF)", "phospholipase A1 activity (MF)", "N-acylsphingosine amidohydrolase activity (MF)" and "ceramidase activity (MF)" and were enriched from the shared up-regulated DEGs after the irradiation. "Circadian regulation of gene expression (BP)", "Transcription corepressor binding (MF)" and "desmosome (CC)" were enriched from the shared down-regulated DEGs after the irradiation.

As a result of KEGG pathway analysis of DEGs shared between male and female, "ola01100:Metabolic pathways", "ola00100:Steroid biosynthesis", "ola03320:PPAR signaling pathway", "ola01040:Biosynthesis of unsaturated fatty acids", "ola01212:Fatty acid metabolism", "ola00592:alpha-Linolenic acid metabolism", "ola04145:Phagosome", "ola01240:Biosynthesis of cofactors", "ola00520:Amino sugar and nucleotide sugar metabolism", "ola00062:Fatty acid elongation", "ola04146:Peroxisome", "ola00380:Tryptophan metabolism", "ola00630:Glyoxylate and dicarboxylate metabolism", "ola00900:Terpenoid backbone biosynthesis", "ola00120:Primary bile acid biosynthesis", "ola01200:Carbon metabolism" and "ola00591:Linoleic acid metabolism" pathways were up-regulated after irradiation (Table. 9), "ola04820:Cytoskeleton in muscle cells", "ola04080:Neuroactive ligand-receptor interaction", "ola00330:Arginine and proline metabolism", "ola04744:Phototransduction", "ola04148:Efferocytosis", "ola01230:Biosynthesis of amino acids", "ola04310:Wnt signaling pathway", "ola04512:ECM-receptor interaction" were down-regulated after irradiation (Table. 10).

Discussions

Transcriptome Analysis of Medaka Intestine After 1 Week of Low Dose Irradiation

Intestinal epithelial cells, including goblet cells, absorptive epithelial cells, Paneth cells, enteroendocrine cells, and intestinal stem cells (ISCs), play vital roles in nutrient absorption and pathogen defense. Among them, the ISCs, which are a group of cells located at the base of crypts, are primarily responsible for replacing rapidly renewing intestinal epithelial cells through continuously differentiating while maintaining their population through mitosis. These ISCs exhibit high sensitivity to ionizing radiation, accelerating their cell division to compensate for damaged and lost epithelial cells during irradiation induced injuries. It has been confirmed that radiation exposure induce cessation of proliferation in intestinal epithelial cells and dysfunction of intestinal epithelial tissue by histological experiments on mouse (Lu et al., 2023; Quastler, 1956). In this part of the study, I investigated transcriptomic response of adult medaka intestinal cells after low dose / low dose rate irradiation.

Cell Cycle Was Disrupted at 1 Week after Irradiation

In the Gene Ontology (GO) enrichment results, terms related to cell cycle were enriched

in the up-regulated DEGs after the irradiation. The up-regulation of the key G1/S phase genes, including all six members of the MCM family (MCM2-7), suggests that the intestinal cells might have been arrested in the G1 phase due to irradiation-induced stress, indicating a resumption of DNA replication. This response is likely a protective mechanism, promoting cells to repair the irradiation-induced DNA damages before proceeding the cell cycle. In KEGG pathway analysis, the pathway related cell cycle was also enriched from the DEGs between the irradiated and non-irradiated group. However, the up- and down-regulated DEGs were both included in this KEGG pathway. Among the 24 DEGs belonging to “Cell cycle” KEGG pathway, 14 DEGs were up-regulated and 10 DEGs were down-regulated after 1 week of the irradiation (Table 4). All of 6 members of the *mcm* family, *mcm2-7*, along with other 8 G1/S phase related genes were listed in the up-regulated DEGs, suggesting that intestinal stem cells (ISC) were arrested at G1 phase and some of them progressed into S phase. This is consistent with the GO enrichment result above, which found DNA replication and MCM complex enriched in the up-regulated DEGs. In the 10 down-regulated DEGs after the irradiation, most of them are genes involved in mitosis or in regulation of transition to mitosis, strongly suggesting that mitotic activity is suppressed after the irradiation, and some of the stem cells were accumulated in S phase in the irradiated intestine. This suppression could serve as an additional protective measure, preventing cells with potential DNA damage from entering mitosis, which could lead to genomic instability. The activation of the DNA replication machinery and suppression of mitosis suggest a strongly tuned cellular response aiming to balance DNA repair and cell cycle progression, ensuring genomic integrity while managing the effects of the irradiation. This interplay between cell cycle phases in

response to stress underscores the complexity of the irradiation response in intestinal cells and is consistent with previous studies indicating that stress adaptation can be accomplished by cell cycle regulation in response to changing environments (Solé et al., 2015).

GO “Pancreatic juice secretion” was down-regulated at 1 Week after irradiation

GO enrichment analysis found GO term: Pancreatic juice secretion in the down-regulated DEGs after the irradiation, which suggests that pancreatic juice secretion reduced at 1 week after the irradiation. However, all 3 genes in this GO term are carboxyl ester lipase (CEL), which is expressed in pancreatic cells, not in intestine in vertebrates (Lombardo, 2001; Lombardo et al., 1978). The pancreas is a small exocrine glands in medaka and irregularly distributed from near the base of the gallbladder in liver surrounding intestine in medaka (岩松, 2018). Considering the distribution of pancreas in medaka anatomy, it is reasonable to assume that the intestine sample that I prepared in this study might also include pancreas tissue.

Despite the fact that the CEL is mainly expression in pancreas, it is still can be discussed that CEL functions in the intestine. CEL is an important nonspecific lipolytic enzyme in the intestine. Its activity depends on bile salts and is essential for hydrolyzing water-insoluble carboxyl esters with long-chain fatty acyl groups (Hui & Howles, 2002). Since lipid metabolism, especially long chain fatty acid biosynthesis processes were up-regulated in whole-body scale as later mentioned in this chapter, the up-regulation of CELs might be expectable. However, the CELs were down-regulated in medaka intestine,

which suggests a suppression of digest function and also possibly pancreas function after the irradiation. Since pancreas is not a radiosensitive organ, this change might be an indirect influence of the irradiation exposure, such as oxidative stress or inflammatory in digestion track. On the other hand, down-regulation of CELs after the irradiation was also observed in ovary, indicative that the down-regulation of CELs after the irradiation might be a whole-body scale response even though CELs are mainly expressed in pancreas, that will be discussed in the whole-body section later.

Overall, clear responses to the low dose / low dose rate irradiation have been revealed in medaka intestine, especially intestinal epithelial cells. As expected, cell proliferation was delayed while repairment activity was promoted after the low dose / low dose rate irradiation. In addition, the down-regulation of CELs expression was unexpectedly found in the intestine cells after the irradiation. Intestinal cell hypertrophy and tissue disintegration induced by high-dose/high-dose rate was confirmed histologically in goldfish (Hyodo, 1965), however, the previous histological examination of low dose / low dose rate irradiated medaka has not reported any intestinal response (Nakazawa, 2020). In this study, medaka intestinal with same irradiation treatment were investigated by RNA sequencing technique, transcriptome profile reveals the intestinal responses under the low dose / low dose rate irradiation, which might be so faint that it may be difficult to detect through histological examination.

Transcriptome Analysis of Medaka Testis After 1 Week of Low Dose Irradiation

Ionizing radiation has a more pronounced impact on actively dividing cells and spermatogenic cells undergoing mitosis and meiosis in testis, those are highly susceptible to ionizing radiation compared to slowly self-renewing somatic cells. Also, it is reported that in vertebrate testis, spermatogonia, along with spermatids and sperm, can undergo DNA damage induced by reactive oxygen species (ROS) (Fang et al., 2013; Fatehi et al., 2018; Vilenchik & Knudson, 2000). In medaka testis, spermatogonia have very high sensitivity to high dose irradiation and apoptotic cell death is induced after the irradiation (Nagata et al., 2022; Yasuda et al., 2012). Medaka testis typically forms cysts, each of which is comprising male germ cells and surrounded by somatic cells, called Sertoli cells. Sertoli cells play crucial roles in supporting and nurturing the germ cells to undergo spermatogenesis within the cysts. Considering the close communication between the supporting Sertoli cells and the germ cells, especially spermatogonia, changes in transcriptome of the supporting somatic cells should not be underestimated. In this study, I conducted RNA-seq analysis in medaka testis at 1 week after the low dose / low dose rate irradiation to understand how chronic low dose irradiation affects the spermatogenesis in medaka at transcriptomic level.

Meiosis and spermiogenesis processes accelerated after low dose irradiation

It is suggested that ribosome and translation has been significantly down-regulated in the irradiated testis. The detected down-regulation of the translation-related processes is consistent with the understanding that mRNA translation is often suppressed during late

spermatogenesis (Sassone-Corsi, 2002), allowing the spermatocytes maturation without additional protein synthesis. In meiotic spermatocytes and spermatids, most of mRNA translation has been suppressed (Kleene, 2004), letting us to assume that this down-regulation of translation was led by increasing of meiotic spermatocytes, through accelerated spermatogenesis and spermiogenesis processes after the irradiation, which has been reported after high-dose irradiation (Kuwahara et al., 2003). Additionally, KEGG pathway analysis of the up-regulated DEGs after the irradiation supports the acceleration of spermatogenesis and spermiogenesis. Furthermore, KEGG pathways related to Leydig cells and testosterone production were also enriched. The up-regulation of those pathways may further support the notion that the low dose / low dose rate irradiation triggers a compensatory mechanism to boost spermatogenesis and spermiogenesis, likely to remove germ cells with irradiation-induced damaged genome. This hypothesis is supported by the previous histological examination in adult male medaka; type B spermatogonia stopped cell proliferation and entered meiosis ,accelerating spermatogenesis to discard damaged spermatogonia or spermatids in medaka testis (Kuwahara et al., 2002, 2003; Yasuda et al., 2012).

Communication between germ cells and supportive cells were activated after low dose irradiation

In medaka testis, germ cells are supported by surrounding somatic cells called Sertoli cells, which transfer nutrition to spermatogonia and form blood-testis-barrier (BTB), and Leydig cells, which regulate spermatogenesis by secreting testosterone and other related

steroid hormones. This nutrition transfer and communication between the Sertoli cell and the germ cells play a key role in vertebrate spermatogenesis. Several cell adhesion related pathways and GO terms were up-regulated after the the low dose / low dose rate irradiation in this study. These results suggest the irradiation-induced strengthening of communication between the Sertoli cells and the germ cells in medaka after the irradiation. Sertoli cells are critical for spermatogenesis as they supply essential nutrients to developing/differentiating germ cells, regulating the blood-testis barrier and remove apoptotic cell debris and wastes in testis through phagocytosis (Jones & Lopez, 2013; Kretser et al., 2016; Rato et al., 2012, 2012). The increase of the interaction between the Sertoli cells and the germ cells indicated that testicular cells are under external or internal stresses after the low dose / low dose rate irradiation. This result suggests that Sertoli cells are inevitable for the low dose / low dose rate irradiation responses in medaka testis, especially, Sertoli cells are likely to enhance their supportive role by increasing nutrient transfer to the germ cells, reinforcing the blood-testis barrier, and actively participating in the clearance of apoptotic cells during the acceleration of meiosis and spermiogenesis. The enhanced interaction between the Sertoli cells and the germ cells can be a protective mechanism to maintain normal spermatogenesis and to ensure survival of healthy germ stem cells and proper differentiation of germ cells under the irradiation stress.

Metabolic and power production activities were suppressed in testis after low dose irradiation

It is reported that metabolic down-regulation is a common response to radiation exposure,

as cells shift their energy and resources focus toward DNA repairing and survival (Tang et al., 2018). In this study, I found that several metabolic pathways were down-regulated in response to the low dose / low dose rate irradiation. KEGG pathway analysis picked up and enriched several metabolic pathways in the down-regulated DEGs, suggesting the suppression of energy-producing activities in cells and GO terms and KEGG pathways related to oxidative phosphorylation and pentose phosphate pathway were enriched from the down-regulated DEGs after the irradiation. This finding suggests a reduction in energy production in the irradiated testis, which may be explained as an adaptive response to conserve resources under stress. On the other hand, an acceleration of spermatogenesis and spermiogenesis was also observed following low dose / low dose rate irradiation in medaka testis (Nakazawa, 2020) and large amount of adenosine triphosphate (ATP) is necessary to support this process (Cao et al., 2024; Yu et al., 2019). This controversy implies that the irradiation-induced accelerated spermatogenesis or spermiogenesis can be different process from the normal spermatogenesis which aims to produce healthy fertile sperms.

Immune response and inflammatory were activated in testis after low dose irradiation

Testis is an immune-privileged organ (Fijak et al., 2017): immune response is regulated to prevent germ cells from autoimmune attack, however, testis is also capable of providing effective immune responses (Washburn et al., 2022). Several immune response related KEGG pathways were picked up from the up-regulated DEGs after the irradiation.

The enriched GO terms strongly suggest that the low dose / low dose rate irradiation might activate immune responses and inflammatory in medaka testis and this finding is consistent with the previous reports of radiation-induced immune activation in mouse, where low dose irradiation stimulates immune cells and promotes clearance of damaged cells (Sharplin & Franko, 1989). The other previous study has revealed that medaka launched in the orbit experiments exhibit the increase in expression of genes related to systemic inflammation and immune responses (Murata et al., 2015), however, the expressions of same immune-related genes mentioned in the space medaka experiment were not found in the DEGs and not altered after the low dose / low dose rate irradiation in my study. Immune responses might be activated in the irradiated testis to ensure the progress of spermatogenesis under the low dose / low dose rate irradiation exposure and GO term of “MHC class II protein complex” and “Calcium” might play a key role in this process. In addition, inflammatory responses influenced by low dose / low dose rate irradiation studied in mouse revealed that low dose / low dose rate irradiation can inhibit inflammatory responses under appropriate conditions, either by reducing pro-inflammatory responses (Mathias et al., 2015) or increasing anti-inflammatory effects (Ebrahimian et al., 2017).

Calcium regulated activities were activated after low dose irradiation

Calcium ions is known to be crucially functional in various stages of spermatogenetic process, including regulating the proliferation and differentiation of spermatogonia (Golpour et al., 2017; Treviño et al., 1998), maturation of spermatozoa (Dadras et al.,

2019; Krasznai et al., 2000; Niksirat & Kouba, 2016) and acrosome reaction (Blas et al., 2002). In addition, calcium ion also crucial for testicular somatic cells, supporting testosterone production in Leydig cells (Costa et al., 2010) and the functions of Sertoli cells (Auzanneau et al., 2006; Gorczynska & Handelsman, 1991), as well as regulating energy metabolism in testis (Herrera et al., 2000). In this study, GO term: “calcium ion binding (MF)”, “calcium ion transmembrane transporter activity (MF)”, “calcium ion transport (BP)”, as well as “ola04020: Calcium signaling pathway” and “ola04270: Vascular smooth muscle contraction” were enriched from the up-regulated DEGs in the medaka testis after the low dose / low dose rate irradiation. The up-regulation of the calcium-related GO terms and KEGG pathways suggests that calcium-regulated activities were significantly enhanced following the low dose / low dose rate irradiation in the medaka testis, which further suggests that spermatogenesis or/and supporting testicular somatic cell functions were promoted following the low dose / low dose rate irradiation. Although both spermatogenesis and supportive testicular somatic cell responses were confirmed by the other GO terms and KEGG pathways enriched in the up-regulated DEGs after the irradiation, further understanding of irradiation-induced calcium-related response in testis is difficult due to the limitation of bulk RNA-seq technique. Further investigation with much higher resolution, such as single cell RNA-seq is needed to separate the irradiation response from germ cells and testicular somatic cells. Finally, as shown later in both male and female whole-body analysis, calcium signalling pathway was found down-regulated after the low dose / low dose rate irradiation, which suggests that the up-regulated calcium related activity observed in the testis after the irradiation might be testis-specific.

These findings underscore the ability of medaka testis to adapt to low dose / low dose rate irradiation through a multifaceted response that balances immune activation, metabolic regulation, sex-hormone homeostasis, as well as an abnormal acceleration of spermatogenesis. While irradiation induces stress, the testis appears to activate defense mechanisms that reduce irradiation induced damage and promote recovery, ensuring the continued production of fertile and healthy sperm. However, bulk RNA-seq has limitations, different cell types in the tissue might have different or even opposite response against certain stimulus, and these differences might become obscured in bulk RNA-seq results. Testis seems to be a suitable candidate for this issue, with a serial of differentiating spermatogenetic cells and unique supporting somatic cells, which interests us to investigate the irradiation response under a higher resolution. Thus, I decided to analysis testis after the irradiation with single cell RNA-seq in the next chapter.

Transcriptome Analysis of Medaka Ovary After 1 Week of Low Dose Irradiation

Radiation is known to significantly effects on rapidly dividing cells, making the male reproductive system particularly sensitive to its impact. In the female ovaries, the development and maturation of oocytes, which occur in carefully regulated stages, also can be disrupted by irradiation. Studies in mammals indicated that radiosensitivity of oocyte vary greatly depending on the stage and species of the follicles/oocytes (Adriaens et al., 2009). It is also reported that low dose irradiation can cause drastic loss of primordial follicles in mouse and Ca^{2+} oscillations in the irradiated oocytes at the time of fertilization was disrupted, indicating the qualitative deterioration of oocytes after irradiation (Pesty et al., 2010). To explore how chronic low dose /low dose rate irradiation

affects the ovarian transcriptome, RNA-seq analysis was conducted on medaka ovaries one week after the low dose / low dose rate irradiation.

Metabolic activity was suppressed after low dose irradiation

The significant impacts of the low dose / low dose rate irradiation on the metabolic and steroidogenic activities in the medaka ovary were detected. *ola01100*: Metabolic pathways were enriched from the down-regulated DEGs after the irradiation (Table 8). Carbon metabolism related pathways were enriched, suggesting a reduction in energy metabolism and a suppression of ovarian activities. The suppression of metabolic pathways, particularly those related to carbon metabolism, suggests a reduced energy demand, which may reflect an overall decrease in ovarian activity, especially in oogenesis which is an energy-needed process. After the irradiation, cells in the ovary may undergo metabolic shifts to conserve energy and manage oxidative stress, which would be adaptive responses aiming to enhance cell survival after the irradiation (Tang et al., 2018).

Steroid hormone biosynthesis was interrupted by low dose irradiation

In this study, I found that several GO terms and KEGG pathways related to lipid and steroid hormone metabolism were enriched in the down-regulated DEGs after the low dose / low dose rate irradiation. Moreover, cytochrome P450 family genes, which play important roles in steroid hormone synthesis and metabolism in ovary, were also notably down-regulated. These findings strongly suggest that steroid hormone synthesis was suppressed not only by lipid deficiency as discussed later, but also by inhibition of

cytochrome P450 family activities.

The down-regulation of biosynthesis of steroid hormones and the inhibition of cytochrome P450 family genes indicated that the chronic low dose / low dose rate irradiation can clearly affect ovary steroidogenic activities. Since the cytochrome P450 enzymes are central to the synthesis of steroid hormones, their inhibition might lead to a disruption in the hormone balance, affecting normal oogenesis and reproductive function in female (Tsuchiya et al., 2005).

Hyaluronic acid binding activity was slightly promoted after low dose irradiation

Glycosaminoglycan related GO term (“glycosaminoglycan binding”) and KEGG pathways (ola00532: Glycosaminoglycan biosynthesis - chondroitin sulfate / dermatan sulfate) were enriched from the up-regulated DEGs after the irradiation in the ovary and was also up-regulated. Another two GO terms (“positive regulation of neuroblast proliferation” and “perineuronal net”) were enriched from the up-regulated DEGs and I found that these three GOs contain the same three genes, which are ENSORLG00000029206 (*hapln1a*), ENSORLG00000001551 (*acanb*; aggrecan b) and ENSORLG00000000100 (*ACAN*; aggrecan;). Both *hapln1a* and *aggrecan* are predicted to have hyaluronic acid binding activity (Kiani et al., 2002). The up-regulation of hyaluronic acid binding activity could represent a compensatory mechanism which aims to maintain extracellular matrix integrity and to support germ cell survival in the irradiated environment in the ovary, since glycosaminoglycans are widely critical for cell signaling and tissue repair (Casale & Crane, 2024).

These findings suggest that low-dose / low dose rate irradiation leads to a complex reprogramming of ovarian function, characterized by the down-regulation of key metabolic and steroidogenic pathways, possibly to conserve energy and protect ovarian tissue. However, the suppression of steroid hormone synthesis can cause significant risks to reproductive activity, emphasizing the need for further study of the long-term effects of low-dose / low dose rate irradiation on vertebrate ovarian function.

Transcriptome Analysis of Medaka Whole body After 1 Week of Low Dose Irradiation

By the RNA-seq analysis of the irradiation-sensitive tissues in this study, I have provided insights into the tissue-specific responses, allowing for a focused examination of tissue-specific responses in gene expression after the low dose / low dose rate irradiation.

However, this approach has limitations, as interactions and systemic effects across the whole organism were overlooked. On the other hand, whole-body sequencing might offer a universal view of the biological response against the irradiation, capturing the complex interplay between organs and tissues. While this method provides a broader perspective, it also would obscure specific organ-level changes.

Lipid metabolism is disrupted after 1 week of low dose / low dose rate gamma-ray irradiation

The interpretation of the KEGG pathway for “fatty acid metabolism” revealed that the catabolic process of fatty acids shorter than C16 in mitochondria is up-regulated, while the opposite process, the synthesis process stays unchanged (Figure 9). C16 and C18 fatty acids are the most common fatty acids in vertebrates, including fish, stored as fat in the form of triglycerides, and served as an energy source for cellular functions through hydrolysis. Among freshwater fish, palmitic acid (C16) is the most prevalent fatty acid within triglycerides, the level of palmitoleic acid has been characterized as a distinctive feature of freshwater fish (Ackman, 1967; Pyz-Łukasik & Kowalczyk-Pecka, 2017). Therefore, the up-regulation of C16 fatty acid (palmitic acid) catabolism observed in medaka after the irradiation suggests that the medaka might be under an energy deficiency following the irradiation. Consequently, it can be hypothesized that medaka was facing an energy-deficiency after the irradiation, leading to the up-regulation of stored body fat utilization to compensate for the energy deficit.

C16 and C18 fatty acids are also key components in the synthesis of long-chain fatty acids. The long-chain fatty acid synthesis pathway starting from C16 was up-regulated in whole-body tissues following the irradiation. Specifically, the up-regulation of unsaturated fatty acid synthesis was observed. Unsaturated fatty acids play the critical role in many physiological functions, including neuroprotection, antioxidant activity, anti-inflammatory effects, and cardiovascular health (Subirade & Chen, 2008). It is reported that unsaturated fatty acids such as omega-3 fatty acids can prevent inflammatory

reactions induced under oxidative stress (Corteselli et al., 2020). Those components may serve as a protective role against immune responses following the irradiation. It is reported that the biosynthesis of docosahexaenoic acid (DHA), an omega-3 fatty acid which is important for maintaining fish health, is connected to the expression of *fads2* (Ishikawa et al., 2019). In the shared DEG list of male and female whole-body tissue, 3 isoforms of *fads2* were found up-regulated after the irradiation, which confirmed the result that unsaturated fatty acid biosynthesis was up-regulated after the irradiation and DHA might be a main product of this process.

Moreover, reactive oxygen species (ROS) produced by low dose / low dose rate irradiation oxidizes unsaturated fatty acids which maintain membrane fluidity and function, and leads to oxidative degradation and even the formation of harmful lipid peroxides, called lipid radicals. β -oxidation of long-chain fatty acids, in addition to the peroxisome proliferation, was up-regulated after the irradiation, and these peroxisomal processes were likely involved in the catabolism of oxidatively damaged lipids. Meanwhile, increase in long-chain fatty acids synthesis may improve and maintain membrane physiological functions by replacing oxidized lipids with newly synthesized lipids.

Lipid synthesis requires energy and NADPH, and further the oxidation of long-chain fatty acids in peroxisomes producing H_2O_2 , which strengthens oxidative stresses. The "Peroxisome" pathway was up-regulated in the irradiated medaka, suggesting enhanced peroxisomal activity and peroxisome proliferation. Peroxisomes are essential organelles involved in lipid metabolism in eukaryotic cells. While medium- and long-chain fatty acids (FAs) are primarily oxidized in mitochondria, very-long-chain fatty acids (VLCFAs)

are mainly metabolized through β -oxidation in peroxisomes (Wanders, 2014). The key enzyme for this process is acyl-CoA oxidase 1 (ACOX1), which converts acyl-CoAs into 2-trans-enoyl-CoAs, generating hydrogen peroxide (H_2O_2) and contributing up to 35% of the total H_2O_2 production in mammalian tissues (Boveris et al., 1972). The up-regulations of ACOX1 and β -oxidation after the irradiation were also confirmed in the KEGG pathway analysis in this study (Figure 10). This additional oxidative stress from peroxisomal fatty acid oxidation might further strengthen the oxidative stress that had been caused by the low dose / low dose rate irradiation. These phenomena could explain why lipid metabolism does not fully recover even one week after the irradiation.

In addition, up-regulation of pex11, which is critical for peroxisome division (Honsho et al., 2016), was also confirmed in the KEGG pathway analysis (Figure 10). Over activation of peroxisome β -oxidation will lead to lipid metabolism disorder, with increase in free fatty acids and overload of liver function (Duszka et al., 2020). In addition, researches have proved that VLCFA and BCFA promote transcription and expression of peroxisome through PPAR α (Lamichane et al., 2018; Tahri-Joutey et al., 2021). The up-regulation of “PPAR signaling pathway” (Figure 11), as well as “long chain fatty acids biosynthesis” was confirmed in both male and female medaka after the irradiation, which strongly suggest that PPAR signaling pathway might play a key role in this lipid metabolism disorder that I found after the low dose / low dose rate irradiation.

Also, the up-regulations of cholesterol synthesis, catabolism, and subsequent synthesis of cholesterol hormones were observed after the irradiation. Cholesterol homeostasis in vertebrate body is maintained primarily through three pathways: *de novo* synthesis via the mevalonate pathway, absorption through LDL, and cholesterol catabolism via the bile

acid synthesis pathway. I have found that CEL (carboxyl ester lipase) was down-regulated in the intestines and even in the ovaries after one week of the irradiation exposure as mentioned above. This suggests that the primary source of cholesterol in adult medaka body comes from *de novo* synthesis rather than intestinal absorption, and that cholesterol uptake might be reduced in some tissues after the irradiation. Regarding cholesterol catabolism, CYP8B1 and LXR α , both involved in cholesterol metabolism through the PPAR signaling pathway, were up-regulated in the irradiated medaka. CYP8B1 is a key enzyme in the synthesis of primary bile acids from cholesterol, and LXR α also plays an important regulatory role in this process. The GO term of “Primary bile acid synthesis” was also up-regulated following the low dose / low dose rate irradiation, suggesting that excess cholesterol might be produced in the irradiated medaka body, and the bile acid synthesis pathway might be activated as a result of the accumulated cholesterol to reduce it and to maintain cholesterol homeostasis in the medaka body.

Finally, cholesterol is also a crucial precursor for steroid hormones and vitamins, and related pathways were also up-regulated in whole-body scale after the irradiation. Steroids and steroid hormones are the crucial components of cellular membranes and signaling molecules for various physiological functions (Olunkwa et al., 2023). Notably, the cortisol degradation pathway was up-regulated following the irradiation (Figure 12). Cortisol is a key marker of stress in vertebrates, also in fish, and is more indicative of acute stress than chronic stress (Sadoul & Geffroy, 2019). The up-regulation of cortisol-related genes is an expectable response to the low dose / low dose rate irradiation, where the up-regulation was detected in the degradation pathway rather than in the synthesis pathway of the cortisol. It can be hypothesized that after one week of irradiation, stress

level represented by cortisol level gradually decreases, and normal hormone levels are restored through the breakdown of excess cortisol. Although the biosynthesis of sex hormones in steroid hormone synthesis pathway was enriched from the up-regulated DEGs after the irradiation, almost all of the up-regulated reactions were catalyzed by the same enzyme which also functions in bile acid synthesis pathway. As mentioned before, even though the Leydig cells were activated in the irradiated testis, noticeable alteration in sex hormone production was not observed in neither the testis nor ovaries after the irradiation. Thus, the impact of low dose / low dose rate irradiation on sex hormone biosynthesis remains to be questionable. As for vitamins, obvious alteration of biosynthesis of vitamins were not found, however, absorption of fat-soluble vitamins like cholecalciferol (vitamin D) or menadione (Vitamin K) might be affected by the change of cholesterol metabolism after the irradiation.

Immune response is activated after 1 week of low dose / low dose rate gamma-ray irradiation

Besides the lipid-related changes, some immune responses were also activated after the low dose / low dose rate irradiation. The enrichment of the GO terms related to immune response and KEGG pathway “Phagosome” in the up-regulated DEGs strongly suggests that immune response remained activated in whole-body scale even 1 week after the irradiation. In addition, the up-regulation of the “Biosynthesis of Unsaturated Fatty Acids”, "alpha-Linolenic Acid Metabolism" and "Linolenic Acid Metabolism" pathways point to the metabolism of omega-3 fatty acids, which is important for anti-inflammatory

processes. It was revealed that 100 mGy gamma-ray irradiation can trigger immune response at a whole-body scale and biosynthesis of anti-inflammatory fatty acids was promoted in the irradiated medaka. This result is consistent with the report of the medaka reared in International Space Station, that genes related to inflammatory responses and stress responses are up-regulated in whole-body scale (Murata et al., 2015). However, only a few immune-related genes mentioned in that report were found in the list of the up-regulated DEGs after the low dose / low dose rate irradiation in this study. It is well known that low dose or low dose rate irradiation induces oxidative stress that can cause chronic inflammatory disease. In contrast, some other studies reported that inflammatory responses can be suppressed by low dose rate irradiation (Ebrahimian et al., 2017; Mathias et al., 2015). This controversy clearly indicates the complexity of regulation of the immune system and the impacts of low dose / low dose rate irradiation. In this study, the typical genes related to “strong” immune response were not significantly activated in the irradiated medaka and it is assumed that the medaka had recovered from the irradiation-induced inflammatory at 1 week after the low dose / low dose rate irradiation, or irradiated dose (100 mGy) was not enough to induce server inflammatory in the medaka. Even though the histological examinations also did not find any sign of activated immune system (Nakazawa, 2020), findings in this study indicate that the impacts of low dose / low dose rate irradiation on vertebrates are present and cannot be ignored.

To summary this chapter, bulk RNA-seq was performed on both tissues and whole-body of medaka, serval responses after the irradiation were observed though comparison of non-irradiated and irradiated expression profiles. With the power of NGS techniques, this study not only confirmed several irradiation responses previously observed through

physiological experiments but also uncovered subtle changes that had not been detected under same condition before. These findings highlight the sensitivity of molecular analyses in capturing subtle biological responses, offering deeper insights into the mechanisms underlying irradiation effects that might have been overlooked in traditional experiments. However, tissue-level RNA-seq has its limitations, as it may not effectively capture the heterogeneity within tissues. When performing RNA-seq on whole tissues, tissue-specific changes can be masked, different cell types within the tissue may also exhibit distinct or even opposing responses. To further investigate irradiation responses in medaka, I plan to employ single-cell RNA-seq, a technique with higher resolution, for analysis. This approach will provide a clearer understanding of the various cell types within the tissue and their specific responses to irradiation. Among the medaka tissues discussed in Chapter 1, I have chosen the testis, a tissue characterized by significant cellular diversity and complex responses, as the focus of the next chapter of this study. Expression profiles of male germ cells and their responses to irradiation in medaka testis will be discussed in the next chapter.

Figures and Tables

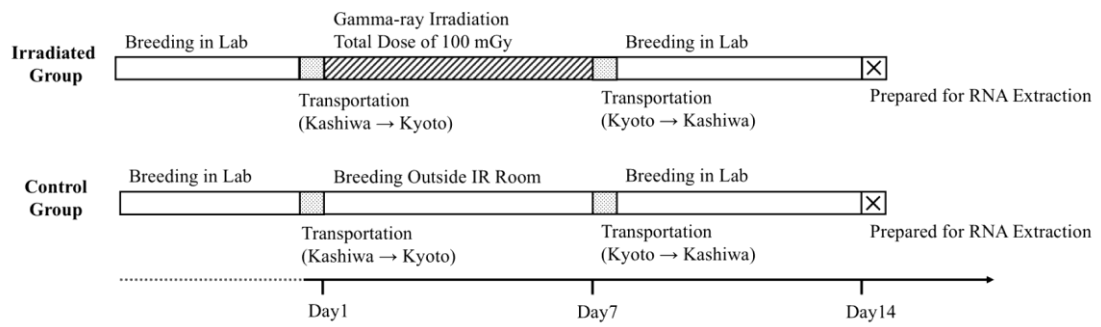
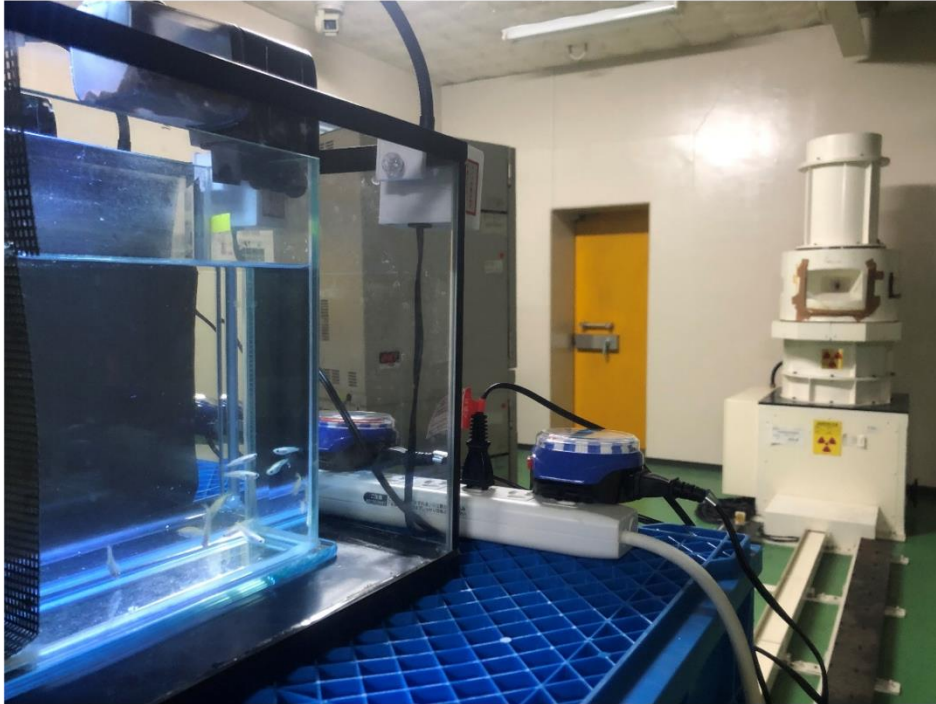


Figure 1. Experiment Schedule of low dose irradiation experiment in Radiation Research Center at Kyoto University.

(A)



(B)

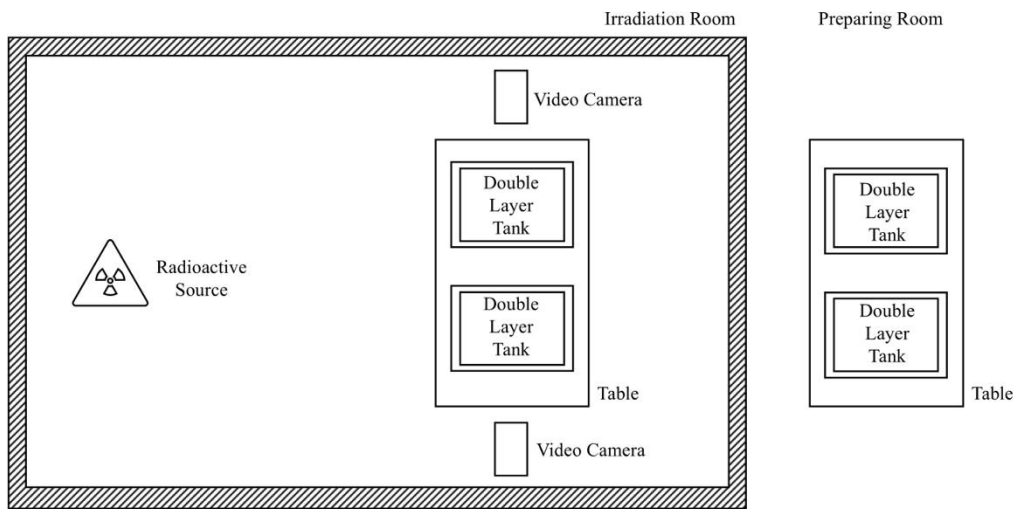
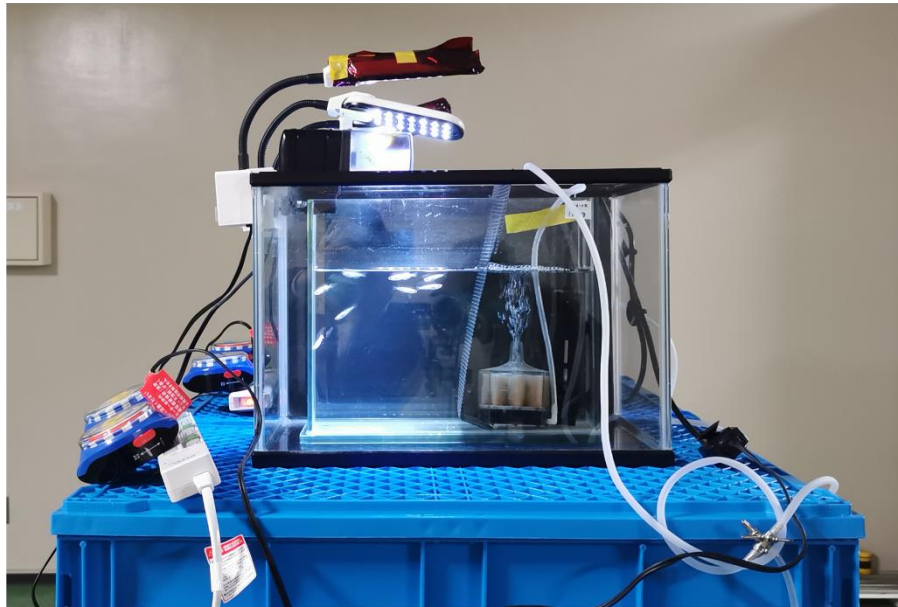


Figure 2. Equipment settings of low dose irradiation experiment in Radiation Research Center at Kyoto University. (A) Photography of equipment settings; (B) Illustration of equipment settings.

(A)



(B)

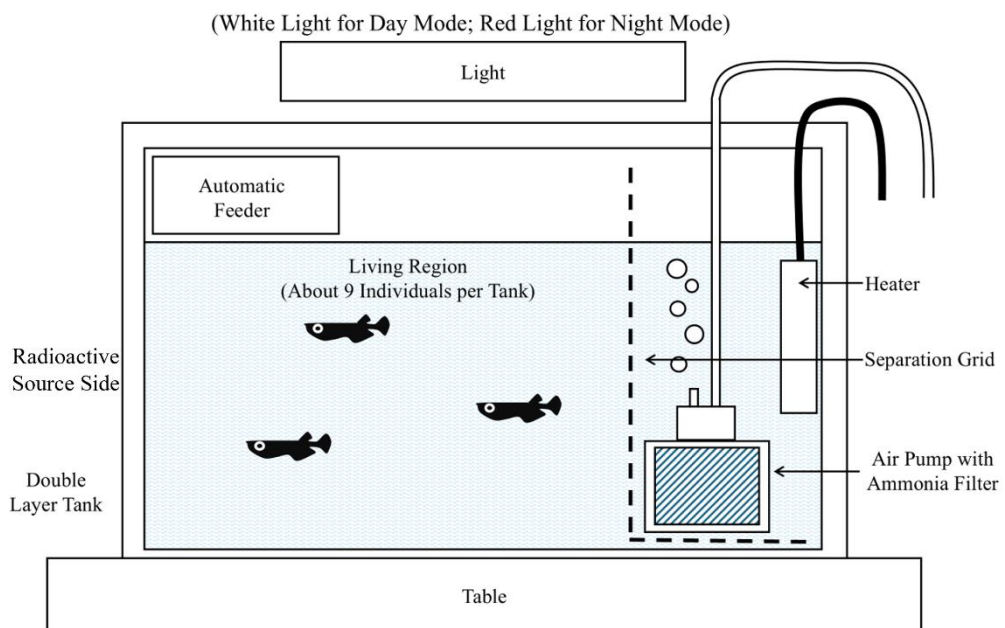


Figure 3. Breeding settings during low dose irradiation experiment in Radiation Research Center at Kyoto University. (A) Photography of breeding settings; (B) Illustration of breeding settings.

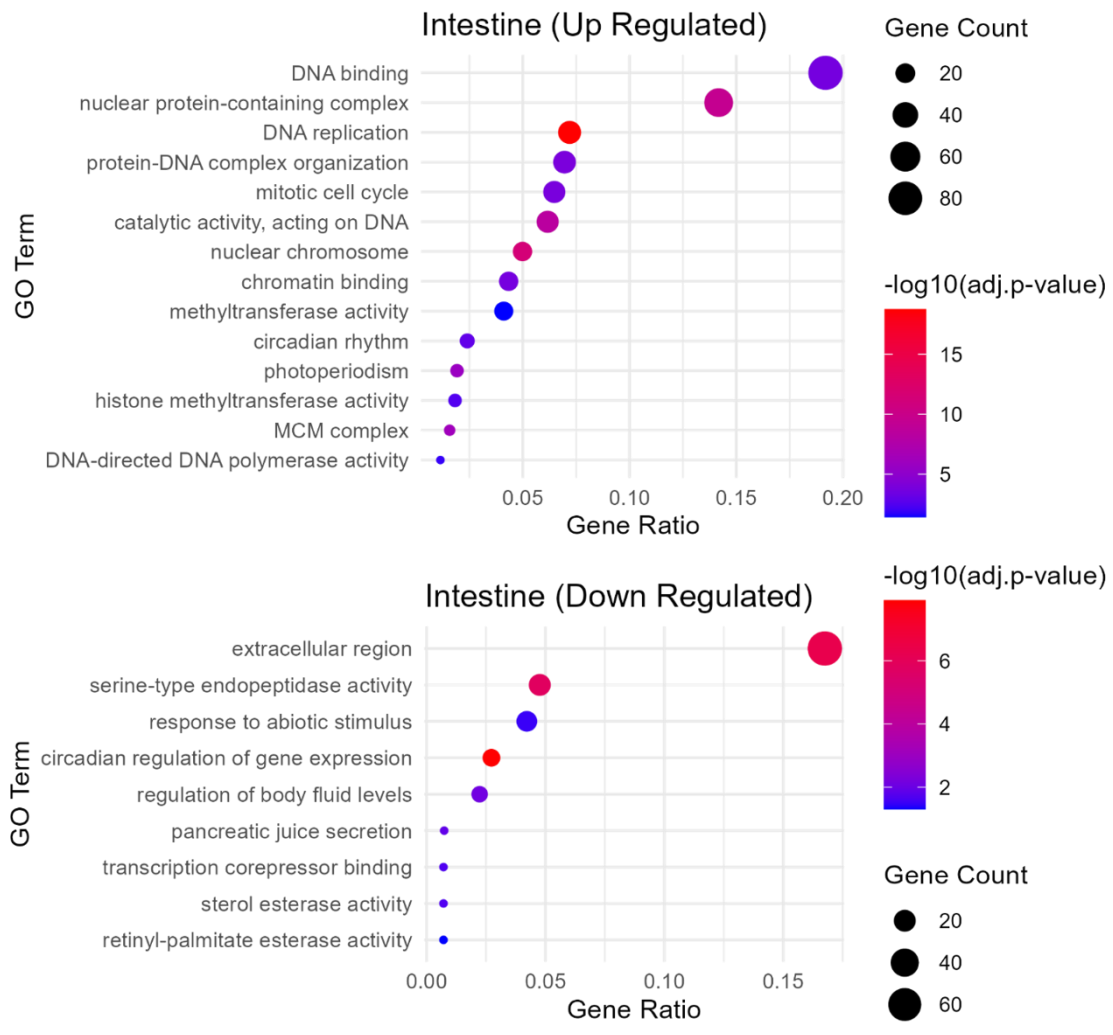


Figure 4. Dot plot of GO terms enriched from up- and down-regulated DEGs after the irradiation of medaka intestine.

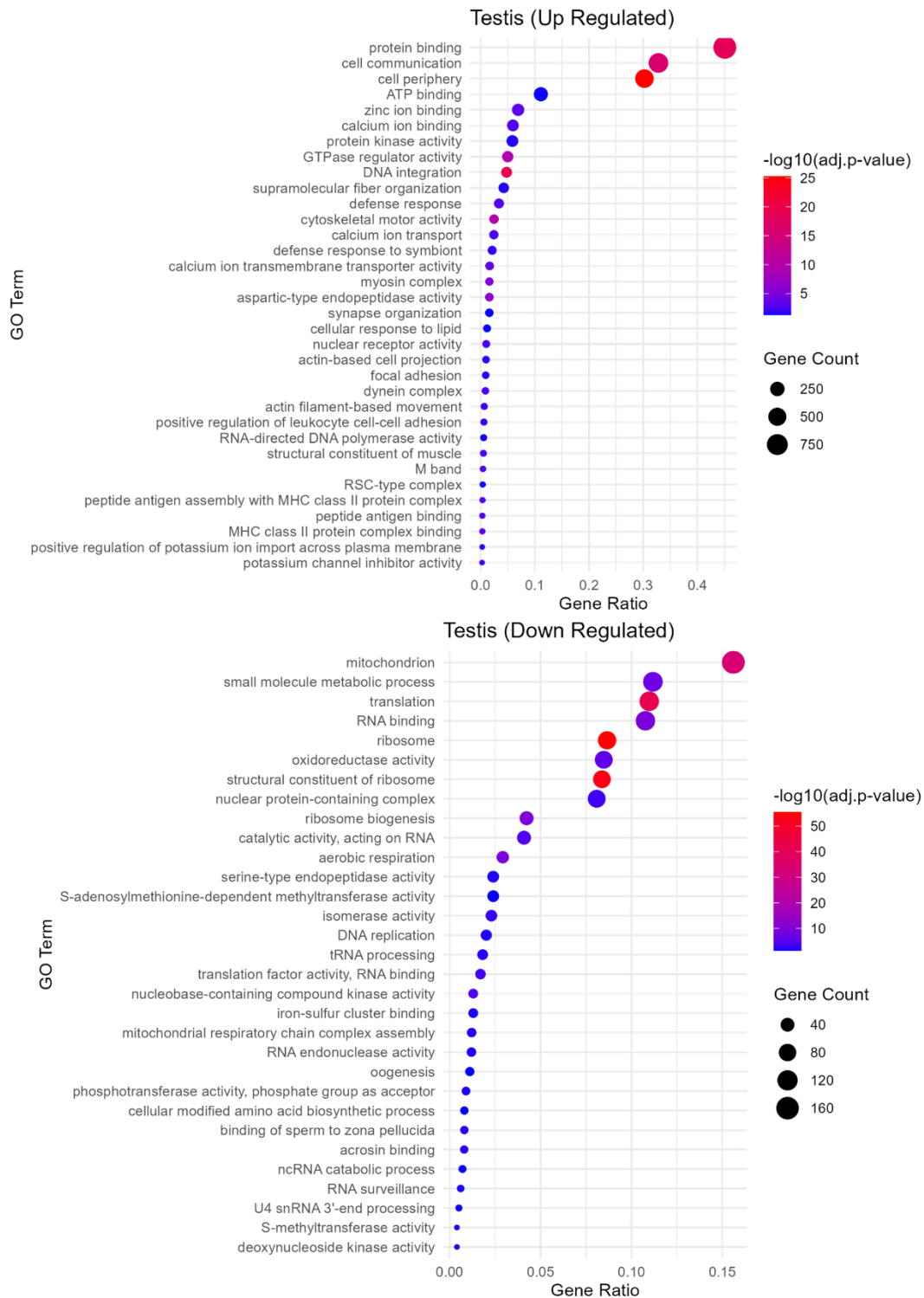


Figure 5. Dot plot of GO terms enriched from up- and down-regulated DEGs after ldr from medaka testis.



Figure 6. Dot plot of GO terms enriched from up- and down-regulated DEGs after ldr from medaka ovary.

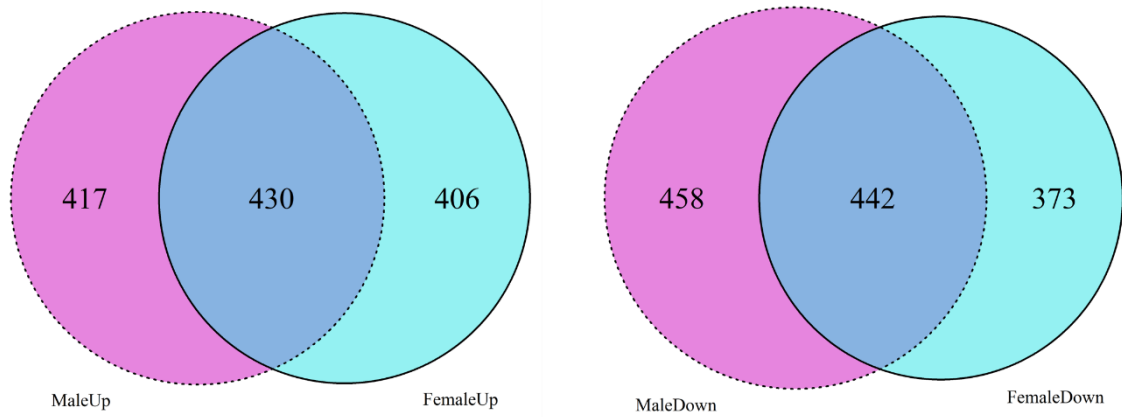


Figure 7. DEGs shared in male and female. MaleUp: DEGs up-regulated after the irradiation in male medaka; FemaleUp: DEGs up-regulated after the irradiation in female medaka; MaleDown: DEGs down-regulated after the irradiation in male medaka; FemaleDown: DEGs down-regulated after the irradiation in female medaka.



Figure 8. Dot plot of GO terms enriched from up- and down-regulated DEGs shared in male and female after the irradiation.

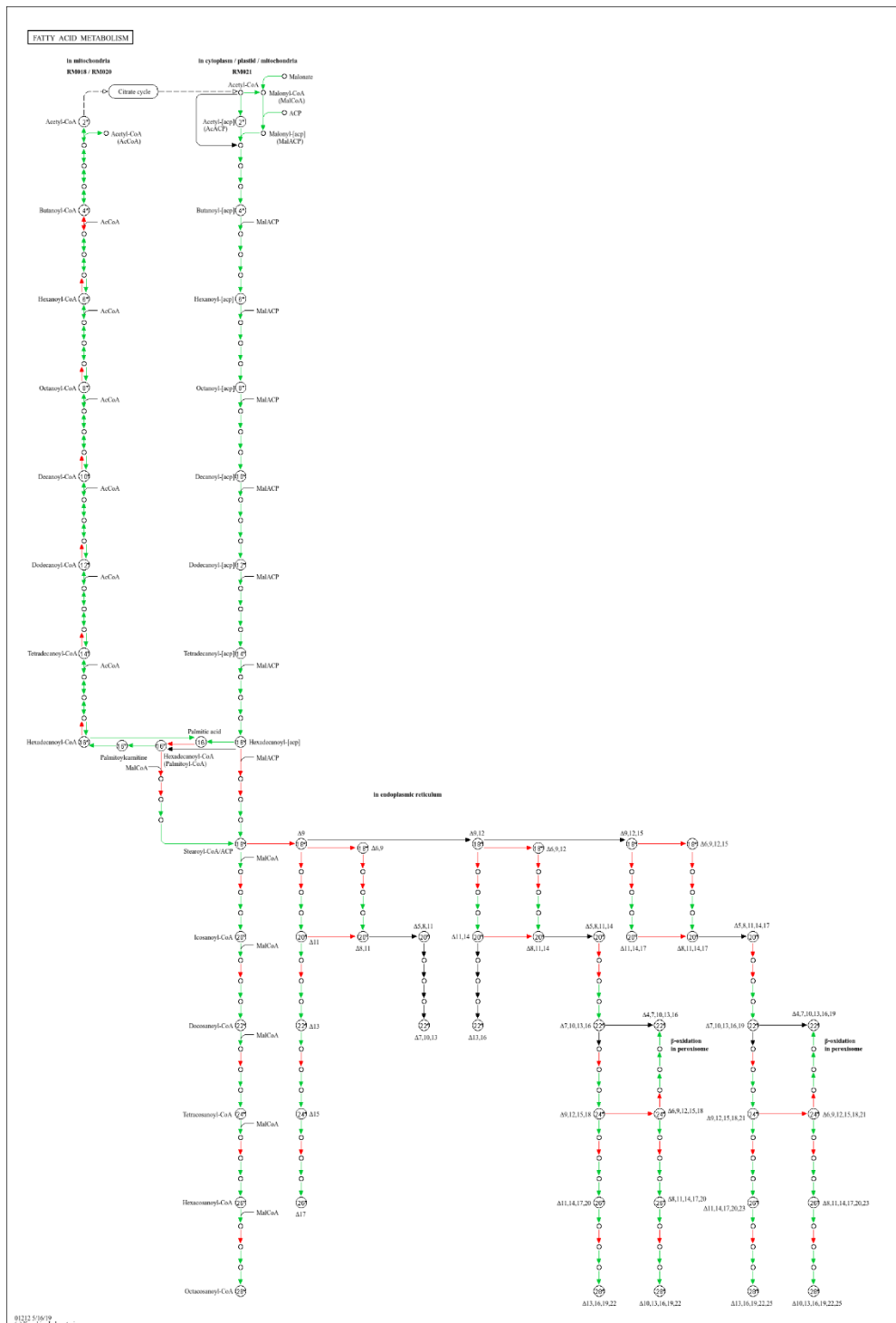


Figure 9. KEGG pathway of “Fatty Acid Metabolism”. Pathways up-regulated after the irradiation in both male and female whole-body are shown by red arrows.

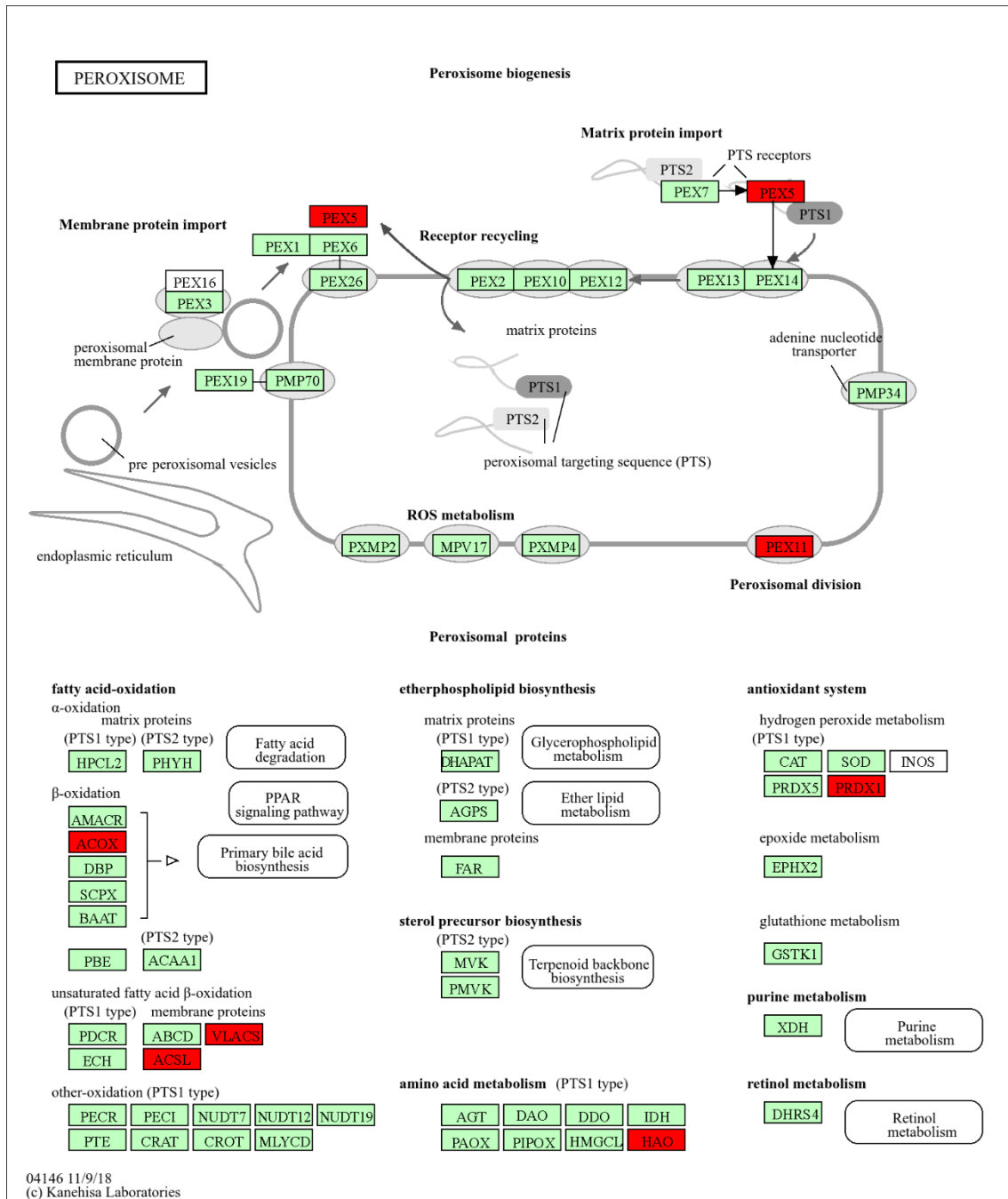


Figure 10. KEGG pathway of “Peroxisome”. Pathways up-regulated after the irradiation in both male and female whole-body are shown in red

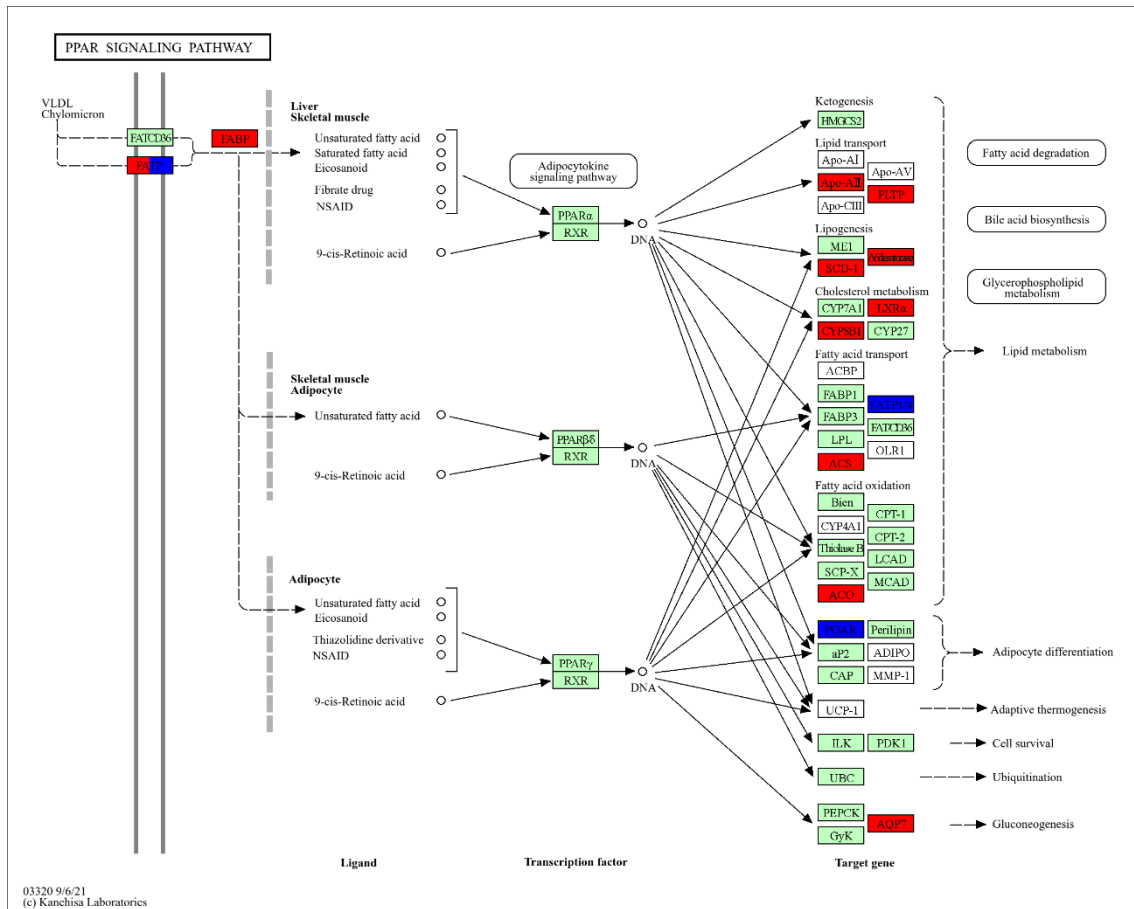


Figure 11. KEGG pathway of “PPAR signaling pathway”. Pathways up-regulated after the irradiation in both male and female whole-body are shown in red; down-regulated are shown in blue.

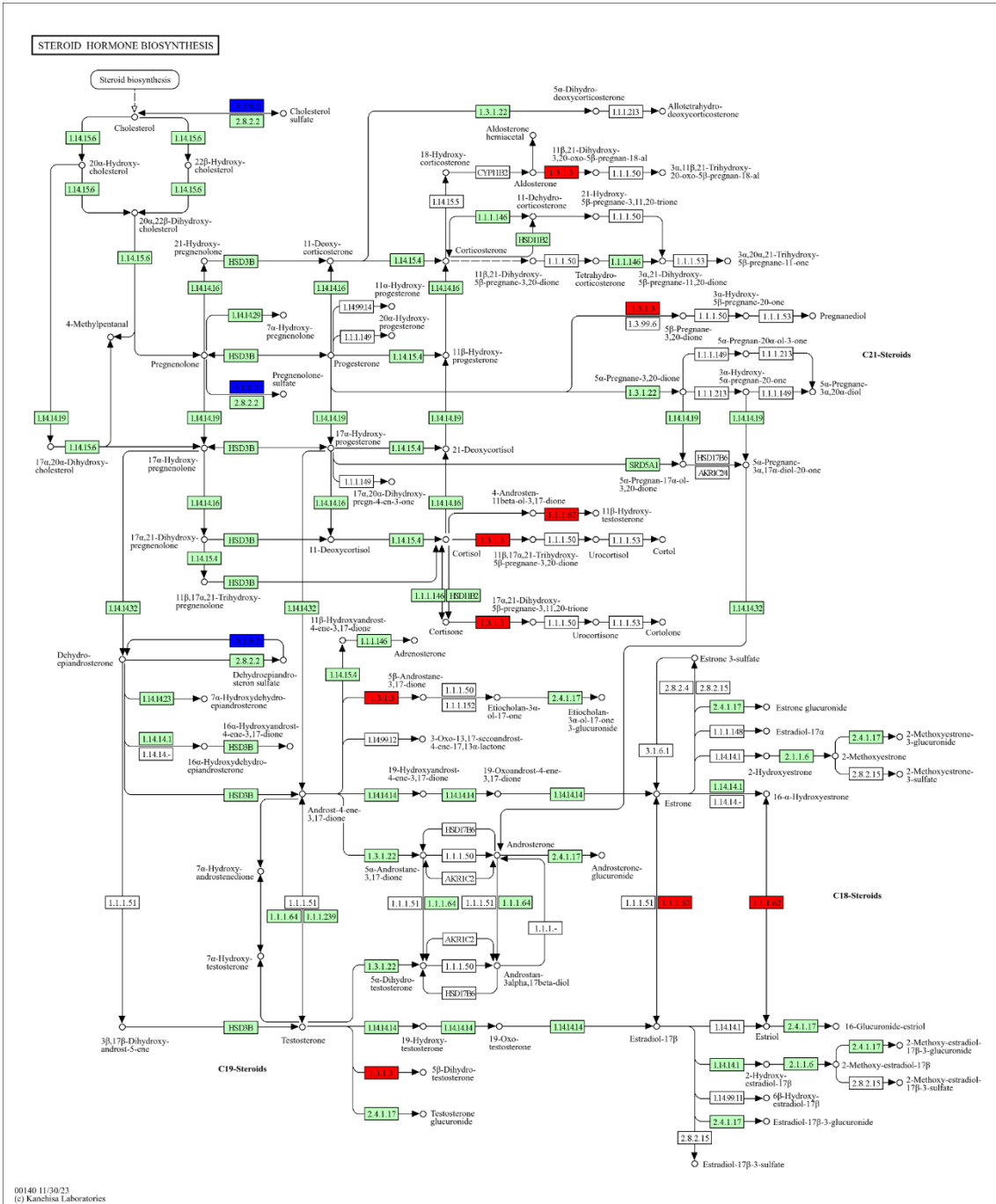


Figure 12. KEGG pathway of “Steroid Hormone Biosynthesis”. Pathways up-regulated after the irradiation in both male and female whole-body are shown in red; down-regulated are shown in blue.

Table 1. Samplelist

| Sample Name | Treatment | Gender | N | Tissue | Read length (bp) | Sampling Date |
|--------------------|-----------|--------|---|------------|------------------|---------------|
| c_f_mus_201910 | Control | Female | 6 | Muscle | 100 | 2019.10 |
| c_f_201910_1 | Control | Female | 3 | Whole-body | 100 | 2019.10 |
| c_f_201910_2 | Control | Female | 3 | Whole-body | 100 | 2019.10 |
| c_m_mus_201910 | Control | Male | 6 | Muscle | 100 | 2019.10 |
| c_m_201910_1 | Control | Male | 3 | Whole-body | 100 | 2019.10 |
| c_m_201910_2 | Control | Male | 3 | Whole-body | 100 | 2019.10 |
| ldr_f_mus_201910 | 100mGy IR | Female | 6 | Muscle | 100 | 2019.10 |
| ldr_f_201910 | 100mGy IR | Female | 3 | Whole-body | 100 | 2019.10 |
| ldr_m_mus_201910 | 100mGy IR | Male | 6 | Muscle | 100 | 2019.10 |
| ldr_m_201910_1 | 100mGy IR | Male | 3 | Whole-body | 100 | 2019.10 |
| ldr_m_201910_2 | 100mGy IR | Male | 3 | Whole-body | 100 | 2019.10 |
| c_int_201903 | Control | Male | 6 | Intestine | 100 | 2019.03 |
| c_ova_201903 | Control | Female | 6 | Ovary | 100 | 2019.03 |
| c_tes_201903 | Control | Male | 6 | Testis | 100 | 2019.03 |
| ldr_int_201903 | 100mGy IR | Male | 6 | Intestine | 100 | 2019.03 |
| ldr_ova_201903 | 100mGy IR | Female | 6 | Ovary | 100 | 2019.03 |
| ldr_tes_201903 | 100mGy IR | Male | 6 | Testis | 100 | 2019.03 |
| c_tes_202111_1 | Control | Male | 6 | Testis | 50 | 2021.11 |
| c_m_mus_202111_1 | Control | Male | 6 | Muscle | 50 | 2021.11 |
| c_int_202111_1 | Control | Male | 6 | Intestine | 50 | 2021.11 |
| ldr_tes_202111_1 | 100mGy IR | Male | 6 | Testis | 50 | 2021.11 |
| ldr_m_mus_202111_1 | 100mGy IR | Male | 6 | Muscle | 50 | 2021.11 |
| c_f_202111_1_1 | Control | Female | 3 | Whole-body | 100 | 2021.11 |
| c_f_202111_2_1 | Control | Female | 3 | Whole-body | 100 | 2021.11 |
| c_m_202111_1 | Control | Male | 3 | Whole-body | 100 | 2021.11 |
| ldr_f_202111_1_1 | 100mGy IR | Female | 3 | Whole-body | 100 | 2021.11 |
| ldr_f_202111_2_1 | 100mGy IR | Female | 3 | Whole-body | 100 | 2021.11 |
| ldr_m_202111_1 | 100mGy IR | Male | 3 | Whole-body | 100 | 2021.11 |
| ldr_int_201111_1 | 100mGy IR | Male | 6 | Intestine | 100 | 2021.11 |

Table 2. KEGG pathway analysis of upregulated DEGs from intestine after irradiation

| Term | Count | PValue |
|---|-------|----------|
| DNA replication | 19 | 2.81E-20 |
| Homologous recombination | 10 | 2.86E-07 |
| Mismatch repair | 8 | 6.75E-07 |
| Nucleotide excision repair | 9 | 6.03E-05 |
| Fanconi anemia pathway | 8 | 2.06E-04 |
| Cell cycle | 14 | 2.69E-04 |
| Base excision repair | 7 | 9.91E-04 |
| Glyoxylate and dicarboxylate metabolism | 4 | 5.69E-02 |
| Pyrimidine metabolism | 5 | 6.52E-02 |
| Fatty acid biosynthesis | 3 | 8.07E-02 |
| Peroxisome | 6 | 8.35E-02 |
| Purine metabolism | 8 | 9.34E-02 |
| Nucleotide metabolism | 6 | 9.51E-02 |
| Alanine, aspartate and glutamate metabolism | 4 | 9.55E-02 |
| Lysine degradation | 5 | 9.89E-02 |

Table 3. KEGG pathway analysis of downregulated DEGs from intestine after irradiation

| Term | Count | PValue |
|--|-------|----------|
| Arginine and proline metabolism | 7 | 1.66E-03 |
| FoxO signaling pathway | 12 | 3.49E-03 |
| Cysteine and methionine metabolism | 7 | 3.96E-03 |
| Glycine, serine and threonine metabolism | 6 | 5.86E-03 |
| p53 signaling pathway | 8 | 6.85E-03 |
| Cell cycle | 11 | 9.03E-03 |
| Metabolic pathways | 55 | 1.74E-02 |
| Steroid biosynthesis | 4 | 1.85E-02 |
| Neuroactive ligand-receptor interaction | 20 | 4.48E-02 |
| Glycerolipid metabolism | 5 | 9.16E-02 |

Table 4. Cell cycle related genes in KEGG pathway ola04110:Cell cycle enriched from medaka intestine DEGs

| Ensembl ID | Gene symbol | Function | Reference | Regulation after ldr |
|--------------------|-------------|---|------------------------------|----------------------|
| ENSORLG00000011329 | mcm6 | S | Simon et al., 2014 | Up |
| ENSORLG00000015908 | orc5 | S | Loo et al., 1995 | Up |
| ENSORLG00000010517 | mcm5 | S | Simon et al., 2014 | Up |
| ENSORLG00000011013 | cdkn1d | G1/S | Laranjeiro et al., 2013 | Up |
| ENSORLG00000003191 | mcm2 | S | Simon et al., 2014 | Up |
| ENSORLG00000015341 | ccne2 | G1/S | Liu et al., 2020 | Up |
| ENSORLG00000015683 | smad2 | G1/S | | Up |
| ENSORLG00000008317 | rb1 | G1/S | Bertoli et al., 2013 | Up |
| ENSORLG00000017467 | mcm4 | S | Simon et al., 2014 | Up |
| ENSORLG00000016187 | mcm3 | S | Simon et al., 2014 | Up |
| ENSORLG00000000527 | mcm7 | S | Simon et al., 2014 | Up |
| ENSORLG00000012394 | skp2 | S | Hume et al., 2021 | Up |
| ENSORLG00000002937 | pna | S | Moldovan et al., 2007 | Up |
| ENSORLG00000000945 | e2f1 | G1/S | Bertoli et al., 2013 | Up |
| ENSORLG00000027369 | cdkn2a/b | G1: prevent into S | Luan et al., 2020 | Down |
| ENSORLG00000025626 | gadd45b | G2/M | Jin et al., 2002 | Down |
| ENSORLG00000013657 | ccnb1 | G2/M | Martínez-Alonso et al., 2020 | Down |
| ENSORLG00000016447 | cdc20 | M | Weinstein et al., 1997 | Down |
| ENSORLG00000009603 | PLK1 | G2/M | Laoukili et al., 2005 | Down |
| ENSORLG00000000284 | cdkn1a | G2/M | Hussain et al., 2017 | Down |
| ENSORLG00000019266 | cdk1 | G2/M | Morgan et al., 1997 | Down |
| ENSORLG00000017163 | mdm2 | inhibition of DNA replication and G1 arrest | Deb et al., 2003 | Down |
| ENSORLG00000008493 | ccnb3 | G2/M | Nguyen et al., 2002 | Down |
| ENSORLG00000000615 | ccnb2 | G2/M | Raina et al., 2021 | Down |

Table 5. KEGG pathway analysis of up-regulated DEGs from testis after irradiation

| Term | Count | PValue |
|--|-------|----------|
| Cell adhesion molecules | 54 | 2.08E-09 |
| Calcium signaling pathway | 72 | 3.04E-09 |
| Intestinal immune network for IgA production | 16 | 1.56E-07 |
| Regulation of actin cytoskeleton | 58 | 2.47E-07 |
| Focal adhesion | 54 | 3.67E-07 |
| Phagosome | 38 | 7.32E-07 |
| ECM-receptor interaction | 28 | 1.59E-06 |
| Apelin signaling pathway | 37 | 2.39E-05 |
| Cytokine-cytokine receptor interaction | 41 | 2.61E-05 |
| Vascular smooth muscle contraction | 32 | 2.37E-04 |
| GnRH signaling pathway | 26 | 2.90E-04 |
| Phosphatidylinositol signaling system | 25 | 3.81E-04 |
| Gap junction | 25 | 4.33E-04 |
| Adherens junction | 27 | 3.98E-03 |
| Efferocytosis | 33 | 6.48E-03 |
| Viral life cycle - HIV-1 | 15 | 8.82E-03 |
| ErbB signaling pathway | 20 | 9.01E-03 |
| Adrenergic signaling in cardiomyocytes | 34 | 1.46E-02 |
| MAPK signaling pathway | 53 | 1.88E-02 |
| Inositol phosphate metabolism | 17 | 2.61E-02 |
| Varion - Herpesvirus | 6 | 3.71E-02 |
| Endocytosis | 43 | 5.18E-02 |
| Motor proteins | 31 | 7.05E-02 |
| ABC transporters | 9 | 8.52E-02 |
| Toll-like receptor signaling pathway | 16 | 9.84E-02 |

Table 6. KEGG pathway analysis of down-regulated DEGs from testis after irradiation

| Term | Count | PValue |
|--|-------|----------|
| Ribosome | 76 | 2.56E-52 |
| Oxidative phosphorylation | 34 | 7.27E-10 |
| Metabolic pathways | 187 | 7.10E-09 |
| Nucleotide metabolism | 20 | 1.46E-04 |
| Biosynthesis of cofactors | 26 | 4.36E-04 |
| RNA degradation | 16 | 1.13E-03 |
| DNA replication | 10 | 1.19E-03 |
| RNA polymerase | 9 | 1.84E-03 |
| Spliceosome | 25 | 2.91E-03 |
| Pyrimidine metabolism | 12 | 6.74E-03 |
| Base excision repair | 10 | 8.90E-03 |
| Drug metabolism - other enzymes | 12 | 9.54E-03 |
| Pentose phosphate pathway | 8 | 1.49E-02 |
| Carbon metabolism | 19 | 1.58E-02 |
| Glyoxylate and dicarboxylate metabolism | 8 | 1.72E-02 |
| Pyruvate metabolism | 9 | 1.83E-02 |
| Tyrosine metabolism | 8 | 2.27E-02 |
| Nicotinate and nicotinamide metabolism | 9 | 2.33E-02 |
| Ribosome biogenesis in eukaryotes | 12 | 2.34E-02 |
| Nucleotide excision repair | 10 | 2.56E-02 |
| Purine metabolism | 20 | 3.18E-02 |
| Arginine and proline metabolism | 9 | 4.37E-02 |
| Glycolysis / Gluconeogenesis | 11 | 4.87E-02 |
| Pentose and glucuronate interconversions | 6 | 5.92E-02 |
| Glycine, serine and threonine metabolism | 8 | 6.73E-02 |
| Metabolism of xenobiotics by cytochrome P450 | 7 | 8.69E-02 |

Table 7. KEGG pathway analysis of upregulated DEGs from ovary after irradiation

| Term | Count | PValue |
|---|-------|----------|
| Glycosaminoglycan biosynthesis - chondroitin sulfate / dermatan sulfate | 2 | 6.81E-02 |
| Porphyrin metabolism | 2 | 7.63E-02 |
| Efferocytosis | 3 | 7.75E-02 |

Table 8. KEGG pathway analysis of downregulated DEGs from ovary after irradiation

| Term | Count | PValue |
|--|-------|----------|
| Metabolic pathways | 67 | 9.09E-13 |
| Steroid hormone biosynthesis | 8 | 2.07E-05 |
| Linoleic acid metabolism | 6 | 3.35E-05 |
| Starch and sucrose metabolism | 6 | 4.08E-04 |
| Retinol metabolism | 6 | 2.25E-03 |
| Drug metabolism - other enzymes | 6 | 5.32E-03 |
| Arachidonic acid metabolism | 6 | 6.41E-03 |
| Tryptophan metabolism | 5 | 9.16E-03 |
| Glycine, serine and threonine metabolism | 5 | 9.16E-03 |
| Ascorbate and aldarate metabolism | 4 | 9.22E-03 |
| Pentose and glucuronate interconversions | 4 | 1.25E-02 |
| beta-Alanine metabolism | 4 | 2.08E-02 |
| Porphyrin metabolism | 4 | 2.24E-02 |
| Cysteine and methionine metabolism | 5 | 2.27E-02 |
| Drug metabolism - cytochrome P450 | 4 | 3.15E-02 |
| Metabolism of xenobiotics by cytochrome P450 | 4 | 3.35E-02 |
| Glutathione metabolism | 5 | 3.77E-02 |
| Pantothenate and CoA biosynthesis | 3 | 4.02E-02 |
| Taurine and hypotaurine metabolism | 3 | 5.25E-02 |
| Biosynthesis of cofactors | 7 | 6.03E-02 |
| Steroid biosynthesis | 3 | 6.14E-02 |
| Amino sugar and nucleotide sugar metabolism | 4 | 6.27E-02 |
| alpha-Linolenic acid metabolism | 3 | 7.56E-02 |
| Peroxisome | 5 | 8.38E-02 |
| Carbon metabolism | 6 | 9.01E-02 |

Table 9. KEGG pathway analysis of upregulated DEGs shared between male and female after irradiation

| Term | Count | PValue |
|---|-------|----------|
| Metabolic pathways | 79 | 6.84E-12 |
| Steroid biosynthesis | 10 | 9.38E-10 |
| PPAR signaling pathway | 13 | 2.10E-07 |
| Biosynthesis of unsaturated fatty acids | 10 | 2.83E-07 |
| Fatty acid metabolism | 11 | 7.72E-06 |
| alpha-Linolenic acid metabolism | 7 | 2.06E-05 |
| Phagosome | 13 | 3.23E-04 |
| Biosynthesis of cofactors | 11 | 3.32E-03 |
| Amino sugar and nucleotide sugar metabolism | 6 | 6.37E-03 |
| Fatty acid elongation | 5 | 1.31E-02 |
| Peroxisome | 7 | 2.05E-02 |
| Tryptophan metabolism | 5 | 2.21E-02 |
| Glyoxylate and dicarboxylate metabolism | 4 | 4.68E-02 |
| Terpenoid backbone biosynthesis | 3 | 8.31E-02 |
| Primary bile acid biosynthesis | 3 | 8.31E-02 |
| Carbon metabolism | 7 | 8.96E-02 |
| Linoleic acid metabolism | 3 | 8.98E-02 |

Table 10. KEGG pathway analysis of downregulated DEGs shared between male and female after irradiation

| Term | Count | PValue |
|---|-------|----------|
| Cytoskeleton in muscle cells | 13 | 3.35E-03 |
| Neuroactive ligand-receptor interaction | 17 | 7.84E-03 |
| Arginine and proline metabolism | 5 | 9.82E-03 |
| Phototransduction | 4 | 3.28E-02 |
| Efferocytosis | 8 | 4.78E-02 |
| Biosynthesis of amino acids | 5 | 4.85E-02 |
| Wnt signaling pathway | 8 | 5.74E-02 |
| ECM-receptor interaction | 5 | 8.38E-02 |

Chapter Two

Single Cell RNA-seq of Medaka Testis

Introduction

In vertebrates, including humans, certain tissues exhibit heightened sensitivity to ionizing radiation, notably the intestines, lymph nodes, bone marrow, and reproductive glands, with the testis being particularly susceptible (Kuwahara et al., 2002, 2003; Nagata et al., 2022; Yasuda et al., 2012, 2018). In adult medaka fish testis, irradiation triggers an acceleration of spermatogenesis to remove damaged spermatogenic cells from the tissue. Furthermore, irradiation induced damage in medaka testis results in cell death specifically in spermatogonia (Kuwahara et al., 2002; Yasuda et al., 2018).

When the tumor suppressor gene *p53* is deficient in medaka, acute exposure by high doses of gamma-ray irradiation (total dose 5 Gy, dose rate 7.3 Gy/min) has been found to induce the formation of a kind of female germ cell like cells, or being called testis-ova, in the testis of male fish (Yasuda et al., 2012). These induced testis-ova are subsequently eliminated from the tissue through a *p53*-independent exclusion mechanism, and the tissue fully recovers within one month after radiation exposure, with normal

spermatogenesis resuming. Additionally, it has long been known that external stresses such as starvation and heat treatment, along with radiation exposure (X-rays), can induce testis-ova in the male testis (Egami, 1955a, 1955b, 1956). However, the detailed mechanisms underlying the induction of testis-ova by irradiation remain to be fully elucidated.

It is suggested that spermatogonia are maintained within cysts of supportive somatic cells (Sertoli cells), and testis-ova are speculated to be induced from type A spermatogonia. To elucidate the mechanism of abnormal differentiation leading to testis-ova, particularly the molecular mechanisms of testis-ova induction resulting from gamma-ray irradiation, it is desired to confirm various responses to radiation exposure at the level of individual cells that have been separated from somatic cells. To understand the molecular mechanisms underlying abnormal differentiation into testis-ova at the level of spermatogonia, it is deemed necessary to conduct gene expression analysis at the single-cell level and to analyze cells separately by cell type.

Along with the remarkable advancements in RNA sequencing technologies, it has become possible to analyse gene expression at the single-cell level (Guo et al., 2018; Hermann et al., 2018; Hwang et al., 2018; Lukassen et al., 2018a, 2018b; Neuhaus et al., 2017). Within the fish testis, there are a dynamic cellular environment including germ cells deriving from spermatogonia into spermatocytes, and then into spermatids, alongside supportive somatic cells like Sertoli cells and Leydig cells (Lacerda et al., 2014). While some studies have explored the transcriptome landscape of fish testis using RNA-seq technique (Qian et al., 2022; Wu et al., 2021), research focus on fish spermatogenesis in distinct differentiating stage remains limited, especially in Japanese medaka.

In this study, we developed a method for retrieving more spermatogonia from medaka testis. Subsequently, utilizing single-cell RNA sequencing and analysis on those cells, we researched into the expression profiles of both spermatogenesis cells and testis-ova. This approach allowed us to gain insights into the molecular signatures and gene expression patterns specifically associated with these cell types within the medaka testicular environment, and the gene expression patterns leading to the development of testis-ova in male medaka testis. Moreover, the single-cell sequencing technique allows us to uncover cell-specific expression profiles in response to irradiation, which were previously obscured by the bulk RNA-seq analysis performed in Chapter One.

Materials and Methods

1. Fish

Wild-type (Hd-rR strain) medaka and *p53*-deficient medaka were used in this study. *p53*-deficient medaka were originally generated by TILLING (Targeting Induced Local Lesions in Genomes) in the Cab genetic background, followed by backcrossing with the Hd-rR strain for 5 generations to establish a *p53*-deficient strain with the inbred Hd-rR genetic background (Taniguchi et al., 2006; Yasuda et al., 2012).

Fish husbandry is same as described in Chapter one.

This research was conducted using protocols approved by the Animal Care and Use Committee of the University of Tokyo (permit number: C-09-01). All surgical procedures were performed on fish anaesthetized with MS-222, and all efforts were made to minimize suffering and the number of fish sacrificed.

2. Gamma-ray Irradiation

Four- to six-month-old male fish were irradiated. For low dose acute irradiation, I irradiated free-swimming fish with ¹³⁷Cs gamma-rays (Gamma cell 3000 Elan, MDS Nordion, Ottawa, ON, Canada) with a dose rate of 7.5 Gy/min and a total dose of 0.5 Gy

at room temperature. Free-swimming fish were kept in a water-containing small cylinder (diameter = 30 mm, depth = 30 mm) during the irradiation. After irradiation, fish were returned to free-swimming rearing condition until sampling.

3. Single-cell Preparation

Adult male medaka were euthanized after anesthesia, and their testes were isolated from the body after abdominal incision. The isolated testes were transferred into a pre-prepared cell dispersion solution (195 μ L L-15 (# 128-06075, FUJIFILM Wako Pure Chemical Corporation, Osaka, Japan), 25 μ L Collagenase H (40 mg/mL PBS (-), Roche Diagnostics, Mannheim, Germany), 250 μ L DispaseII (3.33 mg/mL in L-15、 # 383-02281, FUJIFILM Wako Pure Chemical Corporation, Osaka, Japan), 30 μ L DNase (15 U/ μ L in PBS (-)), Sigma Aldrich, USA) in a 1.5 mL tube. The testicular tissue in the cell dispersion solution was dissociated using scissors for 2 minutes at room temperature. Subsequently, it was pipetted approximately 50 times and subjected to an enzyme reaction at 26°C for 30 minutes. After another round of pipetting (approximately 50 times), an additional enzyme reaction was performed at 26°C for 30 minutes. The mixture was then centrifuged at 1,000 rpm for 10 minutes at 4°C. After discarding the supernatant, pellet was resuspended by pipetting in 1 mL of L-15 medium, and this solution was considered as the cell suspension. The cell suspension was passed through a 42 μ m filter to remove cell clumps, and then centrifuged at 1,000 rpm for 10 minutes at 4°C. The supernatant was discarded, and cells were resuspended again by pipetting in 100 μ L of L-15 medium. To isolate only the spermatogonia from the cell suspension, a density gradient centrifugation

method using Percoll (#P1644 Sigma-Aldrich, USA) was employed. A total of 4.5 mL of Percoll solution and 0.5 mL of L-15 medium were mixed thoroughly using a vortex mixer to prepare the Percoll stock solution. Using this Percoll stock solution, stepwise dilutions of 20%, 40%, 60%, and 80% Percoll solutions were prepared with L-15 medium. 2 mL of each stepwise dilution in descending order of concentration was layered slowly with using a Pasteur pipette in a 15 mL tube (#2325-015, AGC TECHNO GLASS Co., Ltd, Shizuoka, Japan). On top of these layers, 100 μ L of the cell suspension was gently layered. The 15 mL tube was centrifuged using a swing rotor (R4S, Koki Holdings Co., Ltd, Tokyo, Japan) at 2,650 rpm for 30 minutes at 4°C (HIMAC CR-21G, R4S, Koki Holdings Co., Ltd, Tokyo, Japan). After centrifugation, each layer was gently collected into a 1.5 mL tube using a Pasteur pipette. Among the fractionated layers, the layer containing the 40% Percoll solution had a higher abundance of spermatogonia. To remove the Percoll solution from this layer, the tube was centrifuged at 4,000 rpm for 4 minutes at 4°C, and the Percoll solution was aspirated. The pellet was then resuspended in fresh L-15 medium (Sato et al., 2017) (Acknowledgments to Professor Yoshizaki) .

4. Single Cell RNA Sequence

Single Cell 3' Reagent Kits v2 (10X Chromium, USA) was utilized for library adjustment. Cells were suspended in a barcoded solution (Single Cell Master Mix) and dispensed into dedicated well plates for approximately 8,700 cells (Single Cell A Chip, #230027, 10X Chromium, USA). The suspension was loaded onto the Chromium™ Controller (10X Chromium, USA) to enable single-cell resolution. Subsequently, RNA extraction, cDNA

synthesis, and quality checks were performed on the labeled single-cell-derived RNA, followed by sequencing on the Hiseq 2500 (Illumina, Inc., California, USA).

5. Mapping

Reads resulting from single-cell sequencing were mapped to medaka genome reference (Ensemble release 94; ASM223467v1). Cell Ranger pipelines (10X Genomics, USA) were used for single-cell transcriptome analysis, quantification of transcript level of each cell and expression abundance of each gene.

6. Single Cell RNA Sequence Analysis

Filtered output files from Cell Ranger pipeline were imported into Seurat (Hao et al., 2024) for downstream analysis, separately. Each sample was re-filtered in the R environment with following conditions. Cells with nFeature more than 200 and less than 5000, mitochondrial gene less than 5 percent were classified as good quality cells. Those cells passed Seurat re-filtering were collected by subset() function and processed. UMAP method was utilized for dimension reduction. Clusters were clustered by FindCluster() function with default resolution at first. After identifying cell types by expression profile of known markers and DEGs, cluster information was reassigned by re-running FindCluster() function and adjusting the resolution parameter. Cluster numbers were balanced between 4 datasets by adjusting resolution parameter in FindCluster() function in each separate dataset, aiming to have each cell type assigned to similar number of clusters. The resolution of FindCluster() function in non-irradiated Hd-rR, irradiated Hd-

rR, non-irradiated *p53*KO and irradiated *p53*KO dataset was 0.25, 0.4, 0.5 and 0.4.

In addition, DoubletFinder() (McGinnis et al., 2019) package was utilized for identify doublet cells. According to the results of DoubletFinder() and marker gene of each cluster, the cluster which express marker gene belong to more than 2 cell types or has few markers of its own and has majority of cell identified as doublet will be identified as doublet cluster, thus will not be involved in next step analysis.

7. Integrated Analysis

To further observe the consistency and difference between samples, integrated analysis was performed. Samples were integrated following Seurat integration pipeline, and the integrated dataset will go through same downstream processing pipeline including Scale data, Normalization, find variable features, PCA, find neighbor with UMAP method, find clusters.

8. Trajectory and Pseudotime Analysis

Dataset analyzed by Seurat will be imported into Monocle3 (Trapnell et al., 2014) for trajectory analysis, including expression metadata, clustering information and UMAP coordination. Trajectory was tracked by function learn_graph(), and pseudotime was calculated by manually choosing the start node.

Result

Single cell RNA sequence of wild-type control group adult medaka testis and identification of each cell types

Throughout, histological sections have been a common means to observe medaka sperm development. However, in most cases, deducing their developmental stage relies on morphological observations of germ cells, posing significant challenges for researchers. In order to provide a clearer perspective on medaka spermatogenesis and the dynamic changes in transcriptional levels throughout this process, the current experiment conducted single-cell RNA sequencing and analysis of medaka testes. Cell expression profiles were then used to classify these cells. It is well-known that spermatogonia cells, while maintaining their own numbers through mitosis, produce many spermatocytes through differentiation and meiosis, eventually developing into sperm that are released from the body. Consequently, compared to spermatocytes and sperm, the number of spermatogonia cells in the testis/cyst is relatively small. This significant difference in cell quantity can potentially impact the results of single-cell RNA sequencing analysis. In particular, distinguishing and classifying the relatively fewer spermatogonia cells may become challenging.

To mitigate this issue, the current experiment employed the common Percoll method.

Following dissection, a simple purification step was applied to the isolated testicular cells. This step substantially reduced the proportion of small-volume, high-density spermatocytes and sperm, as well as increasing the proportion of large-volume spermatogonia, thereby enhancing the precision of spermatogonia cell analysis.

In this single-cell RNA sequencing analysis of the wild-type medaka control group, 5,488 cells expressing 16,150 different genes were obtained under cluster resolution of 0.25. Among these cells, 5420 cells passed Seurat's filtering criteria. Subsequent analysis led to the classification of these cells into 11 distinct clusters (Figure. 13). Based on the results of the DoubletFinder package and the analysis of specific gene expression in each cluster, the majority of doublet-positive cells were found to originate from cluster 3. Notably, the specific gene expression in cluster 3 was relatively indistinct, lacking strong specificity. As a result, cluster 3 was identified as a doublet cluster and was not included in the subsequent analysis and discussion.

1. Spermatogonia type B

Cells in cluster 0,1,7 express higher level of *ddx4* (*vasa*, ENSORLG00000020672) and *dazl* (deleted in azoospermia-like) (Nicholls et al., 2019; Raz, 2000; Tanaka et al., 2001; Xu et al., 2007), which are markers for germ cells. In addition, cells in those clusters lack expression of stem cell marker genes, which indicates that those cells could be identified as spermatogonia type B cells.

Since type B spermatogonia undergoes mitosis and grows into primary spermatocytes, they can be divided into S phase, G1 phase and G2/M phase type B cells by cell cycle

marker genes separately. Cell cycle phase was identified by CellCycleScore() function in Seurat package, as well as the expression profile of cell cycle markers in each cluster.

Known cell cycle phase markers were utilized to further clarify the identity of type B spermatogonia clusters. *Pcna* (proliferation c antigen) (Moldovan et al., 2007) was especially expressed in cluster 7, which indicated that cell in cluster 7 are in S phase of the mitosis cell cycle; Cells in cluster 0 express *ccnb3* (Mita et al., 2000), which is a marker gene for G2/M phase; Even though cells in cluster 1 were scored as a mixture of G1 and S phase cells, *mcm4* (Simon & Schwacha, 2014) expression clearly identifies them as G1 phase type B cells.

2. Spermatocytes (Meiosis)

Cells in cluster 4 and 5 which are connected to the G1 phase type B spermatogonia express *dmc1* (DNA meiotic recombinase, marker gene of primary meiosis) (J. Chen et al., 2016) and *syce1* (marker gene for late meiosis) (Iwai et al., 2006), as well as *pcna* and *mcm4* at a lower level compared to spermatogonia. Thus, cells in cluster 4 and 5 could be identified as spermatocyte in early and late stage, separately.

3. Spermatid and Sperm

Cluster 2 and 8 have a high expression level of *plcz1* (Ito et al., 2008), which indicated that cells in those 2 clusters might be spermatid and sperm.

4. Somatic cell

Cluster 10 has a specific expression of Leydig marker gene, *cyp17*, which suggests that cells in cluster 10 are Leydig cells. Cells in cluster 6 can be identified as Sertoli cell since the major expression of *rgs13* (a marker gene of Sertoli cells in testis) is in cluster 6.

5. Type A Spermatogonia

Cells in cluster 9 also express spermatogonia marker genes (*ddx4*, *pcna*, *ccnb3*, *mcm4*) at a lower level compared to Spermatogonia type B cells (cluster 0, 1 and 7). Also, some marker genes of germ stem cell like *dnd1* (Gross-Thebing & Raz, 2020; Hong et al., 2016; Suzuki et al., 2016) and *nanos2* (Aoki et al., 2009; S. Nakamura et al., 2011) are only detected in cluster 9. According to those expression profile described above, cluster 9 can be identified as type A spermatogonia.

6. Testis-ova like cells

In addition, some cells, especially cells gathered at the opposite side to type B spermatogonia cluster in type A spermatogonia cluster, have a unique expression profile of ova specific expression genes, like *nanos3*, *nanog*, *mos*, *nobox* (ENSORLG00000028896), *Hlfoo* (ENSORLG00000024434) and *Zpsbp4* (ENSORLG00000023295). This result indicated that those cell group in cluster 9 might be testis-ova reported by previous research and are spontaneously differentiated from spermatogonia type A in Hd-rR medaka testis.

Single cell RNA sequence of irradiated Hd-rR medaka testis and identification of each cell types

To investigate medaka testis response to gamma-ray irradiation, I performed single cell RNA-seq on adult Hd-rR medaka testis 1 week after gamma-ray irradiation (Figure. 14). 17056 genes across 16634 cells were detected under the cluster resolution of 0.4. 7 cell types detected in non-irradiated Hd-rR medaka testis were also detected, while 2 clusters, cluster 2 and 9, exhibited a novel expression pattern and distribution different from all 7 cell types identified in non-irradiated Hd-rR medaka testis.

According to result of DoubletFinder and gene expression pattern, cluster 11 was identified as doublet and removed from the dataset. Cluster 1 and 12 exhibit expression of spermatogonia markers, while ova-specific genes only express in cluster 12, so cluster 1 was identified as type B spermatogonia and cluster 12 type A spermatogonia and testis-ova. Cluster 3,4,6,7 and 8 were identified as spermatocyte for expressing *sycp1* and *scp3*. Cluster 5 and 0 were identified as spermatid and sperm.

For testicular somatic cell, Leydig cell gathered in cluster 13 and Sertoli cell gathered in cluster 14.

As for cluster 2 and 9, both spermatocyte marker (*sycp1* and *scp3*) and spermiogenesis marker (*PLCZ1* and *ccnb2*) expression were detected (Figure 15). Along with the topological information, these 2 clusters were expected to be cells skipping normal spermatogenesis process from type B spermatogonia and accelerating into spermiogenesis due to gamma-ray irradiation. This acceleration was consistent with the

result reported in previous histological studies.

Single cell RNA sequence of non-irradiated *p53* deficient medaka testis and identification of each cell types

To further investigate the effect of *p53* deficiency on spermatogenesis, I performed single cell RNA-seq analysis on non-irradiated *p53* deficient medaka testis. In this analysis, 3348 cells expressing 14547 genes were detected under the cluster resolution of 0.5 (Figure. 16). Using the same markers, I successfully identified 7 cell types within 13 clusters: type A spermatogonia, type B spermatogonia, spermatocytes, spermatids, sperm, Leydig cells and Sertoli cells.

Cells in cluster 12 expressed both spermatogonia and germ stem cell markers, such as *dnd1* and *nanos2*, and were identified as type A spermatogonia. Cluster 2, 9 and 10 also exhibit expression of spermatogonia markers, based on the expression pattern of cell cycle markers, these clusters were identified as G1 phase, G2/M phase and S phase mitotic type B spermatogonia, respectively. Cluster 0, 3, 6, 7 and 8 contained cells expressing meiosis markers and were identified as spermatocytes. Spermatid and sperm marker mainly expressed in cluster 1, 4 and 5, identifying these clusters as spermatid and sperm. Testicular somatic cells have a respectively smaller population compared to non-irradiated Hd-rR medaka dataset and gathered in cluster 11. Within this cluster, the upper part consisted of Leydig cell and lower part of Sertoli cell.

Single cell RNA sequence of irradiated *p53* deficient medaka testis and identification of each cell types

It is reported that testis-ova can be induced from type A spermatogonia by gamma-ray irradiation in *p53* deficient medaka, however, the molecular mechanism during this process is not clear. To further understand this process, single cell RNA sequencing analysis was performed on adult testis of irradiated *p53* deficient medaka by same pipeline as non-irradiated wild type medaka testis.

5220 cells expressing 16596 genes were detected in irradiated *p53* deficient medaka testis under the cluster resolution of 0.4 (Figure. 17). Same markers were used to identify cell types of each cluster, as a result, 6 cell types (type A SPG & TO, type B SPG, spermatocyte, spermatid, leydig and sertoli) were identified successfully as same as other 3 samples. It was also checked for doublets, as a result, cluster 7 in *p53* deficient irradiated dataset was identified as doublets and deleted. Cells in cluster 6 express both spermatogonia markers and some germ stem cell specific genes, suggesting that cluster 6 is type A spermatogonia cluster. Cluster 0, 3 and 10 formed into a loop shape and have an expression of spermatogonia markers and mitotic genes, identifying them as clusters of type B spermatogonia. Spermatocyte marker and spermiogenesis marker identify cluster 4,9, and 5 as spermatocytes and cluster 1, 2 and 8 as spermatids and sperms. Cluster 11 was identified as Sertoli cell by expressing *rgs13*, and cluster 12 was identified as Leydig cells as expressing *cyp17*.

Integrated Single cell RNA sequence dataset of medaka testis and identification of each cell types

In previous work, I analyzed 4 medaka testis single cell RNA-Seq datasets separately, identified cell types of each cluster, which are 2 somatic cell clusters (Sertori and Leydig) and gamete clusters undergoing spermatogenesis.

Cells from 4 datasets (non-irradiated Hd-rR wild-type medaka testis, irradiated Hd-rR wild-type medaka testis, non-irradiated *p53* deficient medaka testis, irradiated *p53* deficient medaka testis) were integrated into a new data set, and re-run same processes as 4 datasets before (Scale data, normalization, find variable features, PCA, find neighbor with UMAP method, find clusters with resolution = 0.2). In addition, cells in integrated dataset were all tagged by information of their original dataset and cluster number, so that every cell in integrated dataset can be traced back to their separate analysis result. 10 clusters were identified, by annotating differential expressed markers in each cluster, and the separated analysis results tagged on each cell, cell type of each cluster in integrated dataset was identified (Figure. 18). Type A Spermatogonia gathered in cluster 7, while type B spermatogonia gathered in cluster 0, continue by spermatocytes as cluster 2,6 and 3, and finished by spermatids and sperm gathered in cluster 4 and 1. Somatic cells were in cluster 8 and 9, identified as Leydig and Sertoli cells, separately. Cluster 5 exhibited the same expression profile and topological features, which identified it as cells accelerating spermatogenesis from spermatogonia into spermatids induced by irradiation.

Spermatogonia stop proliferation and rush into meiosis and spermiogenesis after gamma-ray irradiation with a *p53* dependency

In irradiated Hd-rR medaka testis, a group of spermatogenetic cells, which are not observed in non-irradiated Hd-rR also non-irradiated *p53* deficient medaka testis datasets, were identified as cells accelerating spermatogenesis from spermatogonia into spermatids. Like cells in spermatocytes clusters, those cells express spermatocyte specific markers like *scp3* and *scyp1*, thus those cells can be considered as spermatocytes. However, those cells also express spermiogenesis markers (*PLCZ1*, *ccnb2*, and *spatd1*), which were not expressed in spermatocytes. This expression profile separates this cluster with clusters of spermatocytes and spermatid following normal spermatogenetic process analyzed in this study.

This group of cells only observed in irradiated Hd-rR medaka testis dataset, but not in non-irradiated testis datasets. This result was further confirmed by integration analysis. Cluster 5 in integrated dataset was identified as those accelerated cells, since it exhibits same expression profile and topological feature as cluster 2 and 9 in irradiated Hd-rR dataset. More importantly, most of cells in cluster 5 from integrated dataset were cells from cluster 2 and 9 of irradiated Hd-rR dataset. This result strongly suggests that this acceleration of spermatogenesis was induced by irradiation. Surprisingly, those cells were not observed in irradiated *p53* deficient medaka dataset, which indicated that this acceleration has a *p53* dependency.

In integrated dataset, compared to non-irradiated group, expression of G2/M phase marker (*ccnb1*, *ccnb3*) reduced in type B spermatogonia in irradiated Hd-rR medaka

dataset (Figure. 19), which clearly shows a cessation of mitotic cell division of type B spermatogonia after gamma-ray irradiation. In addition, the accelerated cluster is close to type B spermatogonia in S phase, cells close to type B spermatogonia cluster express S phase marker like *pcna* and *skp2*, and this expression of S phase marker in cluster 5 faded in cells far away from spermatogonia. This result indicated that this irradiation induced transformation from proliferation to accelerated spermatogenesis might be activated during S phase or G2 check point.

Spermatogenesis is not significantly affected by *p53* deficiency

Comparing between non-irradiated Hd-rR and non-irradiated *p53* deficient medaka dataset, surprisingly, same cell type and distribution were observed in both datasets. In integrated dataset, same type of cells from 2 datasets were clustered into same clusters, and not clear impact was observed, which indicated that spermatogenic process was similar in non-irradiated Hd-rR and *p53* deficient medaka testis. It further suggests that Spermatogenesis is not significantly affected by *p53* deficiency.

Testis-ova constantly differentiating from type A spermatogonia

It is reported that gamma ray irradiation induces the formation of testis-ova *p53* deficient medaka testis (Nagata et al., 2022; Yasuda et al., 2012). To investigate the molecular mechanisms underlying this irradiation induced formation of testis-ova, single-cell RNA-seq analysis was conducted on irradiated *p53* deficient medaka testis. The expression of spermatogonia marker and *nanos2*, which is a type A spermatogonia marker for medaka,

and the topology with type B spermatogonia identified cluster 6 as type A spermatogonia.

In type A spermatogonia cluster, a group of cells, which located on the side opposite to where the cluster of type A spermatogonia is connected to the cluster of type B spermatogonia, has a unique expression feature of oogenesis-specific genes (*mos*, *nobox* (ENSORLG00000028896), *hlf8* (*hlf8*, ENSORLG00000024434)) (Figure. 20, Figure. 21) (Aoki et al., 2009; Beer & Draper, 2013; Kajiura-Kobayashi et al., 2000; Kikuchi et al., 2020; Monti & Redi, 2009; Tanaka et al., 2001). This expression profile strongly suggesting that those cells in type A cluster were type A spermatogonia differentiating to early-stage testis-ova.

Interestingly, cells with similar expression profile and location features were observed in not only irradiated *p53* deficient dataset, but also other 3 datasets in this study. All cells exhibit similar features like expression of both type A spermatogonia specific genes and oogenesis-specific genes, as well as their UMAP location on the side of type A spermatogonia away from the type B spermatogonia clusters. This expression of oogenesis-specific in a group type A spermatogonia were not affected by efficiency, nor irradiation. Surprisingly, these findings strongly suggest that there is part of type A spermatogonia constantly mis-differentiating into testis-ova in testis of Hd-rR strain medaka.

Discussion

In this chapter, single-cell RNA sequencing on medaka testis was performed on the wild-type Hd-rR strain and the *p53* deficient medaka 7 days after the gamma-ray irradiation of 0.5 Gy, in addition to their non-irradiated groups. In all datasets, serial spermatogenic cell types were identified: type A and type B spermatogonia, meiotic spermatocyte, spermatid and sperm, and 2 testicular somatic cells: Sertoli cells and Leydig cells. All spermatogenic cells were arranged continuously in the order of spermatogenesis by UMAP analysis, except type A spermatogonia of which clusters were located apart from the other clusters in the 2 non-irradiated testes. Somatic cells were located apart from the germ cell clusters, too. This distribution confirmed that spermatogenesis is a continuous process in medaka. Furthermore, in this study, Percoll method was used to raise the proportion of spermatogonia in the testicular cells prepared for single-cell RNA-seq analysis. The abundance of spermatogonia, especially type B spermatogonia, enabled me a further investigation of type B spermatogonia dynamics in this study. On the UMAP analysis, the clusters of type B spermatogonia were looped, recalling the mitotic cell cycling of type B spermatogonia. Cell cycle score, which is one of Seurat functions to evaluate cell cycle phase, and the expression of cell cycle markers confirmed that type B spermatogonia in S phase, G1 phase and G2/M phase were clearly clustered in 3 different clusters, and the cluster of the type B spermatogonia in G1 phase was continuous with the

meiotic spermatocyte cluster. In contrast in the irradiated Hd-rR dataset, type B spermatogonia also can be separated into 3 “regions” on UMAP analysis, however, only one cluster was assigned to type B spermatogonia (Figure 14A). This is because the resolution of clustering (which decides the cluster number in one dataset on UMAP) must be compromised to balance the cluster numbers between the 4 datasets. Type B spermatogonia undergo extensive mitotic divisions to proliferate and greatly increase in their numbers before proceeding into meiosis, and this phenomenon was clearly confirmed by single-cell RNA-seq analysis here.

In addition, compared to type A spermatogonia, type B spermatogonia exhibit both low gene expression levels and fewer number of expressing genes (Figure. 22), which strongly suggests that the differentiation of type A spermatogonia into type B spermatogonia may be accompanied by the suppression of specific gene expressions rather than the activation of a novel set of gene expressions. This suggests that silencing of certain gene pathways is a key to maintain the undifferentiated state and to start the differentiation, and crucial for proper spermatogenesis and germ stem cells function.

Among the “wild-type” Hd-rR datasets, a novel group of germ cells were detected only in the irradiated testis, those were absent in the normal spermatogenesis in the Hd-rR medaka. On the UMAP analysis, those cells were located alongside the spermatocyte clusters, also connecting the type B spermatogonia cluster and spermatid cluster. The spermatocyte and spermatid clusters were annotated by their specifically expressed marker genes. On the other hand, those novel cells appeared in the irradiated Hd-rR testis have an expression profile of expressing both meiosis and spermiogenesis markers. It has been reported in the previous histological studies that gamma-ray irradiation induces

spermatogenesis acceleration in medaka testis (Kuwahara et al., 2003; Yasuda et al., 2012). Furthermore, I found the abnormal acceleration of spermatogenesis and spermiogenesis in the low dose / low dose rate gamma-ray irradiated medaka testis by bulk RNA-seq in the chapter 1 of this thesis. These findings strongly suggest that the novel cell cluster appeared in the irradiated Hd-rR testis were type B spermatogonia and spermatocytes abnormally rushed into meiosis and spermiogenesis after the irradiation. Surprisingly, in the *p53* deficient testis, this novel cell cluster was not present both in the non-irradiated nor irradiated dataset. I further conducted integrated analysis of the 4 dataset and confirmed that almost all of the novel cells, which expressing both meiosis and spermiogenesis markers, came from the irradiated Hd-rR dataset, not from the *p53* deficient dataset. This result strongly suggests that the irradiation-induced acceleration of spermatogenesis depends on *tp53* functions. In addition, it should be noticed that there is no obvious impact of the irradiation to the topology of clusters of spermatocyte, spermatid and sperm in the regular process of spermatogenesis in all the 4 datasets.

Irradiation impact was also found in type B spermatogonia in the irradiated Hd-rR medaka testis. *cnb1* and *cnb3*, which are marker genes of G2/M phase of mitotic cell cycle, were down-regulated in the type B spermatogonia from the irradiated Hd-rR dataset, suggesting that type B spermatogonia proliferation was suppressed. The suppressed proliferation of type B spermatogonia was also reported previously in the gamma-ray irradiated medaka (Kuwahara et al., 2003). It can be considered that irradiated cells make time for DNA repair before DNA replication through cell cycle delay (ap Rhys & Bohr, 1996; Lydall & Weinert, 1996; Wang, 1998). Cells from the Hd-rR and the *p53* deficient testis were clustered into same integrated clusters, suggesting that there is no obvious

impact on spermatogenesis by *p53* deficiency. This finding is consistent with the histological results by the previous studies (Nagata et al., 2019; Yasuda et al., 2012). In addition, expression of the genes related to *p53* were not altered by *p53* deficiency nor gamma-ray irradiation in this study. *p21 (cdkn1)*, the most famous downstream gene of *tp53* pathway, was barely detected in any of the 4 datasets of medaka testis in this study. As for the other members of the *tp53* pathway, *tp63* expressed in a few cells in the type A spermatogonia cluster and *tp73* was not detected in any datasets, both expressions were not affected by *p53* deficiency nor irradiation.

Ova-like cells in testis are known as testis-ova and can be induced by gamma-ray irradiation in the *p53* deficient medaka testis (Nagata et al., 2019, 2022; Yasuda et al., 2012). Several oogenesis-specific genes (*nanos3*, *nanog*, *mos*, *nobox*, *hlf8* (H1foo) and *sox19b*) and I found that these oogenesis-markers were expressed only in cells in the type A spermatogonia cluster in the 4 datasets. In addition, cells expressing these oogenesis-markers localized at the side of the type A spermatogonia cluster opposite to the side at which the type A and type B spermatogonia clusters were connected. Surprisingly, these cells are observed not only in the irradiated *p53* deficient dataset, but also they were identified in all of the other 3 datasets with similar expression profile and topological feature on the UMAP analysis. This result strongly suggests that a part of type A spermatogonia is constantly differentiating into testis-ova in Hd-rR strain medaka, regardless of the irradiation nor the *p53* deficiency. My hypothesis is that those mis-differentiating type A spermatogonia would be removed by *p53* through apoptosis. However, they might further differentiate into larger testis-ova when *p53* is absent, so that the large grown “oocytes” would be identified easily by the histological studies.

In chapter 1, by bulk RNA-seq analysis, I revealed that the low dose / low dose irradiation induced several alterations in spermatogenesis in medaka testis such as the acceleration of meiosis and spermiogenesis, metabolic suppression, alteration in testicular somatic cell functions, immune activation and up-regulation of calcium related activities. In this chapter, I confirmed the acceleration of meiosis and spermiogenesis by single cell RNA-seq and further I demonstrated that the acceleration is an abnormal process and different from the normal spermatogenesis. This acceleration of meiosis and spermiogenesis might affect the calcium related activities in medaka testis. I have focused mainly on the male germ cells and process of spermatogenesis in the single cell RNA-seq in this chapter, so that the testicular somatic cells were not fully collected from the testes and it was difficult to investigate the impacts of the irradiation on the testicular somatic cells precisely. The further single cell RNA-seq analysis that focus on the testicular somatic cells might be highly helpful to understand the impact of irradiation on testicular responses and development of the appropriate protocols to prepare the singled cells those are focused in the organs/tissues will be important.

Figures

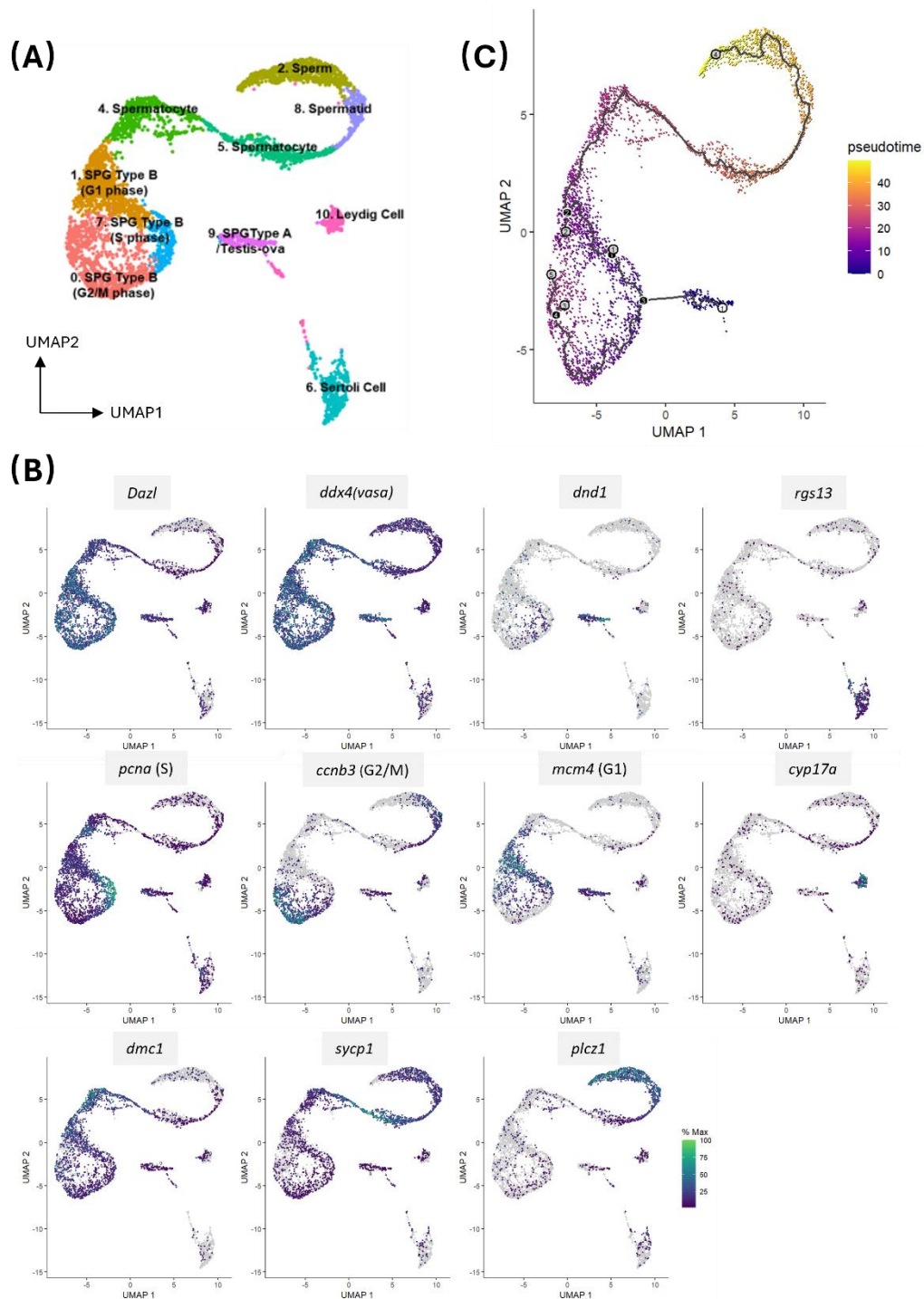


Figure 13. Single cell RNA sequence analysis of non-irradiated Hd-rR medaka testis. (A) UMAP plot of 5420 medaka testicular cells across 16150 features, 11 clusters were identified at the resolution of 0.25 and each one was assigned to a unique color. (B) Known markers for each cell type have been shown each single cell.

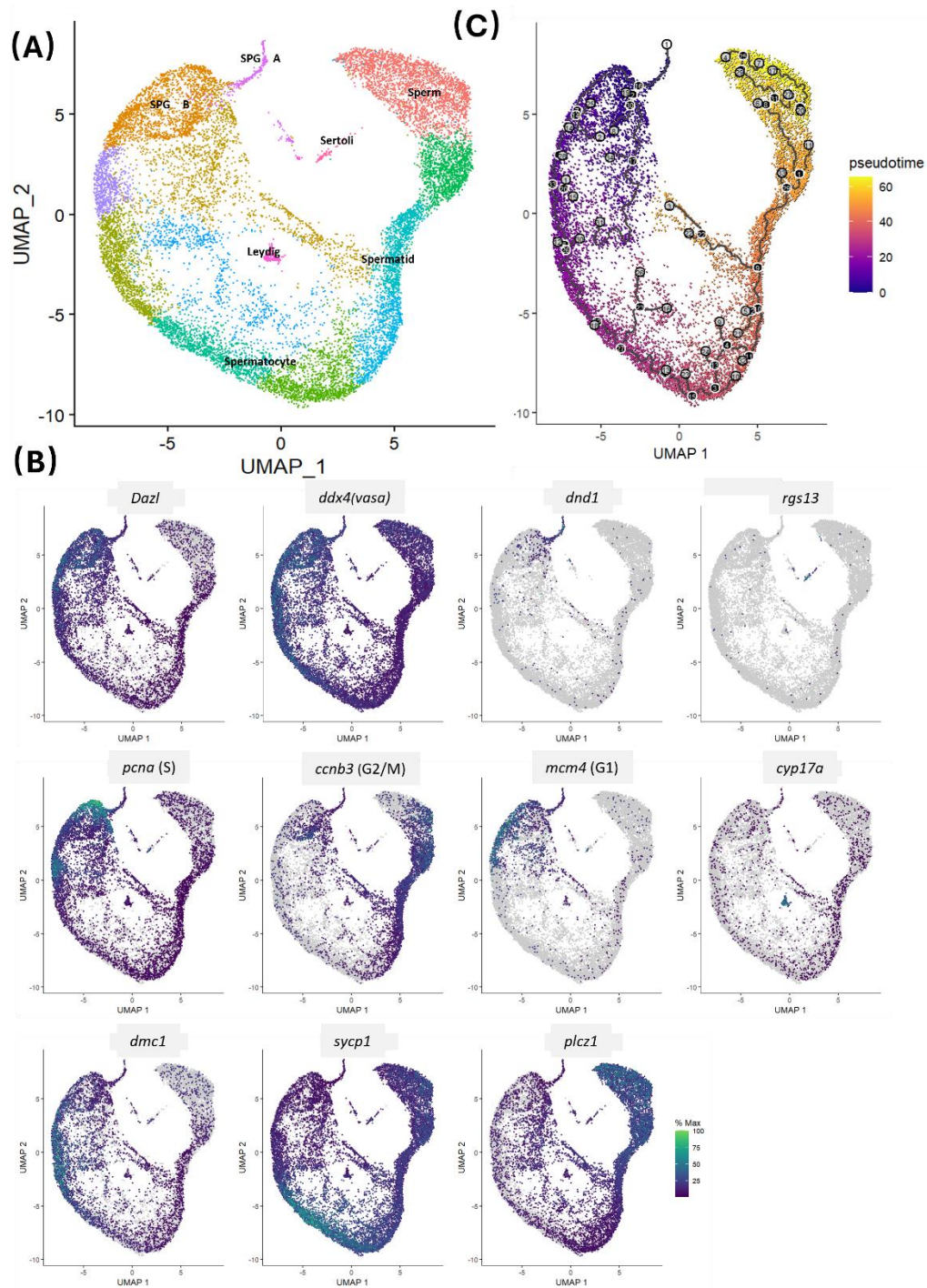


Figure 14. Single cell RNA sequence analysis of 0.5 Gy gamma ray irradiated Hd-rR medaka testis. (A) UMAP plot of 16634 medaka testicular cells across 17056 features, 13 clusters were identified at the resolution of 0.25 and each one was assigned to a unique color. (B) Known markers for each cell type have been shown each single cell.

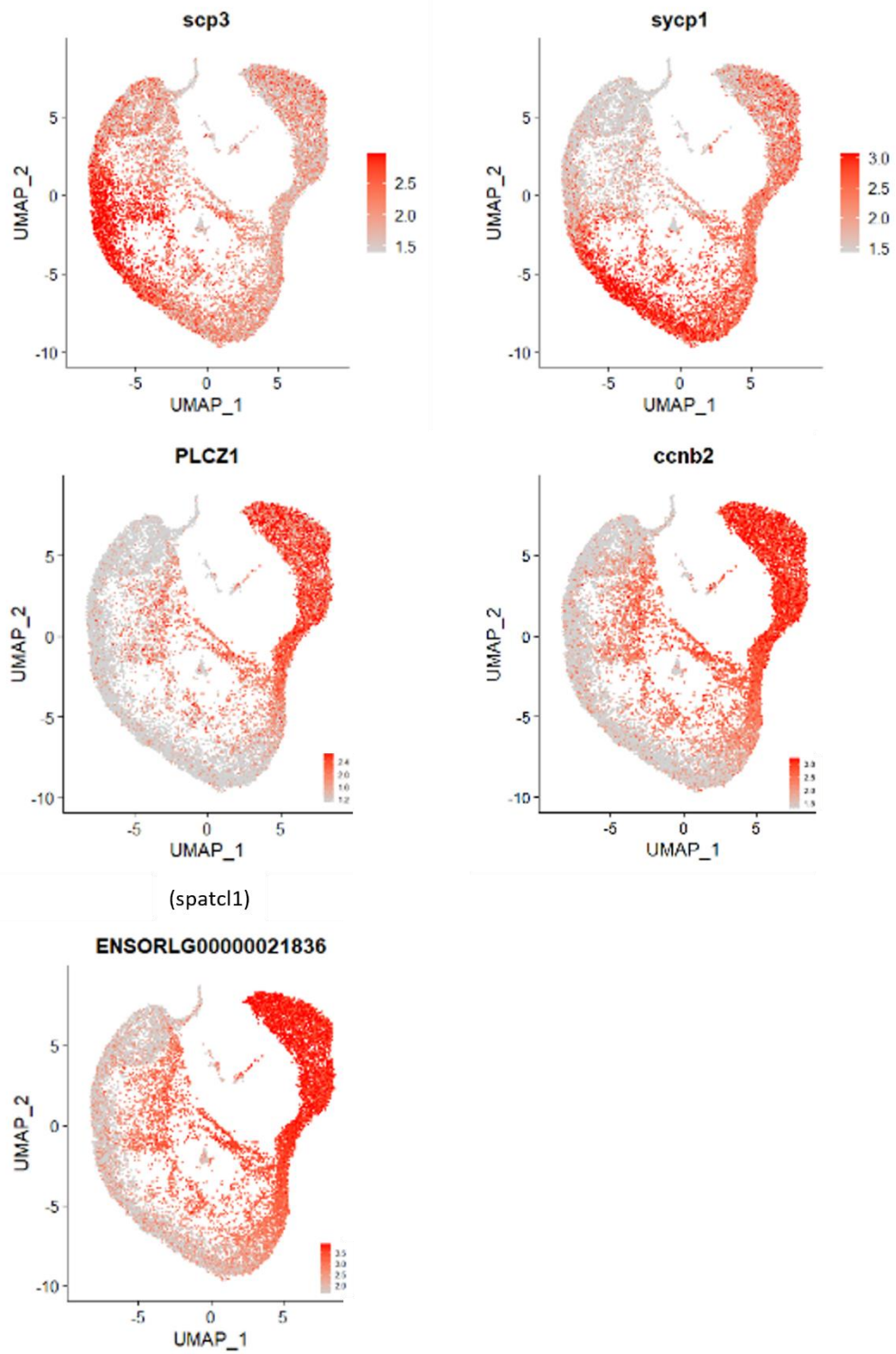


Figure 15. Expression level of spermatocytes marker (scp3 and sycp1) and spermiogenesis marker (PLCZ1, ccnb2 and spatcl1) in each cell of irradiated Hd-rR medaka testis.

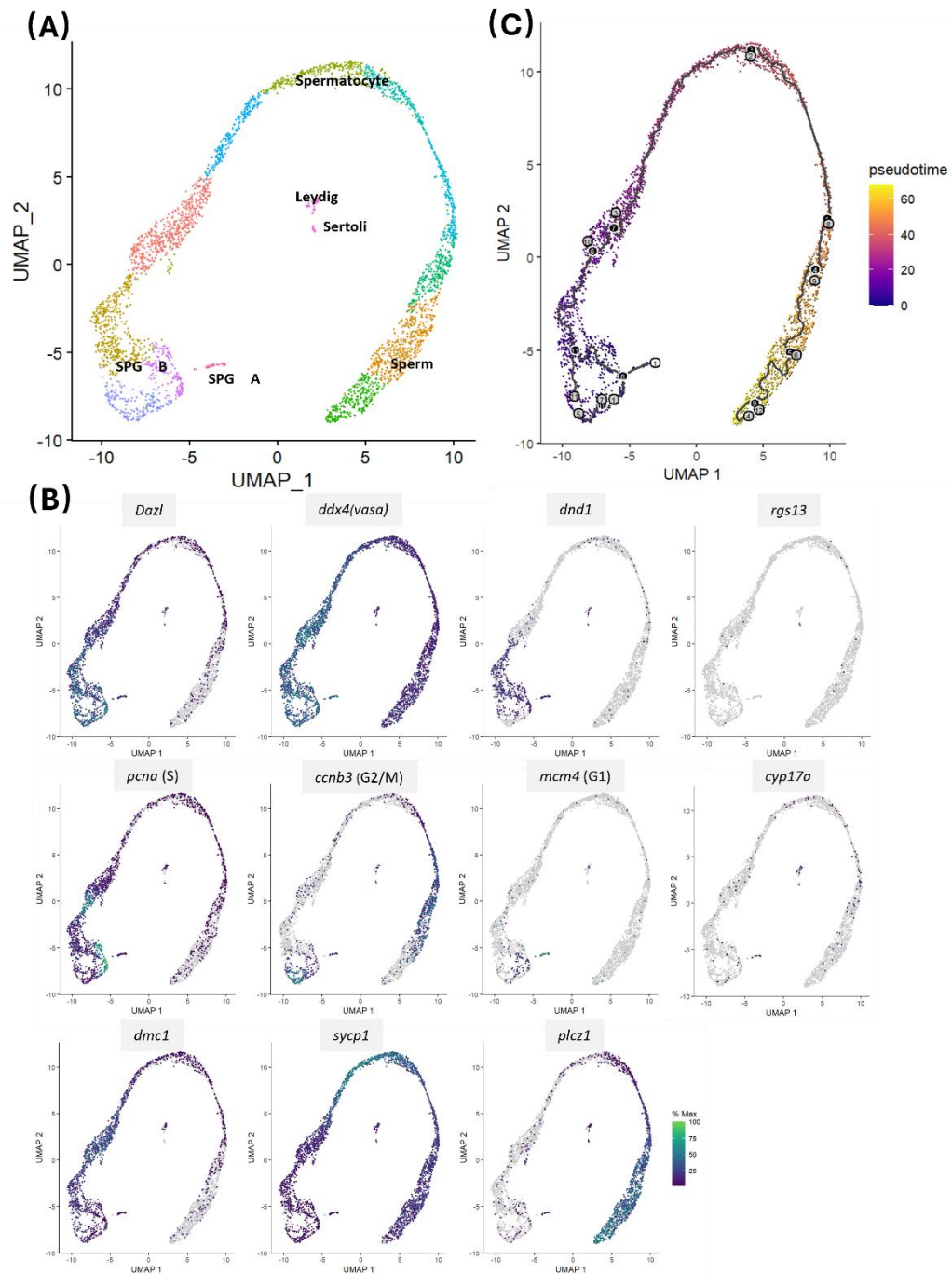


Figure 16. Single cell RNA sequence analysis of non-irradiated p53 knockout medaka testis. (A) UMAP plot of 3348 medaka testicular cells across 14547 features, 13 clusters were identified at the resolution of 0.25 and each one was assigned to a unique color. (B) Known markers for each cell type have been shown each single cell.

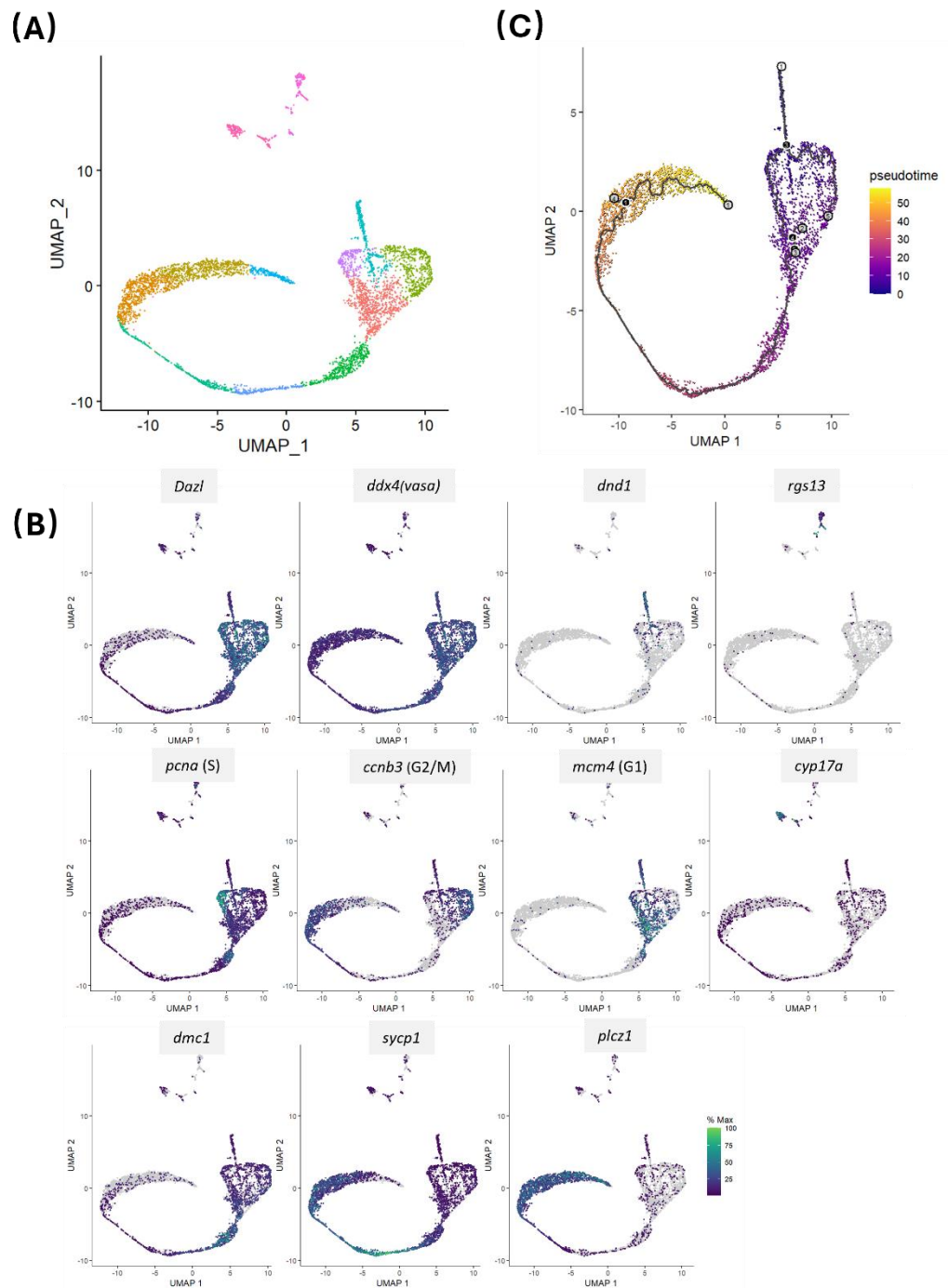


Figure 17. Single cell RNA sequence analysis of 0.5 Gy gamma ray irradiated p53 knockout medaka testis. (A) UMAP plot of 5220 medaka testicular cells across 16596 features, 12 clusters were identified at the resolution of 0.25 and each one was assigned to a unique color. (B) Known markers for each cell type have been shown each single cell.

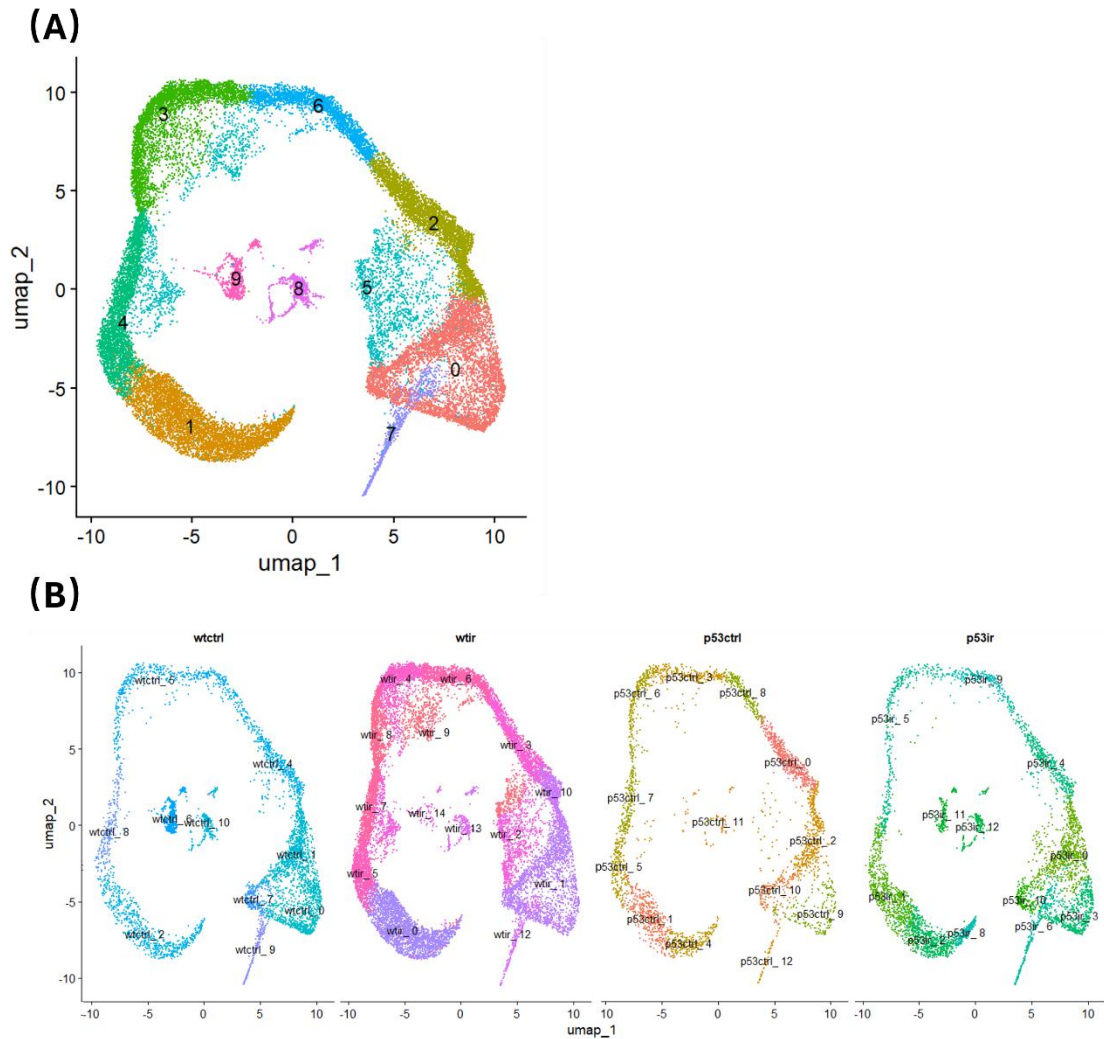


Figure 18. Integrated analysis of 4 single cell RNA sequence datasets, non-irradiated Hd-rR medaka testis (wtctrl), 0.5 Gy gamma ray irradiated Hd-rR medaka testis (wtir), non-irradiated p53 knockout medaka testis (p53ctrl) and 0.5 Gy gamma ray irradiated p53 knockout medaka testis (p53ir). (A) UMAP plot of 29062 medaka testicular cells across 19806 features, 10 clusters were identified at the resolution of 0.25 and each one was assigned to a unique color. (B) UMAP of integrated dataset split by 4 conditions and grouped by original cluster number.

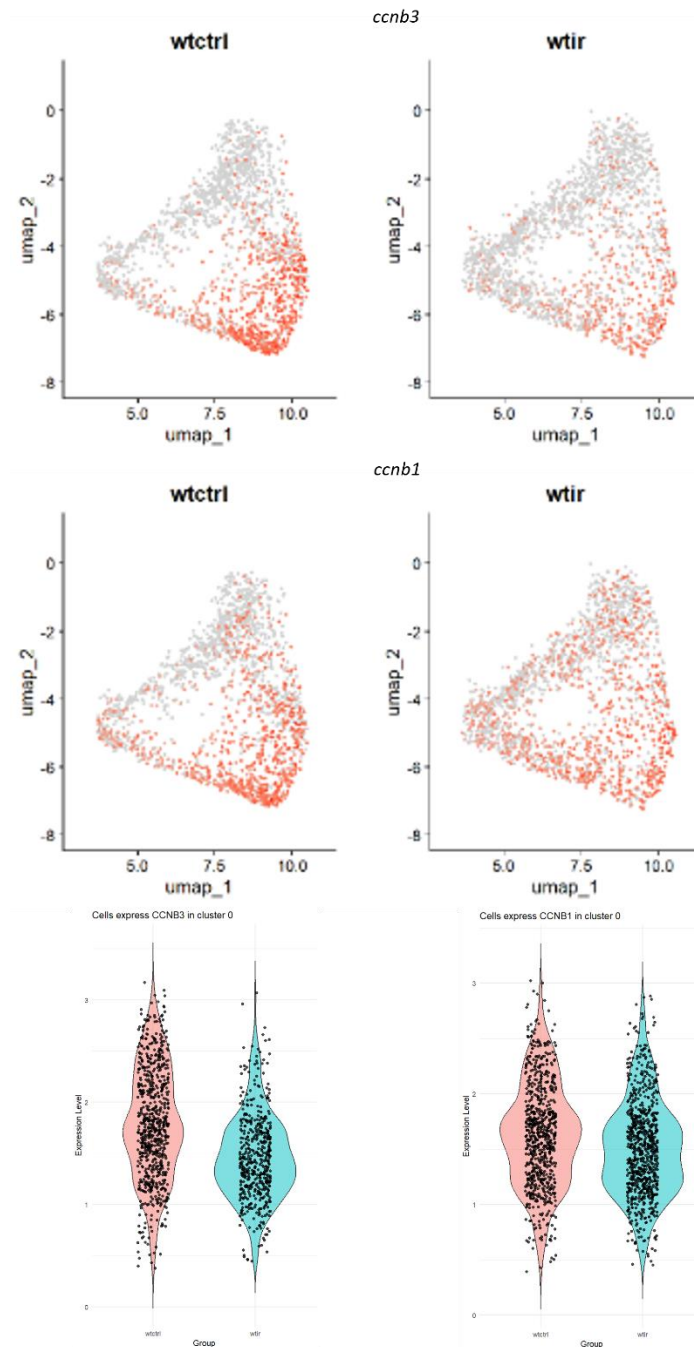


Figure 19. Mitotic marker (*ccnb3* and *ccnb1*) expressed higher in irradiated medaka testis. (A) Expression of mitotic marker (*ccnb3* and *ccnb1*) in each non-irradiated and irradiated Hd-rR medaka type B spermatogonia. (B) Expression level of *ccnb3* in non-irradiated and irradiated Hd-rR medaka *ccnb3* express type B spermatogonia (P value = $2.2e-16$). (C) Expression level of *ccnb1* in non-irradiated and irradiated Hd-rR medaka *ccnb3* express type B spermatogonia (P value = $7.901e-08$).

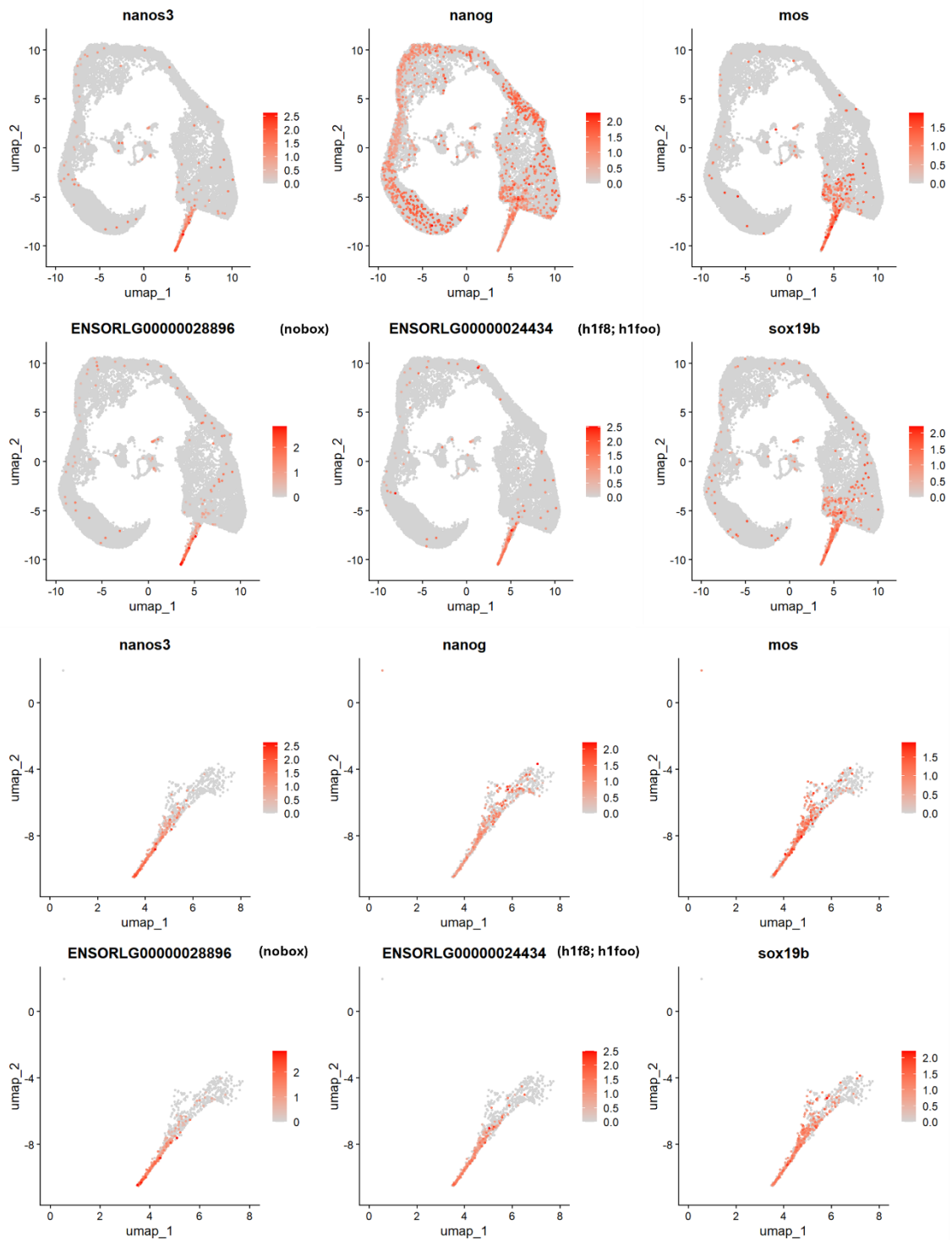


Figure 20. Expression level of oogenesis markers (nano3, nanog, mos, nobox, h1foo and sox19b). (A) Expression level of oogenesis markers in cell from integrated dataset; (B) Expression level of oogenesis markers in each type A spermatogonia. from integrated dataset.

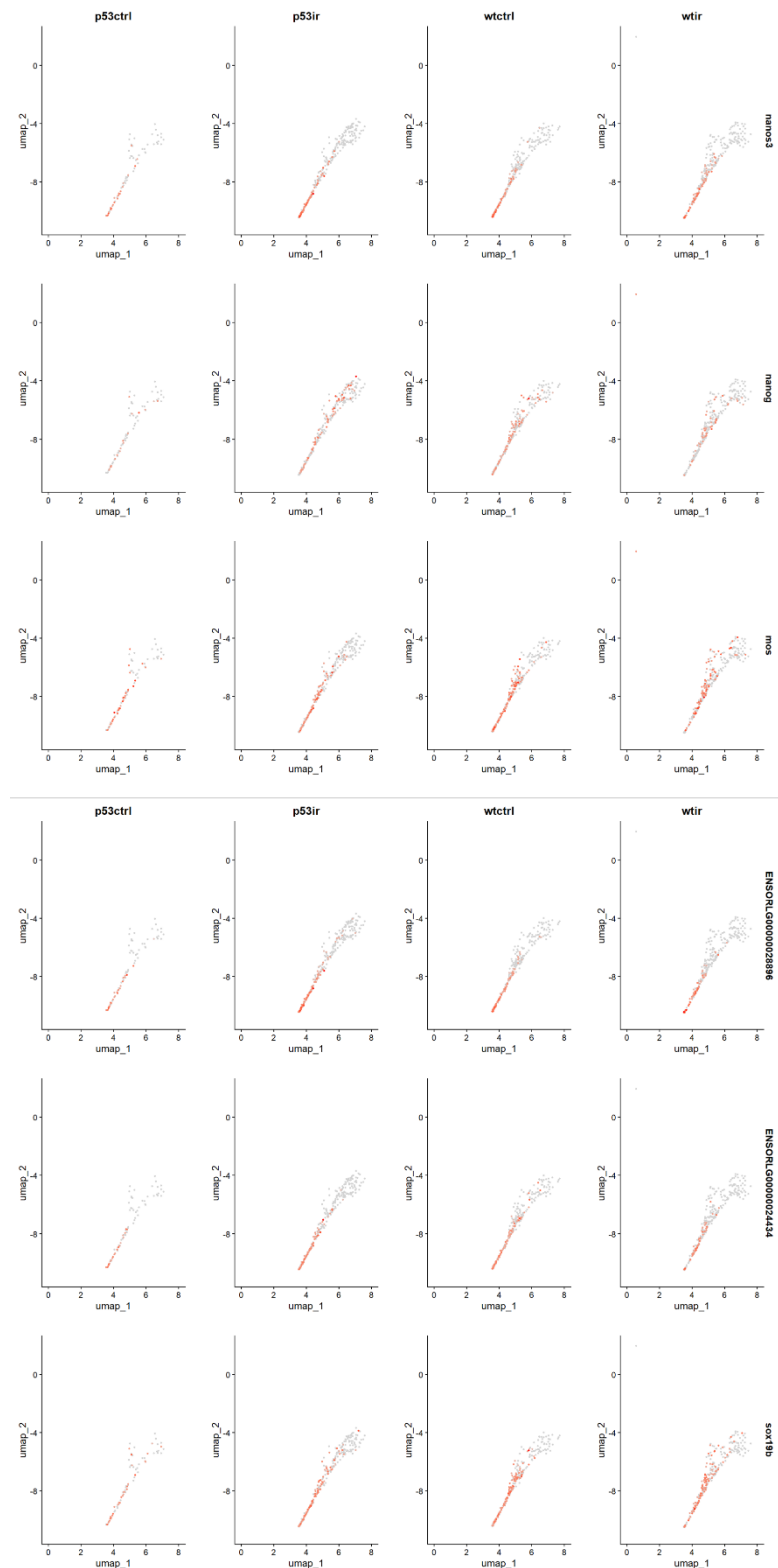


Figure 21. Expression level of oogenesis markers in each type A spermatogonia. from integrated dataset, cells were separated by 4 conditions.

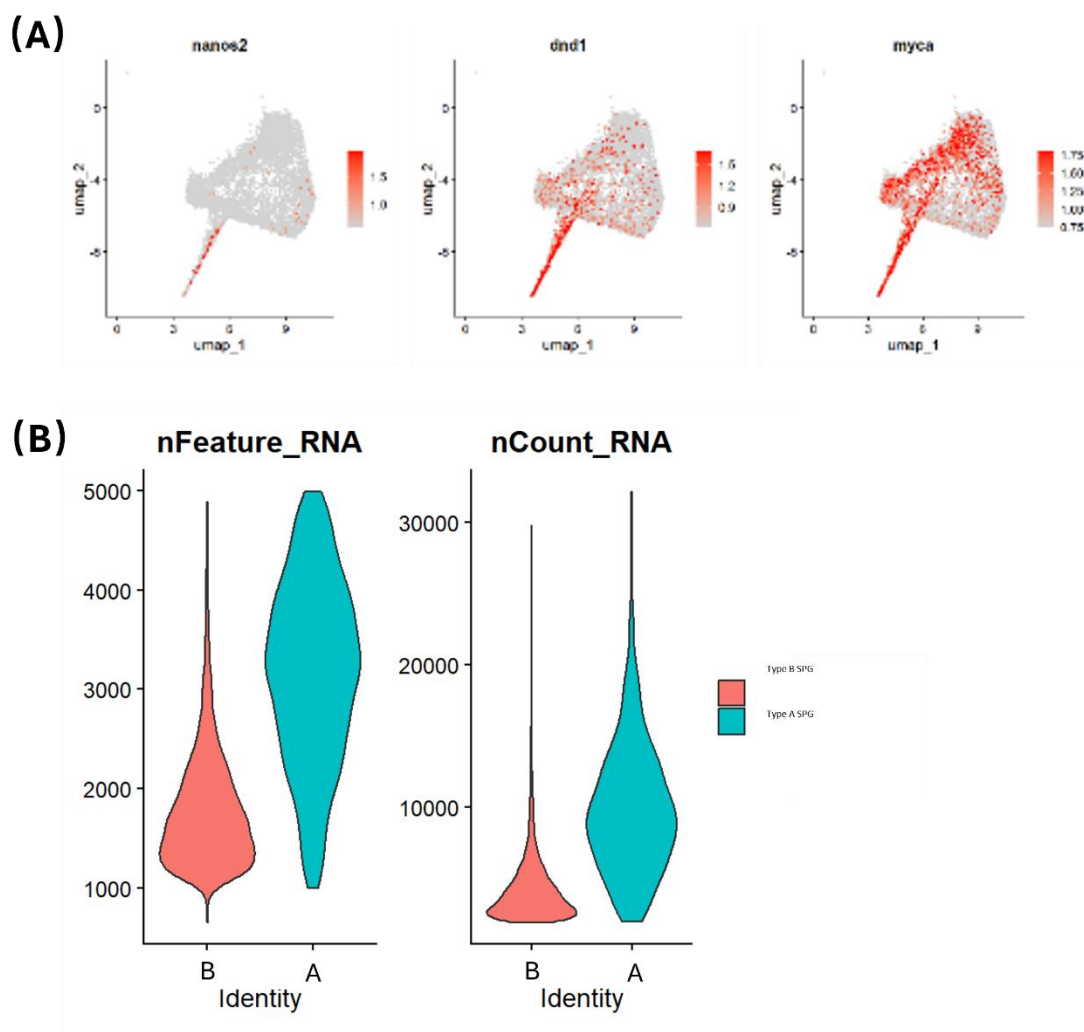


Figure 22. Type A spermatogonia expression profile in integrated dataset. (A) Type A spermatogonia markers (*nanos2*, *dnd1* and *myca*) expressed in spermatogonia; (B) Expressed gene number and total expression depth were compared between type A and type B spermatogonia.

General Discussion

In chapter 1, I conducted bulk RNA-seq analysis on medaka tissues (intestine, testis and ovary) and whole-body, finding out DEGs between the control group and the group irradiated by low dose / low dose rate gamma-ray (total dose of 100 mGy in 7 days). The DEGs were further annotated by GO enrichment and KEGG pathway analysis, for a better understanding of biological responses under low dose / low dose rate irradiation. Tissues like intestine, testis and ovary exhibited varying degrees of metabolic suppression, which may represent an adaptive response of the organism to this irradiation dose. At the same time, some tissue specific responses were also observed after the irradiation. Mitosis in intestinal tissues, especially in the intestinal stem cells, slowed down after the irradiation. In testis, spermatogenesis accelerates, accompanied by behavioral changes in supporting cells and activation of immune responses. Ovarian tissues, as anticipated, do not exhibit particularly significant changes. I also chose to analyze whole-body tissues as a comprehensive unit, comparing responses between male and female in an attempt to identify broader responses after the irradiation. In whole-body tissue, metabolic suppression presented in tissues after the irradiation was not observed. In contrast, up-regulated metabolic activity, especially lipid metabolism was observed in both male and female whole-body tissue after the irradiation, representing the most characteristic

response under this irradiation condition. I made several hypotheses for the reasons of the increased lipid metabolism observed after the irradiation. For instance, the oxidative stress induced by low-dose radiation may lead to an energy deficit within the organism, prompting medaka body to utilize fat reserves to bridge this energy gap. Additionally, oxidative stress can damage functional lipid molecules, necessitating increased lipid metabolism to supply materials for lipid biosynthesis and replacing damaged lipids. Cholesterol and steroid hormones, which are closely related to lipid metabolism, also changed after the irradiation with more complex mechanisms, reflecting the complexity of low dose radiation responses.

Similarly, increased immune responses were observed at the whole-body level, along with the up-regulated biosynthesis of certain anti-inflammatory molecules. In contrast to adaptive immune changes typically seen at higher irradiation doses, the immune-related changes under the low dose / low dose rate conditions in this study primarily involved the innate immune system, likely targeting the clearance of cellular debris or toxic molecules within the organism. The outcomes related to immune responses often vary depending on irradiation dose and dose rate, and experimental conditions. However, determining an exact threshold for these effects remains challenging, highlighting a key issue in low dose irradiation research and underscoring the need for further studies to clarify these responses.

Bulk RNA-seq analysis of tissues and the whole-body tissue has revealed both tissue-specific and more extensive systemic responses following low dose / low dose rate gamma-ray exposure. However, this technique does not capture the cell-specific responses that may occur within different cell populations in the same tissue. Therefore,

in Chapter 2, I focused on the testis, performing a more refined transcriptomic analysis through single-cell RNA sequencing. This approach allows for the classification of germ cells and testicular somatic cells, with a particular focus on the response of germ cells under the irradiation. Furthermore, this study aims to uncover the mechanisms behind testis-ova formation in medaka testis, which were suggested in previous research (Nagata et al., 2019; Yasuda et al., 2012).

Continuous process of spermatogenesis was confirmed in non-irradiated Hd-rR medaka testis. Similar process was confirmed in irradiated Hd-rR medaka testis, but with a novel type of cell, which seems to be the spermatogonia accelerating into the spermatogenesis process after the irradiation. Same analysis were conducted on *p53* deficient medaka testis as well, similar spermatogenesis process presented by both non-irradiated and irradiated medaka testis confirmed that *p53* deficient does not affect the regular spermatogenesis, however, acceleration of spermatogenesis induced by the irradiation was not present in irradiated *p53* deficient medaka testis, indicating that this irradiation induced acceleration has a *p53* dependency. Since it is reported that testis-ova can be induced in gamma-ray irradiated *p53* deficient medaka testis, and some early oogenesis marker genes were used as testis-ova marker, those markers were used for searching testis-ova in this study. The expression profiles indicated that testis-ova were differentiated from type A spermatogonia, and surprisingly, testis-ova not only induced in irradiated *p53* deficient medaka testis, but also non-irradiated *p53* deficient medaka testis and even Hd-rR medaka testis. Thus, here I hypothesises that type A spermatogonia is constantly differentiating into testis-ova in Hd-rR strain medaka testis, and this process used to be terminated by *p53* dependent apoptosis, with induction of irradiation of *p53* deficiency, this process

continues to progress so that can be detected by histological examinations.

In this study, responses after low dose irradiation in medaka were analyzed by NGS techniques. Some results are consistent with the histological experiment results in previous studies, however, new discoveries are also made while they might be difficult to notice by histological examinations. These new discoveries prove that NGS techniques as a powerful tool for revealing slight variations, like the physiological responses after low dose irradiation, compared to responses of high dose irradiation. However, this technique still has its limitations, such as, the subtle alteration can be overlapped by other variations between experiment batches, even between samples. More powerful statistic tools and much larger sample pool might be need. As for low dose irradiation research, the responses related to irradiation dose and dose rate is also ambiguous, results can differ between studies with similar conditions, which indicated more experiments data is necessary. With the accessibility of public data and advancements in technology, I am optimistic that the effects of low dose irradiation and potential countermeasures will become clearer in near future. This will contribute to improving human lives and ecosystems under radiation impacts and may also allow people to respond more effectively in handling radioactive materials and dealing with accidents.

References

- Ackman, R. G. (1967). Characteristics of the fatty acid composition and biochemistry of some fresh-water fish oils and lipids in comparison with marine oils and lipids. *Comparative Biochemistry and Physiology*, 22(3), 907–922. [https://doi.org/10.1016/0010-406X\(67\)90781-5](https://doi.org/10.1016/0010-406X(67)90781-5)
- Adriaens, I., Smits, J., & Jacquet, P. (2009). The current knowledge on radiosensitivity of ovarian follicle development stages. *Human Reproduction Update*, 15(3), 359–377. <https://doi.org/10.1093/humupd/dmn063>
- Aoki, Y., Nakamura, S., Ishikawa, Y., & Tanaka, M. (2009). Expression and Syntenic Analyses of Four nanos Genes in Medaka. *Zoological Science*, 26, 112–118. <https://doi.org/10.2108/zsj.26.112>
- ap Rhys, C. M., & Bohr, V. A. (1996). Mammalian DNA repair responses and genomic instability. *EXS*, 77, 289–305. https://doi.org/10.1007/978-3-0348-9088-5_19
- Ashburner, M., Ball, C. A., Blake, J. A., Botstein, D., Butler, H., Cherry, J. M., Davis, A. P., Dolinski, K., Dwight, S. S., Eppig, J. T., Harris, M. A., Hill, D. P., Issel-Tarver, L., Kasarskis, A., Lewis, S., Matese, J. C., Richardson, J. E., Ringwald, M., Rubin, G. M., & Sherlock, G. (2000). Gene Ontology: Tool for the unification of biology. *Nature Genetics*, 25(1), 25–29. <https://doi.org/10.1038/75556>

- Auzanneau, C., Norez, C., Noël, S., Jougla, C., Becq, F., & Vandebrouck, C. (2006). Pharmacological profile of inhibition of the chloride channels activated by extracellular acid in cultured rat Sertoli cells. *Reproduction Nutrition Development*, 46(3), 241–255. <https://doi.org/10.1051/rnd:2006013>
- Azzam, E. I., Jay-Gerin, J.-P., & Pain, D. (2012). Ionizing radiation-induced metabolic oxidative stress and prolonged cell injury. *Cancer Letters*, 327(0), 48–60. <https://doi.org/10.1016/j.canlet.2011.12.012>
- Beer, R. L., & Draper, B. W. (2013). *Nanos3* maintains germline stem cells and expression of the conserved germline stem cell gene *nanos2* in the zebrafish ovary. *Developmental Biology*, 374(2), 308–318. <https://doi.org/10.1016/j.ydbio.2012.12.003>
- Blas, G. D., Michaut, M., Treviño, C. L., Tomes, C. N., Yunes, R., Darszon, A., & Mayorga, L. S. (2002). The Intraacrosomal Calcium Pool Plays a Direct Role in Acrosomal Exocytosis *. *Journal of Biological Chemistry*, 277(51), 49326–49331. <https://doi.org/10.1074/jbc.M208587200>
- Bolger, A. M., Lohse, M., & Usadel, B. (2014). Trimmomatic: A flexible trimmer for Illumina sequence data. *Bioinformatics*, 30(15), 2114–2120. <https://doi.org/10.1093/bioinformatics/btu170>
- Boveris, A., Oshino, N., & Chance, B. (1972). The cellular production of hydrogen peroxide. *Biochemical Journal*, 128(3), 617–630. <https://doi.org/10.1042/bj1280617>
- Cao, H., Li, L., Liu, S., Wang, Y., Liu, X., Yang, F., & Dong, W. (2024). The multifaceted role of extracellular ATP in sperm function: From spermatogenesis to fertilization.

Theriogenology, 214, 98–106.

<https://doi.org/10.1016/j.theriogenology.2023.10.019>

Casale, J., & Crane, J. S. (2024). Biochemistry, Glycosaminoglycans. In *StatPearls*.

StatPearls Publishing. <http://www.ncbi.nlm.nih.gov/books/NBK544295/>

Chen, J., Cui, X., Jia, S., Luo, D., Cao, M., Zhang, Y., Hu, H., Huang, K., Zhu, Z., & Hu,

W. (2016). Disruption of *dmc1* Produces Abnormal Sperm in Medaka (*Oryzias*

latipes). *Scientific Reports*, 6(1), 30912. <https://doi.org/10.1038/srep30912>

Chen, Y., Chen, L., Lun, A. T. L., Baldoni, P. L., & Smyth, G. K. (2024). *edgeR 4.0:*

Powerful differential analysis of sequencing data with expanded functionality and improved support for small counts and larger datasets (p. 2024.01.21.576131).

bioRxiv. <https://doi.org/10.1101/2024.01.21.576131>

Corteselli, E. M., Gold, A., Surratt, J., Cui, T., Bromberg, P., Dailey, L., & Samet, J. M.

(2020). Supplementation with omega-3 fatty acids potentiates oxidative stress in

human airway epithelial cells exposed to ozone. *Environmental Research*, 187,

109627. <https://doi.org/10.1016/j.envres.2020.109627>

Costa, R. R., Varanda, W. A., & Franci, C. R. (2010). A calcium-induced calcium release

mechanism supports luteinizing hormone-induced testosterone secretion in mouse

Leydig cells. *American Journal of Physiology-Cell Physiology*, 299(2), C316–

C323. <https://doi.org/10.1152/ajpcell.00521.2009>

Dadras, H., Boryshpolets, S., Golpour, A., Policar, T., Blecha, M., & Dzyuba, B. (2019).

Effects of temperature on sperm motility of burbot *Lota lota*: Spontaneous

activation and calcium dependency. *Journal of Fish Biology*, 95(4), 1137–1144.

<https://doi.org/10.1111/jfb.14110>

- Dobin, A., Davis, C. A., Schlesinger, F., Drenkow, J., Zaleski, C., Jha, S., Batut, P., Chaisson, M., & Gingeras, T. R. (2013). STAR: Ultrafast universal RNA-seq aligner. *Bioinformatics*, 29(1), 15–21. <https://doi.org/10.1093/bioinformatics/bts635>
- Duszka, K., Gregor, A., Guillou, H., König, J., & Wahli, W. (2020). Peroxisome Proliferator-Activated Receptors and Caloric Restriction-Common Pathways Affecting Metabolism, Health, and Longevity. *Cells*, 9(7), 1708. <https://doi.org/10.3390/cells9071708>
- Ebrahimian, T. G., Beugnies, L., Surette, J., Priest, N., Gueguen, Y., Gloaguen, C., Benderitter, M., Jourdain, J. R., & Tack, K. (2017). Chronic Exposure to External Low-Dose Gamma Radiation Induces an Increase in Anti-inflammatory and Antioxidative Parameters Resulting in Atherosclerotic Plaque Size Reduction in ApoE^{-/-} Mice. *Radiation Research*, 189(2), 187–196. <https://doi.org/10.1667/RR14823.1>
- Egami, N. (1955a). Production of testis-ova in adult males of *Oryzias latipes*. III. Testis-ova production in starved males. *Jour Fac Sci Tokyo U Sect Iv Zool*, 7(3), Article 3.
- Egami, N. (1955b). Production of testis-ova in adult males of *Oryzias latipes* IV. Effect of X-ray irradiation on testis-ovum production. *JSci. Univ. Tokyo (Zool.)*, 429–442.
- Egami, N. (1956). Production of testis-ova in adult males of *Oryzias latipes* VI Effect on testis-ovum production of exposure to high temperature. *Annot Zool Japon*, 11–

18.

- Fang, F., Gong, P. S., Zhao, H. G., Bi, Y. J., Zhao, G., Gong, S. L., & Wang, Z. C. (2013). Mitochondrial Modulation of Apoptosis Induced by Low-dose Radiation in Mouse Testicular Cells. *Biomedical and Environmental Sciences*, 26(10), 820–830. <https://doi.org/10.3967/bes2013.005>
- Fatehi, D., Mohammadi, M., Shekarchi, B., Shabani, A., Seify, M., & Rostamzadeh, A. (2018). Radioprotective effects of Silymarin on the sperm parameters of NMRI mice irradiated with γ -rays. *Journal of Photochemistry and Photobiology B: Biology*, 178, 489–495. <https://doi.org/10.1016/j.jphotobiol.2017.12.004>
- Fijak, M., Bhushan, S., & Meinhardt, A. (2017). The Immune Privilege of the Testis. In W. K. H. Krause & R. K. Naz (Eds.), *Immune Infertility: Impact of Immune Reactions on Human Fertility* (pp. 97–107). Springer International Publishing. https://doi.org/10.1007/978-3-319-40788-3_5
- Golpour, A., Pšenička, M., & Niksirat, H. (2017). Subcellular distribution of calcium during spermatogenesis of zebrafish, *Danio rerio*. *Journal of Morphology*, 278(8), 1149–1159. <https://doi.org/10.1002/jmor.20701>
- Gorczyńska, E., & Handelsman, D. J. (1991). The role of calcium in follicle-stimulating hormone signal transduction in Sertoli cells. *Journal of Biological Chemistry*, 266(35), 23739–23744. [https://doi.org/10.1016/S0021-9258\(18\)54345-3](https://doi.org/10.1016/S0021-9258(18)54345-3)
- Gross-Thebing, T., & Raz, E. (2020). Chapter Seven - Dead end and Detour: The function of the RNA-binding protein Dnd in posttranscriptional regulation in the germline. In F. L. Marlow (Ed.), *Current Topics in Developmental Biology* (Vol. 140, pp. 181–208). Academic Press. <https://doi.org/10.1016/bs.ctdb.2019.12.003>

- Guo, J., Grow, E. J., Mlcochova, H., Maher, G. J., Lindskog, C., Nie, X., Guo, Y., Takei, Y., Yun, J., Cai, L., Kim, R., Carrell, D. T., Goriely, A., Hotaling, J. M., & Cairns, B. R. (2018). The adult human testis transcriptional cell atlas. *Cell Research*, 28(12), 1141–1157. <https://doi.org/10.1038/s41422-018-0099-2>
- Halliwell, B. (1991). Reactive oxygen species in living systems: Source, biochemistry, and role in human disease. *The American Journal of Medicine*, 91(3), S14–S22. [https://doi.org/10.1016/0002-9343\(91\)90279-7](https://doi.org/10.1016/0002-9343(91)90279-7)
- Halliwell, B., & Aruoma, O. I. (1991). DNA damage by oxygen-derived species Its mechanism and measurement in mammalian systems. *FEBS Letters*, 281(1–2), 9–19. [https://doi.org/10.1016/0014-5793\(91\)80347-6](https://doi.org/10.1016/0014-5793(91)80347-6)
- Hao, Y., Stuart, T., Kowalski, M. H., Choudhary, S., Hoffman, P., Hartman, A., Srivastava, A., Molla, G., Madad, S., Fernandez-Granda, C., & Satija, R. (2024). Dictionary learning for integrative, multimodal and scalable single-cell analysis. *Nature Biotechnology*, 42(2), 293–304. <https://doi.org/10.1038/s41587-023-01767-y>
- Hermann, B. P., Cheng, K., Singh, A., Cruz, L. R.-D. L., Mutoji, K. N., Chen, I.-C., Gildersleeve, H., Lehle, J. D., Mayo, M., Westernströer, B., Law, N. C., Oatley, M. J., Velte, E. K., Niedenberger, B. A., Fritze, D., Silber, S., Geyer, C. B., Oatley, J. M., & McCarrey, J. R. (2018). The Mammalian Spermatogenesis Single-Cell Transcriptome, from Spermatogonial Stem Cells to Spermatids. *Cell Reports*, 25(6), 1650-1667.e8. <https://doi.org/10.1016/j.celrep.2018.10.026>
- Herrera, E., Salas, K., Lagos, N., Benos, D. J., & Reyes, J. G. (2000). Energy metabolism and its linkage to intracellular Ca²⁺ and pH regulation in rat spermatogenic cells. *Biology of the Cell*, 92(6), 429–440. <https://doi.org/10.1016/S0248->

4900(00)01082-0

- Hong, N., Li, M., Yuan, Y., Wang, T., Yi, M., Xu, H., Zeng, H., Song, J., & Hong, Y. (2016). Dnd Is a Critical Specifier of Primordial Germ Cells in the Medaka Fish. *Stem Cell Reports*, 6(3), 411–421. <https://doi.org/10.1016/j.stemcr.2016.01.002>
- Honsho, M., Yamashita, S., & Fujiki, Y. (2016). Peroxisome homeostasis: Mechanisms of division and selective degradation of peroxisomes in mammals. *Biochimica et Biophysica Acta (BBA) - Molecular Cell Research*, 1863(5), 984–991. <https://doi.org/10.1016/j.bbamcr.2015.09.032>
- Huang, D. W., Sherman, B. T., & Lempicki, R. A. (2009). Systematic and integrative analysis of large gene lists using DAVID bioinformatics resources. *Nature Protocols*, 4(1), 44–57. <https://doi.org/10.1038/nprot.2008.211>
- Hui, D. Y., & Howles, P. N. (2002). Carboxyl ester lipase. *Journal of Lipid Research*, 43(12), 2017–2030. <https://doi.org/10.1194/jlr.R200013-JLR200>
- Hwang, B., Lee, J. H., & Bang, D. (2018). Single-cell RNA sequencing technologies and bioinformatics pipelines. *Experimental & Molecular Medicine*, 50(8), 1–14. <https://doi.org/10.1038/s12276-018-0071-8>
- Hyodo, T. Y. (1965). Effect of X-Irradiation on the Intestinal Epithelium of the Goldfish *Carassius auratus*: II. Influence of Temperature on the Development of Histopathological Changes in the Intestine. *Radiation Research*, 24(1), 133–141. <https://doi.org/10.2307/3571723>
- Ina, Y., & Sakai, K. (2005). Further Study of Prolongation of Life Span Associated with Immunological Modification by Chronic Low-Dose-Rate Irradiation in MRL-lpr/lpr Mice: Effects of Whole-Life Irradiation. *Radiation Research*, 163(4), 418–

423.

- Ishida, Y., Takabatake, T., Kakinuma, S., Doi, K., Yamauchi, K., Kaminishi, M., Kito, S., Ohta, Y., Amasaki, Y., Moritake, H., Kokubo, T., Nishimura, M., Nishikawa, T., Hino, O., & Shimada, Y. (2010). Genomic and gene expression signatures of radiation in medulloblastomas after low-dose irradiation in *Ptch1* heterozygous mice. *Carcinogenesis*, *31*(9), 1694–1701. <https://doi.org/10.1093/carcin/bgq145>
- Ishikawa, A., Kabeya, N., Ikeya, K., Kakioka, R., Cech, J. N., Osada, N., Leal, M. C., Inoue, J., Kume, M., Toyoda, A., Tezuka, A., Nagano, A. J., Yamasaki, Y. Y., Suzuki, Y., Kokita, T., Takahashi, H., Lucek, K., Marques, D., Takehana, Y., ... Kitano, J. (2019). A key metabolic gene for recurrent freshwater colonization and radiation in fishes. *Science*, *364*(6443), 886–889. <https://doi.org/10.1126/science.aau5656>
- Ito, M., Shikano, T., Oda, S., Horiguchi, T., Tanimoto, S., Awaji, T., Mitani, H., & Miyazaki, S. (2008). Difference in Ca²⁺ Oscillation-Inducing Activity and Nuclear Translocation Ability of PLCZ1, an Egg-Activating Sperm Factor Candidate, Between Mouse, Rat, Human, and Medaka Fish1. *Biology of Reproduction*, *78*(6), 1081–1090. <https://doi.org/10.1095/biolreprod.108.067801>
- Iwai, T., Yoshii, A., Yokota, T., Sakai, C., Hori, H., Kanamori, A., & Yamashita, M. (2006). Structural components of the synaptonemal complex, SYCP1 and SYCP3, in the medaka fish *Oryzias latipes*. *Experimental Cell Research*, *312*(13), 2528–2537. <https://doi.org/10.1016/j.yexcr.2006.04.015>
- Jones, R. E., & Lopez, K. H. (2013). *Human Reproductive Biology*. Academic Press.
- Kajiura-Kobayashi, H., Yoshida, N., Sagata, N., Yamashita, M., & Nagahama, Y. (2000).

- The Mos/MAPK pathway is involved in metaphase II arrest as a cytostatic factor but is neither necessary nor sufficient for initiating oocyte maturation in goldfish. *Development Genes and Evolution*, 210(8–9), 416–425. <https://doi.org/10.1007/s004270000083>
- Kanehisa, M., & Goto, S. (2000). KEGG: Kyoto encyclopedia of genes and genomes. *Nucleic Acids Research*, 28(1), 27–30. <https://doi.org/10.1093/nar/28.1.27>
- Kanehisa, M., Sato, Y., & Kawashima, M. (2022). KEGG mapping tools for uncovering hidden features in biological data. *Protein Science*, 31(1), 47–53. <https://doi.org/10.1002/pro.4172>
- Kiani, C., Chen, L., Wu, Y. J., Yee, A. J., & Yang, B. B. (2002). Structure and function of aggrecan. *Cell Research*, 12(1), 19–32. <https://doi.org/10.1038/sj.cr.7290106>
- Kikuchi, M., Nishimura, T., Ishishita, S., Matsuda, Y., & Tanaka, M. (2020). Foxl3, a sexual switch in germ cells, initiates two independent molecular pathways for commitment to oogenesis in medaka. *Proceedings of the National Academy of Sciences*, 117(22), 12174–12181. <https://doi.org/10.1073/pnas.1918556117>
- Kleene, K. C. (2004). Patterns, mechanisms, and functions of translation regulation in mammalian spermatogenic cells. *Cytogenetic and Genome Research*, 103(3–4), 217–224. <https://doi.org/10.1159/000076807>
- Kolberg, L., Raudvere, U., Kuzmin, I., Adler, P., Vilo, J., & Peterson, H. (2023). g:Profiler—Interoperable web service for functional enrichment analysis and gene identifier mapping (2023 update). *Nucleic Acids Research*, 51(W1), W207–W212. <https://doi.org/10.1093/nar/gkad347>
- Krasznai, Z., Márián, T., Izumi, H., Damjanovich, S., Balkay, L., Trón, L., & Morisawa,

- M. (2000). Membrane hyperpolarization removes inactivation of Ca²⁺ channels, leading to Ca²⁺ influx and subsequent initiation of sperm motility in the common carp. *Proceedings of the National Academy of Sciences*, 97(5), 2052–2057. <https://doi.org/10.1073/pnas.040558097>
- Kretser, D. M. de, Loveland, K. A. L., & O'Bryan, M. K. (2016). Spermatogenesis. In *Endocrinology: Adult & Pediatric* (pp. 2325–2353). Elsevier. <https://research.monash.edu/en/publications/spermatogenesis>
- Kuwahara, Y., Shimada, A., Mitani, H., & Shima, A. (2002). A Critical Stage in Spermatogenesis for Radiation-Induced Cell Death in the Medaka Fish, *Oryzias latipes*. *Radiation Research*, 157(4), 386–392. [https://doi.org/10.1667/0033-7587\(2002\)157\[0386:ACSISF\]2.0.CO;2](https://doi.org/10.1667/0033-7587(2002)157[0386:ACSISF]2.0.CO;2)
- Kuwahara, Y., Shimada, A., Mitani, H., & Shima, A. (2003). γ -Ray exposure accelerates spermatogenesis of medaka fish, *Oryzias latipes*. *Molecular Reproduction and Development*, 65(2), 204–211. <https://doi.org/10.1002/mrd.10261>
- Lacerda, S. M. dos S. N., Costa, G. M. J., & de França, L. R. (2014). Biology and identity of fish spermatogonial stem cell. *General and Comparative Endocrinology*, 207, 56–65. <https://doi.org/10.1016/j.ygcen.2014.06.018>
- Lamichane, S., Dahal Lamichane, B., & Kwon, S.-M. (2018). Pivotal Roles of Peroxisome Proliferator-Activated Receptors (PPARs) and Their Signal Cascade for Cellular and Whole-Body Energy Homeostasis. *International Journal of Molecular Sciences*, 19(4), 949. <https://doi.org/10.3390/ijms19040949>
- Li, B., & Dewey, C. N. (2011). RSEM: Accurate transcript quantification from RNA-Seq data with or without a reference genome. *BMC Bioinformatics*, 12(1), 323.

<https://doi.org/10.1186/1471-2105-12-323>

- Lombardo, D. (2001). Bile salt-dependent lipase: Its pathophysiological implications. *Biochimica et Biophysica Acta (BBA) - Molecular and Cell Biology of Lipids*, 1533(1), 1–28. [https://doi.org/10.1016/S1388-1981\(01\)00130-5](https://doi.org/10.1016/S1388-1981(01)00130-5)
- Lombardo, D., Guy, O., & Figarella, C. (1978). Purification and characterization of a carboxyl ester hydrolase from human pancreatic juice. *Biochimica et Biophysica Acta (BBA) - Enzymology*, 527(1), 142–149. [https://doi.org/10.1016/0005-2744\(78\)90263-2](https://doi.org/10.1016/0005-2744(78)90263-2)
- Lowe, D., Roy, L., Tabocchini, M. A., Rühm, W., Wakeford, R., Woloschak, G. E., & Laurier, D. (2022). Radiation dose rate effects: What is new and what is needed? *Radiation and Environmental Biophysics*, 61(4), 507–543. <https://doi.org/10.1007/s00411-022-00996-0>
- Lu, Q., Liang, Y., Tian, S., Jin, J., Zhao, Y., & Fan, H. (2023). Radiation-Induced Intestinal Injury: Injury Mechanism and Potential Treatment Strategies. *Toxics*, 11(12), Article 12. <https://doi.org/10.3390/toxics11121011>
- Lukassen, S., Bosch, E., Ekici, A. B., & Winterpacht, A. (2018a). Characterization of germ cell differentiation in the male mouse through single-cell RNA sequencing. *Scientific Reports*, 8(1), 6521. <https://doi.org/10.1038/s41598-018-24725-0>
- Lukassen, S., Bosch, E., Ekici, A. B., & Winterpacht, A. (2018b). Single-cell RNA sequencing of adult mouse testes. *Scientific Data*, 5(1), 180192. <https://doi.org/10.1038/sdata.2018.192>
- Lydall, D., & Weinert, T. (1996). From DNA damage to cell cycle arrest and suicide: A budding yeast perspective. *Current Opinion in Genetics & Development*, 6(1), 4–

11. [https://doi.org/10.1016/s0959-437x\(96\)90003-9](https://doi.org/10.1016/s0959-437x(96)90003-9)
- Matés, J. M. (2000). Effects of antioxidant enzymes in the molecular control of reactive oxygen species toxicology. *Toxicology*, *153*(1), 83–104. [https://doi.org/10.1016/S0300-483X\(00\)00306-1](https://doi.org/10.1016/S0300-483X(00)00306-1)
- Mathias, D., Mitchel, R. E. J., Barclay, M., Wyatt, H., Bugden, M., Priest, N. D., Whitman, S. C., Scholz, M., Hildebrandt, G., Kamprad, M., & Glasow, A. (2015). Low-Dose Irradiation Affects Expression of Inflammatory Markers in the Heart of ApoE $-/-$ Mice. *PLOS ONE*, *10*(3), e0119661. <https://doi.org/10.1371/journal.pone.0119661>
- McGinnis, C. S., Murrow, L. M., & Gartner, Z. J. (2019). DoubletFinder: Doublet Detection in Single-Cell RNA Sequencing Data Using Artificial Nearest Neighbors. *Cell Systems*, *8*(4), 329–337.e4. <https://doi.org/10.1016/j.cels.2019.03.003>
- Mita, K., Ohbayashi, T., Tomita, K., Shimizu, Y., Kondo, T., & Yamashita, M. (2000). Differential Expression of Cyclins B1 and B2 during Medaka (*Oryzias latipes*) Spermatogenesis. *Zoological Science*, *17*(3), 365–374. <https://doi.org/10.2108/jsz.17.365>
- Moldovan, G.-L., Pfander, B., & Jentsch, S. (2007). PCNA, the Maestro of the Replication Fork. *Cell*, *129*(4), 665–679. <https://doi.org/10.1016/j.cell.2007.05.003>
- Monti, M., & Redi, C. (2009). Oogenesis specific genes (Nobox, Oct4, Bmp15, Gdf9, Oogenesisin1 and Oogenesisin2) are differentially expressed during natural and gonadotropin-induced mouse follicular development. *Molecular Reproduction*

and Development, 76(10), 994–1003. <https://doi.org/10.1002/mrd.21059>

Murata, Y., Yasuda, T., Watanabe-Asaka, T., Oda, S., Mantoku, A., Takeyama, K., Chatani, M., Kudo, A., Uchida, S., Suzuki, H., Tanigaki, F., Shirakawa, M., Fujisawa, K., Hamamoto, Y., Terai, S., & Mitani, H. (2015). Histological and Transcriptomic Analysis of Adult Japanese Medaka Sampled Onboard the International Space Station. *PLOS ONE*, 10(10), e0138799. <https://doi.org/10.1371/journal.pone.0138799>

Nagata, K., Yasuda, T., Oda, S., & Mitani, H. (2019). Low-dose-rate irradiation induces the testis-ova in medaka testis. *Hoshasen Seibutsu Kenkyu (Online)*, 54(3), 200–211.

Nagata, K., Yasuda, T., Suzuki, M., Funayama, T., Mitani, H., & Oda, S. (2022). Testis-ova Induction by Microbeam Irradiation in P53-Deficient Medaka Testis. *CYTOLOGIA*, 87(1), 1–2. <https://doi.org/10.1508/cytologia.87.1>

Nakamura, H., Fukami, H., Hayashi, Y., Tachibana, A., Nakatsugawa, S., Hamaguchi, M., & Ishizaki, K. (2005). Cytotoxic and Mutagenic Effects of Chronic Low-Dose-Rate Irradiation on TERT-Immortalized Human Cells. *Radiation Research*, 163(3), 283–288. <https://doi.org/10.1667/RR3310>

Nakamura, S., Kobayashi, K., Nishimura, T., & Tanaka, M. (2011). Ovarian Germline Stem Cells in the Teleost Fish, Medaka (*Oryzias latipes*). *International Journal of Biological Sciences*, 7(4), 403–409.

Neuhaus, N., Yoon, J., Terwort, N., Kliesch, S., Seggewiss, J., Hüge, A., Voss, R., Schlatt, S., Grindberg, R. V., & Schöler, H. R. (2017). Single-cell gene expression analysis reveals diversity among human spermatogonia. *Molecular Human Reproduction*,

- molehr;gaw079v2. <https://doi.org/10.1093/molehr/gaw079>
- Nicholls, P. K., Schorle, H., Naqvi, S., Hu, Y.-C., Fan, Y., Carmell, M. A., Dobrinski, I., Watson, A. L., Carlson, D. F., Fahrenkrug, S. C., & Page, D. C. (2019). Mammalian germ cells are determined after PGC colonization of the nascent gonad. *Proceedings of the National Academy of Sciences*, *116*(51), 25677–25687. <https://doi.org/10.1073/pnas.1910733116>
- Niksirat, H., & Kouba, A. (2016). Subcellular localization of calcium deposits in the noble crayfish *stacus astacus* spermatophore: Implications for post-mating spermatophore hardening and spermatozoon maturation. *Journal of Morphology*, *277*(4), 445–452. <https://doi.org/10.1002/jmor.20509>
- Olunkwa, U. E., Iheanacho, K. M. E., Igwe, C. U., Nwaogu, L. A., Iheanacho, J. N., Olunkwa, U. E., Iheanacho, K. M. E., Igwe, C. U., Nwaogu, L. A., & Iheanacho, J. N. (2023). Bioactive component analysis of aqueous seed extract of *Aframomum melengueta*. *GSC Biological and Pharmaceutical Sciences*, *25*(2), Article 2. <https://doi.org/10.30574/gscbps.2023.25.2.0458>
- Pesty, A., Doussau, M., Lahaye, J.-B., & Lefèvre, B. (2010). Whole-body or isolated ovary (60)Co irradiation: Effects on in vivo and in vitro folliculogenesis and oocyte maturation. *Reproductive Toxicology (Elmsford, N.Y.)*, *29*(1), 93–98. <https://doi.org/10.1016/j.reprotox.2009.10.007>
- Pyz-Łukasik, R., & Kowalczyk-Pecka, D. (2017). Fatty Acid Profile of Fat of Grass Carp, Bighead Carp, Siberian Sturgeon, and Wels Catfish. *Journal of Food Quality*, *2017*(1), 5718125. <https://doi.org/10.1155/2017/5718125>
- Qian, P., Kang, J., Liu, D., & Xie, G. (2022). Single Cell Transcriptome Sequencing of

- Zebrafish Testis Revealed Novel Spermatogenesis Marker Genes and Stronger Leydig-Germ Cell Paracrine Interactions. *Frontiers in Genetics*, 13. <https://doi.org/10.3389/fgene.2022.851719>
- Quastler, H. (1956). The Nature of Intestinal Radiation Death. *Radiation Research*, 4(4), 303–320. <https://doi.org/10.2307/3570211>
- Rato, L., Alves, M. G., Socorro, S., Duarte, A. I., Cavaco, J. E., & Oliveira, P. F. (2012). Metabolic regulation is important for spermatogenesis. *Nature Reviews Urology*, 9(6), 330–338. <https://doi.org/10.1038/nrurol.2012.77>
- Raz, E. (2000). The function and regulation of vasa-like genes in germ-cell development. *Genome Biology*, 1(3), reviews1017.1. <https://doi.org/10.1186/gb-2000-1-3-reviews1017>
- Sadoul, B., & Geffroy, B. (2019). Measuring cortisol, the major stress hormone in fishes. *Journal of Fish Biology*, 94(4), 540–555. <https://doi.org/10.1111/jfb.13904>
- Sassone-Corsi, P. (2002). Unique Chromatin Remodeling and Transcriptional Regulation in Spermatogenesis. *Science*, 296(5576), 2176–2178. <https://doi.org/10.1126/science.1070963>
- Sato, M., Hayashi, M., & Yoshizaki, G. (2017). Stem cell activity of type A spermatogonia is seasonally regulated in rainbow trout†. *Biology of Reproduction*, 96(6), 1303–1316. <https://doi.org/10.1093/biolre/iox049>
- Schofield, P. N., & Kondratowicz, M. (2018). Evolving paradigms for the biological response to low dose ionizing radiation; the role of epigenetics. *International Journal of Radiation Biology*, 94(8), 769–781. <https://doi.org/10.1080/09553002.2017.1388548>

- Sharplin, J., & Franko, A. J. (1989). A Quantitative Histological Study of Strain-Dependent Differences in the Effects of Irradiation on Mouse Lung during the Early Phase. *Radiation Research*, *119*(1), 1–14. <https://doi.org/10.2307/3577363>
- Shima, A., & Mitani, H. (2004). Medaka as a research organism: Past, present and future. *Mechanisms of Development*, *121*(7), 599–604. <https://doi.org/10.1016/j.mod.2004.03.011>
- Simon, N. E., & Schwacha, A. (2014). The Mcm2-7 Replicative Helicase: A Promising Chemotherapeutic Target. *BioMed Research International*, *2014*(1), 549719. <https://doi.org/10.1155/2014/549719>
- Solé, C., Nadal-Ribelles, M., de Nadal, E., & Posas, F. (2015). A novel role for lncRNAs in cell cycle control during stress adaptation. *Current Genetics*, *61*(3), 299–308. <https://doi.org/10.1007/s00294-014-0453-y>
- Subirade, M., & Chen, L. (n.d.). *Food-protein-derived materials and their use as carriers and delivery systems for active food components*.
- Subirade, M., & Chen, L. (2008). 10—Food-protein-derived materials and their use as carriers and delivery systems for active food components. In N. Garti (Ed.), *Delivery and Controlled Release of Bioactives in Foods and Nutraceuticals* (pp. 251–278). Woodhead Publishing. <https://doi.org/10.1533/9781845694210.2.251>
- Suzuki, A., Niimi, Y., Shinmyozu, K., Zhou, Z., Kiso, M., & Saga, Y. (2016). Dead end1 is an essential partner of NANOS2 for selective binding of target RNAs in male germ cell development. *EMBO Reports*, *17*(1), 37–46. <https://doi.org/10.15252/embr.201540828>
- Tahri-Joutey, M., Andreoletti, P., Surapureddi, S., Nasser, B., Cherkaoui-Malki, M., &

- Latruffe, N. (2021). Mechanisms Mediating the Regulation of Peroxisomal Fatty Acid Beta-Oxidation by PPAR α . *International Journal of Molecular Sciences*, 22(16), 8969. <https://doi.org/10.3390/ijms22168969>
- Tanaka, M., Hennebold, J. D., Macfarlane, J., & Adashi, E. Y. (2001). A mammalian oocyte-specific linker histone gene H1oo: Homology with the genes for the oocyte-specific cleavage stage histone (cs-H1) of sea urchin and the B4/H1M histone of the frog. *Development*, 128(5), 655–664. <https://doi.org/10.1242/dev.128.5.655>
- Tang, L., Wei, F., Wu, Y., He, Y., Shi, L., Xiong, F., Gong, Z., Guo, C., Li, X., Deng, H., Cao, K., Zhou, M., Xiang, B., Li, X., Li, Y., Li, G., Xiong, W., & Zeng, Z. (2018). Role of metabolism in cancer cell radioresistance and radiosensitization methods. *Journal of Experimental & Clinical Cancer Research*, 37(1), 87. <https://doi.org/10.1186/s13046-018-0758-7>
- Taniguchi, Y., Takeda, S., Furutani-Seiki, M., Kamei, Y., Todo, T., Sasado, T., Deguchi, T., Kondoh, H., Mudde, J., Yamazoe, M., Hidaka, M., Mitani, H., Toyoda, A., Sakaki, Y., Plasterk, R. H., & Cuppen, E. (2006). Generation of medaka gene knockout models by target-selected mutagenesis. *Genome Biology*, 7(12), R116. <https://doi.org/10.1186/gb-2006-7-12-r116>
- Trapnell, C., Cacchiarelli, D., Grimsby, J., Pokharel, P., Li, S., Morse, M., Lennon, N. J., Livak, K. J., Mikkelsen, T. S., & Rinn, J. L. (2014). The dynamics and regulators of cell fate decisions are revealed by pseudotemporal ordering of single cells. *Nature Biotechnology*, 32(4), 381–386. <https://doi.org/10.1038/nbt.2859>
- Treviño, C. L., Santi, C. M., Beltrán, C., Hernández-Cruz, A., Darszon, A., & Lomeli, H.

- (1998). Localisation of inositol trisphosphate and ryanodine receptors during mouse spermatogenesis: Possible functional implications. *Zygote*, 6(2), 159–172. <https://doi.org/10.1017/S0967199498000094>
- Tsuchiya, Y., Nakajima, M., & Yokoi, T. (2005). Cytochrome P450-mediated metabolism of estrogens and its regulation in human. *Cancer Letters*, 227(2), 115–124. <https://doi.org/10.1016/j.canlet.2004.10.007>
- Vilenchik, M. M., & Knudson, A. G. (2000). Inverse radiation dose-rate effects on somatic and germ-line mutations and DNA damage rates. *Proceedings of the National Academy of Sciences*, 97(10), 5381–5386. <https://doi.org/10.1073/pnas.090099497>
- Wanders, R. J. A. (2014). Metabolic functions of peroxisomes in health and disease. *Biochimie*, 98, 36–44. <https://doi.org/10.1016/j.biochi.2013.08.022>
- Wang, J. Y. (1998). Cellular responses to DNA damage. *Current Opinion in Cell Biology*, 10(2), 240–247. [https://doi.org/10.1016/s0955-0674\(98\)80146-4](https://doi.org/10.1016/s0955-0674(98)80146-4)
- Washburn, R. L., Hibler, T., Kaur, G., & Dufour, J. M. (2022). Sertoli Cell Immune Regulation: A Double-Edged Sword. *Frontiers in Immunology*, 13, 913502. <https://doi.org/10.3389/fimmu.2022.913502>
- Wu, X., Yang, Y., Zhong, C., Wang, T., Deng, Y., Huang, H., Lin, H., Meng, Z., & Liu, X. (2021). Single-Cell Atlas of Adult Testis in Protogynous Hermaphroditic Orange-Spotted Grouper, *Epinephelus coioides*. *International Journal of Molecular Sciences*, 22(22), 12607. <https://doi.org/10.3390/ijms222212607>
- Xu, H., Li, M., Gui, J., & Hong, Y. (2007). Cloning and expression of medaka *dazl* during embryogenesis and gametogenesis. *Gene Expression Patterns*, 7(3), 332–338.

<https://doi.org/10.1016/j.modgep.2006.08.001>

Yasuda, T., Ishikawa, Y., Shioya, N., Itoh, K., Kamahori, M., Nagata, K., Takano, Y., Mitani, H., & Oda, S. (2018). Radical change of apoptotic strategy following irradiation during later period of embryogenesis in medaka (*Oryzias latipes*). *PLoS ONE*, *13*(8), e0201790. <https://doi.org/10.1371/journal.pone.0201790>

Yasuda, T., Oda, S., Li, Z., Kimori, Y., Kamei, Y., Ishikawa, T., Todo, T., & Mitani, H. (2012). Gamma-ray irradiation promotes premature meiosis of spontaneously differentiating testis-ova in the testis of p53-deficient medaka (*Oryzias latipes*). *Cell Death & Disease*, *3*(10), e395–e395. <https://doi.org/10.1038/cddis.2012.133>

Yasuko, H.-T., & Nobuo, E. (1985). Establishment of inbred strains of the medaka *Oryzias latipes* and the usefulness of the strains for biomedical research. *Zoological Science*, *2*(3), 305–316. <https://doi.org/10.34425/zs000132>

Yu, J., Chen, B., Zheng, B., Qiao, C., Chen, X., Yan, Y., Luan, X., Xie, B., Liu, J., Shen, C., He, Z., Hu, X., Liu, M., Li, H., Shao, Q., & Fang, J. (2019). ATP synthase is required for male fertility and germ cell maturation in *Drosophila* testes. *Molecular Medicine Reports*, *19*(3), 1561–1570. <https://doi.org/10.3892/mmr.2019.9834>

岩松鷹司. (2018). *メダカ学全書*. 大学教育出版.

中澤拓哉 (2020). *メダカを用いた全身組織切片とトランスクリプトーム解析による低線量（率）放射線の生物影響の解明*. 修士論文.

Acknowledgement

First and foremost, I would like to express my deepest gratitude to my supervisor, Professor Oda, for his unwavering support and invaluable guidance throughout my research. I am also immensely grateful to my second supervisor, Professor Mitani, who continued to offer his wisdom and encouragement.

I would like to extend my heartfelt thanks to Doctor Yasuda, who collaborated with me on my previous projects. Your cooperation and expertise were crucial to the success of this work.

I am particularly thankful to Doctor Nagata and Nakazawa for their insightful guidance and significant contributions to the previous research. I also want to acknowledge the support of my classmates, who assisted me with the transportation and care of the fish used in the experiments.

I am deeply appreciative of the support provided by Kyoto University, which was instrumental in the execution of my experimental projects.

Last but certainly not least, I wish to express my profound gratitude to all medaka sacrifices for my studies, whose sacrifices were essential for the advancement of this research.